NBSIR 86-338

Punching Shear Resistance of Lightweight Concrete Offshore Structures for the Arctic: Literature Review

David I. McLean
H. S. Lew
Long T. Phan
Mary Sansalone

U.S. DEPARTMENT OF COMMERCE
National Bureau of Standards
Center for Building Technology
Gaithersburg, MD 20899

May 1986

Sponsored by:
Technology Assessment and Research Branch
Mineral Management Service
. Department of the Interior
ton, Virginia 22091

NBSIR 86-3388

PUNCHING SHEAR RESISTANCE OF LIGHTWEIGHT CONCRETE OFFSHORE STRUCTURES FOR THE ARCTIC: LITERATURE REVIEW

David I. McLean
H. S. Lew
Long T. Phan
Mary Sansalone

U.S. DEPARTMENT OF COMMERCE
National Bureau of Standards
Center for Building Technology
Gaithersburg, MD 20899

May 1986

Sponsored by:
Technology Assessment and Research Branch
Mineral Management Service
U.S. Department of the Interior
Reston, Virginia 22091

U.S. DEPARTMENT OF COMMERCE, Malcolm Baldrige, *Secretary*
NATIONAL BUREAU OF STANDARDS, Ernest Ambler, *Director*

ABSTRACT

The punching shear resistance of lightweight concrete offshore structures for the Arctic is being investigated at the National Bureau of Standards on the behalf of The Minerals Management Service of the U.S. Department of the Interior in cooperation with five American oil companies. This report serves as an introduction to the project and reviews current knowledge on material relevant to the punching shear behavior of concrete offshore structures subjected to Arctic ice loads. A brief review of available information on Arctic ice loads and a discussion of some of the proposed offshore structural concepts are presented. The general mechanics of punching shear failures and the factors affecting punching resistance are discussed along with a comparison of current U.S. and European code provisions on punching shear. Available literature on experimental and analytical investigations on punching shear relevant to this project is also reviewed.

Keywords: Arctic environment; lightweight concrete; literature review; offshore structure; punching shear; reinforced concrete.

PREFACE

In 1984, under the sponsorship of the Minerals Management Service, Department of the Interior, the National Bureau of Standards (NBS) initiated a study of the punching shear behavior of lightweight concrete offshore structures. This project was conceived following the 1983 International Workshop on the Performance of Offshore Concrete Structures in the Arctic Environment, which identified the behavior of lightweight concrete elements subjected to high local ice forces as a major research area.

The authors of this report gratefully acknowledge the support, encouragement, and cooperation provided by Mr. Charles E. Smith of the Minerals Management Service and the significant technical contributions made to this project by Professor Richard N. White of Cornell University.

Any opinions, findings, and conclusions or recommendations expressed in this report are those of the authors and do not necessarily reflect the views of the Minerals Management Service, Department of the Interior.

TABLE OF CONTENTS

		Page
	ABSTRACT	ii
	PREFACE	iii
	LIST OF TABLES	vi
	LIST OF FIGURES	vii
1.0	INTRODUCTION	1
	1.1 Background	1
	1.2 Purpose and Scope of Research	3
	1.3 Purpose of This Report	4
2.0	ICE LOADS ON ARCTIC STRUCTURES	5
	2.1 Introduction	5
	2.2 Nature of Arctic Ice	5
	2.3 Predicting Ice Forces	8
	2.4 Design Values of Ice Loads	12
3.0	CONCRETE OFFSHORE STRUCTURES FOR THE ARCTIC	15
	3.1 Introduction	15
	3.2 Structure Classification	15
	3.2.1 Island Structures	15
	3.2.2 Gravity Structures	16
	3.2.3 Floating Structures	18
	3.3 Review of Proposed Designs	18
4.0	PUNCHING SHEAR BEHAVIOR OF CONCRETE SLABS AND SHELLS	24
	4.1 Introduction	24
	4.2 Comparison of Beam and Punching Shear	25
	4.3 Mechanism of Punching Shear	27
	4.4 Factors Affecting Punching Shear Strength	29
	4.5 Predicting Punching Shear Resistance	40

TABLE OF CONTENTS (continued)

Page

4.6 Code Provisions on Punching Shear Strength 42
4.6.1 ACI 318-83 43
4.6.2 CEB-FIP 44
4.6.3 CP110 46
4.6.4 Comparison of the Codes 47
4.6.5 Limitations of Code Provisions on Punching Shear Strength 48

5.0 RECENT RESEARCH IN PUNCHING SHEAR 51
5.1 Punching Shear in Thick Slabs 51
5.2 Punching Shear in Nuclear Reactor Structures .. 53
5.2.1 Reactor Vessel End Slabs Under Pressure Loading 54
5.2.2 Impact Loading on Nuclear Reactor Containment Structures 57
5.3 Fiber Reinforced Concrete Subjected to Punching and Impact Loads 59
5.4 Punching Shear in Offshore Structures 61
5.4.1 BWA Punching Shear Study 62
5.4.2 Punching Shear in Prestressed Cylindrical Shells: Norwegian Work 71
5.4.3 Other Punching Shear Studies on Offshore Structures 73
5.5 Finite Element Predictions of Punching Shear Strength 75

6.0 SUMMARY 82

7.0 REFERENCES 84

LIST OF TABLES

Table		Page
1	Comparison of effective ice pressures for vertical piles and piers	100
2	Expressions for ultimate shear strength	101
3	Summary of code provisions on punching shear	103

LIST OF FIGURES

Figure		Page
1	Possible ice failure modes	104
2	Local ice pressure design curves	105
3	Example configurations of Arctic offshore structures	106
4	SOHIO Arctic Mobile Structure (SAMS)	107
5	Brian Watt Associates Caisson System (BWACS)	108
6	Artist's sketch of the Arctic Cone Exploration Structure (ACES)	109
7	Typical details of initial constuction (ACES)	110
8	Concrete Island Drilling System: Super Series (Super CIDS)	111
9	Super CIDS brick dimensions and details	112
10	Tarsiut Island, general arrangement	113
11	Structural arrangement for concrete ice wall	113
12	Shear transfer mechanisms in a cracked beam	113
13	Crack formation in the column area of a slab	114
14	Arching action in slabs	114
15	Typical curves for an underreinforced slab	115
16	Punch load vs. flexural reinforcement for the simple and restrained slabs tested by Taylor and Hayes	116
17	Shear test data vs. Eq. 11-37 of ACI 318-83 for two-way prestressed slabs	116
18	Idealized connection model of Kinnunen and Nylander	117

LIST OF FIGURES (continued)

Figure		Page
19	Punching test results compared with code predictions	118
20	Comparison of punching shear provisions for selected parameters: ACI vs. CEB-FIP	119
21	Comparison of punching shear provisions for selected parameters: ACI vs. CP110	120
22	Different types of cracks observed in pressure vessels	121
23	Shear-flexure interaction curve	122
24	General characteristics of a typical test panel used in the BWA study	123
25	BWA punching shear study loading system	124
26	Effect of shear reinforcement quantity on ultimate shear resistance in BWA study	125
27	Test results of BWA study compared with "conventional slab methods"	126
28	Test results of BWA study compared with "conventional slab method" (CP110)	127
29	Comparison of tested vs. calculated ultimate shear resistance, Vu ("ACI modified punching shear method") from BWA study	128
30	Geometry and dimensions for shell specimens of Reference 149	129
31	Results of punching tests of Reference 152 ..	130
32	Finite element predictions of punching shear strength: load vs. deflection curves	131

1.0 INTRODUCTION

1.1 BACKGROUND

Potentially great sources of oil and natural gas are contained within the Arctic Ocean region of North America. To exploit these reserves will require the design, construction, and maintenance of permanent offshore structures that can withstand the harsh conditions imposed by the Arctic environment. Few permanent Arctic offshore structures actually exist and little information is available on the environmental loads that these structures might experience. Further, the structural configurations being proposed are sufficiently different from standard construction that uncertainties exist in predicting the behavior of these Arctic structures under load. For safety and economic reasons, more research is clearly needed if the mineral resources of the Arctic are to be developed.

Designs of Arctic offshore structures have utilized both concrete and steel as the construction material, and increasing attention is being given to composite structures incorporating both concrete and steel into the design [1,2]. Use of concrete as the construction material has many inherent advantages in the harsh Arctic environment. Properly constructed concrete structures can be extremely durable and maintenance free when exposed to marine environments, and concrete can provide a structure with the mass and rigidity needed to withstand the extreme loading conditions of the Arctic [3]. Offshore structures for the Arctic will normally be built in temperate climates and towed to the Arctic region. The structure's weight, buoyancy, floating stability, dynamic response during tow, and deployment in shallow or ice-covered waters must all be considered in design [4]. These requirements make it desirable to use lightweight, high-strength concrete in the construction of Arctic offshore structures.

Over the last 15 years, concrete has been used successfully in the construction of offshore structures in the North Sea [3,5,6]. Concrete has also been used for lighthouses both in Canada and in Northern Europe for over 50 years [6]. While this experience with concrete structures in temperate and sub-arctic regions provides valuable information, unknowns in structural performance still exist as a result of the severe ice loading conditions that exist in the Arctic. Much more research is needed in this area to better understand and quantify ice loads on structures in the Arctic.

Proposed designs of offshore structures for the Arctic typically have a concrete wall extending around the perimeter of the structure. These exterior walls will be subjected to tremendous loads resulting from the impact of ice on the structures. Designs of the exterior walls call for thick, lightweight, high-strength concrete sections which are heavily reinforced and possibly prestressed to improve flexural and shear capacities. Both flat and curved exterior surfaces have been proposed for use. The proper design of this exterior ice wall is of particular importance to the integrity of the structure, and it substantially influences the cost.

The design of offshore structures in the Arctic requires an understanding of the behavior of the concrete exterior walls under high intensity ice loads. Both global and local effects of the ice loading must be considered. Estimates of the ice contact pressures are typically in the range of 3 to 15 MPa (400 to 2200 psi), depending on the area of contact between the ice and the structure [6]. These structures should be designed so that under high intensity ice loads punching shear is not the primary mode of failure. A shear failure is undesirable because it is sudden and it could lead to the progressive collapse of the structure.

Information on the punching shear behavior of thick, heavily reinforced, lightweight concrete sections of the type being

proposed for Arctic structures is limited. Provisions in existing standards pertaining to punching resistance have been derived from tests conducted on thin and lightly reinforced sections. The increased thickness, the large amount of reinforcement, and the possible presence of arch action and prestressing all will influence the punching load capacity. Thus, there is a need to investigate the punching shear resistance of heavily reinforced thick slab and shell sections [3].

1.2 PURPOSE AND SCOPE OF RESEARCH

This research project is being conducted by the National Bureau of Standards (NBS) to investigate the punching shear resistance of heavily reinforced, high-strength, lightweight concrete slab and shell sections in order to aid in the establishment of criteria for the design of Arctic offshore concrete structures. The project was undertaken on the behalf of The Minerals Management Service of the U.S. Department of the Interior in cooperation with the following five oil companies:

- Chevron Oil Company;
- Exxon Company, U.S.A.;
- Mobil Corporation;
- Shell Oil Company; and
- Standard Oil Company of Ohio.

The research project will consist of both analytical studies and physical model studies. The analytical phase is directed towards the development of a finite element analysis program that will incorporate non-linear material models and failure criteria under multi-axial states of stress. The physical modeling tests will be conducted on representative slab and shell sections of Arctic offshore structures. Both prestressed and non-prestressed sections will be studied. The physical tests will initially be conducted on 1/6-scale models, with larger-scale model tests to follow.

1.3 PURPOSE OF THIS REPORT

This report is the first in a series of progress reports on the project being conducted at NBS to investigate the punching shear resistance of lightweight concrete offshore structures. The purpose of this report is to introduce the problem and to review current knowledge on the punching shear behavior of concrete offshore structures subjected to Arctic ice loads. A general review of material relevant to the subject is also presented.

The shape and design of proposed Arctic offshore structures are a direct result of the ice loads that the structures will be expected to resist. A review of available information on Arctic ice loads is presented, followed by a discussion of typical structural concepts that have been proposed. The general mechanics of punching shear failures and the factors affecting punching resistance are discussed along with a comparison of current U.S. and European punching shear code provisions. Finally, available literature on experimental and analytical research on punching shear relevant to this research is reviewed.

2.0 ICE LOADS ON ARCTIC STRUCTURES

2.1 INTRODUCTION

Offshore structures in the Arctic will be exposed to severe ice loading and successfully designing these structures to resist the ice forces is a major aspect of the overall design of the structure. The perimeter wall surrounding an offshore structure represents a substantial portion of the weight and cost of the structure. Design of this perimeter wall (sometimes referred to as the ice wall of the structure) is controlled by the extremely high ice pressures that develop as an ice formation is crushed against it. Past experience with marine structures in sub-arctic and temperate regions, while valuable, does not include information on loading conditions as severe as those expected for the Arctic. Development of an understanding of ice action in the Arctic and quantification of design values of ice loads are clearly in their early stages. Much more research is needed in this area. This chapter presents a review of the publicly available information (much of the recent research is proprietary) on ice loads in the Arctic.

2.2 NATURE OF ARCTIC ICE

The proposed locations of the offshore Arctic structures will result in the structures being exposed to a wide variety of ice forms. Both freshwater ice and sea ice formations are found in the Arctic Ocean. Freshwater ice formations, such as icebergs and ice islands, are of glacial origin. Ice islands are the largest freshwater ice formations and can be as large as 1000 km^2 (400 square miles) in area and have thicknesses up to 60 m (200 ft) [7]. Sea ice is usually classified by age into first-year and multi-year ice. First-year ice is sea ice of one winter's growth, with thicknesses ranging from 0.3 to 2 m (1 to 7 ft). Multi-year ice is ice that has survived at least two summers, and

consolidated multi-year ice thicknesses of up to 7 m (23 ft) have been recorded [7]. Pressure ridges are the result of ice sheets deforming due to pressure and may be 20 m (65 ft) thick. Pack ice is a term commonly used to refer to any accumulation of sea ice. Floes are any relatively flat pieces of sea ice having lateral dimensions on the order of 20 m (65 ft) or more. More detailed information on the classification of ice formations can be found in the literature review on ice loading performed by The American Bureau of Shipping [8].

Ice conditions are a function of the specific region in the Arctic and the hydrography of that particular location. Bays and shallow waters are stationary ice areas. For most of the year the ice is frozen to the sea bed, creating what is known as an ice foot [7]. When melting occurs during the summer, pieces of the ice foot can move, resulting in loads on a structure. However, since the geography of stationary areas limits ice foot movements, the impact forces imposed on a structure are much less than those that would be experienced by a structure located in the open sea. In the Arctic seas the ice cover is made up of moving pack ice. Winter ice conditions are more predictable than those that occur during breakup of the ice cover in the warmer months. The most dangerous ice formations occur during the spring and summer when multi-year floes invade the southern Arctic waters.

Action of ice on offshore structures requires calculation of both local contact pressures and global forces. Forces due to ice pressure result from thermal expansion, static loads, or dynamic loads. Some of the possible failure modes for ice impinging upon a structure are shown in Figure 1 (adapted from References 7,9 and 10). The ice loads imposed on vertical structures are usually based on the buckling or crushing strength of an ice sheet [8]. As buckling occurs only for relatively thin ice floes, ice loads are more commonly specified by the compressive strength of the ice formation. Ice loads on structures with a

sloping surface around their perimeter (usually the structures are conical in shape) are a function of both the compressive and flexural strength of the ice [8]. When moving ice collides with an inclined surface, it tends to ride up the slope, and local crushing occurs along the bottom of the ice sheet which is in contact with the structure. As the contact force is normal to the sloping surface, bending stresses are induced in the ice sheet. When the tensile strength of the ice sheet is exceeded, the sheet fails by cracking.

The possibility of dynamic loading conditions for any particular location depends upon the hydrography of the location. Very fast currents and strong winds can cause impact loading of an ice mass on a structure. Dynamic stresses can also occur when failure of an ice mass in contact with a structure causes instant unloading [11]. Ice-induced vibration of offshore structures is usually not a problem, except perhaps for slender, flexible structures in which the natural frequency of the structure is in the range of the frequency of ice load oscillation (0.5 to 15 Hz) [8]. However, stresses induced by continuous crushing of an ice mass in contact with a structure (ratchetting effects) may cause structural fatigue.

The forces imposed on a structure by moving ice are influenced by many factors. Engelbrektson [11] has identified the following factors as being of predominant importance:

- structural shape (vertical or inclined face, shape of cross section, width);
- structural response (rigid, flexible, vibrating);
- ice feature (sheet ice, rafted ice, ice ridges, icebergs);
- ice failure mode (ductile or brittle crushing, bending, shearing);
- contact between ice and structure (contact area, degree of momentary contact, variation of contact); and

- ice strength, which is in turn governed by:
    - crystalline form and grain size;
    - ice temperature;
    - brine volume;
    - stress condition (confinement); and
    - strain rate.

Ice is elastic at low load levels and high strain rates, but exhibits inelastic behavior under higher load levels and lower strain rates [8]. Typical strength values for sea ice with a salinity of 4.7% and at -10°C are [8,12]:

flexural	0.6 - 1.0 MPa (85 - 145 psi)
compressive, unconfined with an ice thickness of 1.5 m (5 ft)	3.5 - 4.1 MPa (500 - 600 psi)
elastic modulus	4100 MPa (0.6×10^6 psi)
Poisson's ratio	0.30 - 0.35

A more complete discussion of the physical and mechanical properties of ice is given in Reference 8.

2.3 PREDICTING ICE FORCES

Evaluating the effects of ice forces is an important design consideration for any structure that will be required to function in an ice environment. Predicting ice effects on marine structures requires calculation of both local ice contact pressures and total ice forces. Bridges, piers, lighthouses, and ships have existed or operated in ice-infested regions for many years. With the discovery of oil and gas in the Arctic, increasing attention is being given to the problem of predicting ice forces on Arctic structures. A substantial amount of research has been conducted in recent years by individual companies and by joint industry groups such as the Alaska Oil and Gas Association (AOGA) and the Arctic Petroleum Operators

Association of Canada (APOA); however, much of this work is proprietary [8]. Despite these considerable efforts, knowledge and understanding of ice loading on Arctic structures is limited.

Ice forces have been determined using many different techniques and approaches. It is a very complex problem and no general consensus yet exists on what values should be selected for design pressures. An indication of the wide range of ice pressure values that can be calculated using different theories is given in Table 1, taken from Croasdale [13]. While this table is for piles and piers, it nevertheless indicates the difference in opinions that can exist.

In general, three approaches have been taken in the prediction of ice loads on structures: theoretical analyses, experimental laboratory studies, and monitoring of existing structures in situ. A brief discussion of the three approaches is given, and some problems and shortcomings associated with these efforts are noted. A more complete literature survey of the research work that has been performed on the problem of predicting ice loads on structures can be found in Reference 8.

Theoretical approaches have applied classical mechanics to the problem of predicting ice forces, using theories of elasticity and plasticity. The forces are usually specified by solving an indentation problem whereby an ice sheet, represented as a visco-elastic-plastic medium, moves into a rigid indentor [8]. Work by Korzhavin [14] and Ralston [15] has led to the development of indentation equations for predicting the horizontal force exerted by ice crushing against a structure. Ralston's equation appears in API Bulletin 2N [16] and is as follows:

$$F = I f_c C_x D t \qquad (2\text{-}1)$$

where F = horizontal ice force;
I = indentation factor;

f_c = contact factor;
C_x = unconfined compressive strength of the ice;
D = diameter or width of the structure at the region of ice contact; and
t = ice thickness.

The indentation factor, I, depends on:

- crystallographic structure of the ice;
- multi-axial strength of the ice;
- strain rate; and
- geometry of the interaction between the ice and the structure.

The strain rate for the ice is a function of the ice approach velocity and the structure dimension, D. The contact factor, f_c, depends on:

- ice movement rate;
- local geometric effects; and
- active defense mechanisms.

Besides the obvious complexity of using this equation, there are other problems. Parameters to be used in this equation will depend on the location and configuration of the offshore structure. Yet there is no rational basis that currently exists for choosing appropriate values for the parameters. Also, due to the random nature of the loading, an assessment needs to be made to determine what conditions and values will be selected, i.e. what return interval should be used. There are other considerations. Portions of the structure may interact, altering the failure mode of the ice feature. Also, non-simultaneous failure of the ice may occur across the width of large structures. Therefore, even if the theory that is used in the prediction of the ice forces has a rational basis, enough unknowns exist to render the current applicability of this and

similar equations to design questionable [17].

A number of small-scale laboratory tests have been conducted on the interaction of ice with a structure. Both real and artificial ice have been used in these model tests. The U.S. Army Cold Regions Research and Engineering Laboratory has studied the action of sheet ice on model bridge piers using their large refrigerated test basin facility (33.5 m long by 9.15 m wide by 2.4 m deep) [18]. Various parameters were investigated, including the geometry of the bridge piers and the velocity, thickness, and flexural strength of the ice. It was observed in the tests that the magnitude of the force required to fail the ice sheet was strongly influenced by the slope angle of the inclined structure. The investigators compared their test results with forces predicted by Ralston's theoretical approach, and observed some agreement. However, the experimental results tended to be higher than the theoretical ice forces calculated from Ralston's formulation. Other model studies have been conducted on cylindrically- and conically-shaped structures [8,19]. These and other model tests have led to the development of empirical design formulas, but the validity of the formulas are questionable for actual structures because of scale effects [8] and many of the same reasons discussed previously for the theoretical approaches that have been used.

In situ tests involving monitoring of existing structures in the Arctic have been performed [17]. However, the measured response of any structure will be influenced by the particular configuration of that structure. Also, monitoring of actual Arctic structures has not been performed over a sufficient period of time to allow appropriate design and overload values to be selected. Further, much of this work of monitoring of existing structures in the Arctic is currently proprietary. Continued coordinated efforts combining analytical and experimental studies with results of in situ tests are needed before realistic values of Arctic ice loads can be determined.

The discussion of the random nature of the loads that structures in the Arctic will experience intuitively leads to the conclusion that the ice and other environmental loads should be treated in a statistical sense, i.e. by applying a reliability-based design methodology. This has been proposed by Engelbrektson [11], Kry [20], Vivatrat and Slomski [21], and others. Even though this is a logical and promising approach, not enough statistical information has been collected on conditions in the Arctic to provide the basis for developing such a reliability- based design method.

The problem of predicting Arctic ice loads is extremely complex, and the development of design criteria for Arctic structures is still in its early stages. With the increased activity in this region, the need for more research into the interaction of structures with ice is urgent.

2.4 DESIGN VALUES OF ICE LOADS

Despite the lack of a practical and accurate method for predicting ice loads in the Arctic, offshore structures have been designed and a limited number are currently in use in the Arctic. Values must therefore have been assigned to the ice forces in these designs. From the limited amount of design information publicly available, it appears that considerable engineering judgement was used in selecting design ice pressures.

Although both local ice pressures and global ice forces must be considered in design, it is local ice pressures that will control the thickness of the perimeter ice wall of the structure. Local ice pressures can result in a punching shear mode of failure in the exterior wall, although other modes of failure may also occur. As the exterior wall represents a substantial portion of the total cost and weight of the structure, careful judgement must be exercised in selecting a value for the local contact

pressures.

Published codes give very little guidance on values of local ice pressures to be used in design. The American Petroleum Institute has issued Bulletin 2N, "Planning, Designing and Constructing Fixed Offshore Structures in Ice Environments," 1982 [16]. While not a design code per se, the bulletin does identify design considerations for Arctic offshore structures. No design values are given for local ice contact pressures. The bulletin simply states that ice contact failure pressures will be considerably larger than the uniaxial ice strength because of confinement effects, but that the relationship between unconfined and confined compressive strengths is not well established. Values of local confined pressures of sea ice as high as 24 MPa (3500 psi) have been reported [7]. Proprietary research is currently being conducted in this area.

Bulletin 2N states that the design of concrete structures should follow the provisions of ACI 357 R-78 (1978), "Guide For The Design and Construction of Fixed Offshore Concrete Structures" [22]. No provisions for ice force values are given in ACI 357 R-78. Also, no load factor for ice is specified other than stating that it should be determined for the specific site and location.

A survey of available design information on proposed and existing structures indicates that a wide range of local ice contact pressures have been reported as a basis for design:

- 1200 psi on any 50 ft^2, Imperial Oil (ESSO), 1983 [23];
- 1300 psi on any 5 ft^2 (exploratory structure) and 2000 psi on any 5 ft^2 (production structure), R. G. Bea, 1983 [24];
- 590 to 670 psi over 310 to 200 ft^2 respectively, SOHIO, 1984 [25];
- 1600 psi on 10 ft^2 or less and 1000 psi on 210 ft^2, ACES, 1984 [26]; and
- 900 psi on 5 ft X 5 ft area, Super CIDS, 1984 [27].

The only agreement on local ice pressure design values is that as the contact area gets larger, the pressure should decrease. Bruen et al. [28] have proposed design curves, shown in Figure 2a, taking into account this relationship. A similar ice pressure design curve, from Byrd et al. [26], is shown in Figure 2b. Values from the curves are to be considered as uniformly distributed pressures. It is also stated that these curves should be calibrated by large-scale field tests.

3.0 CONCRETE OFFSHORE STRUCTURES FOR THE ARCTIC

3.1 INTRODUCTION

Although very few Arctic offshore structures have been built, a large number of innovative concepts for offshore structures have been proposed. The exterior walls extending around the perimeter of offshore structures must be able to resist both large global loads and local contact pressures exerted on the walls by moving ice. The shape of a structure plays an important role in how the structure will resist the severe ice forces as the failure mode of the oncoming ice is a function of how the ice features interact with the structure. However, the choice of the shape and configuration for an offshore structure is also influenced by the depth of water in which it will operate, cost, constructibility, towing requirements, etc. This chapter will discuss the general types of structural configurations that have been proposed for Arctic offshore structures. Relevant design details from several specific proposals are also presented.

3.2 STRUCTURE CLASSIFICATION

Proposed configurations of offshore structures for the Arctic can generally be classified into three categories [3,23]:

- island structures: non-retained and retained;
- gravity structures: conical, vertical- and step-sided; and
- floating structures.

Representative drawings of the different categories of structures are shown in Figure 3. Hybrid structures combining features may also exist.

3.2.1 ISLAND STRUCTURES

Island structures are most applicable for shallow water areas. Since 1972, about 30 structures of this type have been built in the Beaufort Sea off Canada and Alaska [23]. Island structures

may be non-retained, in effect an artificial island, or the fill material used to construct the island may be retained with caissons.

Non-retained islands (Figure 3a) are economical for use in shallow water regions of 25 m (80 ft) or less [23]. The island is formed by making a mound using fill material upon which the working area is constructed. Ice forces are resisted as a result of the large mass of the structure. Rubble formation around the island enhances the resistance, however it makes accessability to the structure difficult. This type of structure has a large work area which can accomodate many wells. A large amount of locally available gravel or other suitable construction material is required for these structures [3].

Retained islands (Figure 3b) have been proposed for water depths in which non-retained islands would be uneconomical because of their large material requirements. Retained islands are reported to be cost effective for water depths of 25 to 60 m (80 to 200 ft) [23]. Retained islands are formed by constructing a rigid perimeter wall of either steel or concrete and backfilling the wall with earth. The walls will normally be constructed in temperate locations and towed to the Arctic. Like non-retained islands, the retained islands achieve their strength as a result of their large mass [3].

3.2.2 GRAVITY STRUCTURES

Gravity structures have been proposed for use in water depths in which island structures are uneconomical. Proposed designs call for use of gravity structures in water depths of up to 200 m (650 ft) [23,29]. Gravity structures may rest on the sea bed, or they may be attached to the bottom using piles. The structures may also be placed on a submerged berm. Proposed configurations of gravity structures have included structures with sloping sides (usually the structure is conical in shape), vertical sides, and

stepped sides. The different configurations are a result of attempts to reduce the ice forces that the structure must resist.

Conical structures (Figure 3c) and other structures with sloping sides have been proposed as a way of reducing ice forces on the structure by causing the ice to fail in bending rather than crushing. Conical structures will normally have a large base to provide stability and a small top section to reduce the ice force on the structure. The small top section will also result in the disadvantage of having a small working area [3].

Vertical-sided caisson gravity structures (Figure 3d) are normally very large and polygonal in shape. The vertical walls will induce a crushing failure in oncoming ice features, which will result in high local contact pressures developing on the structure's exterior wall. The exterior walls of the vertical-sided gravity structures may be configured as an arch shape to induce arching action, thereby reducing principal tension stresses in the wall [25].

Stepped-sided gravity structures (Figure 3e) have been proposed for production platforms in water depths of 50 to 200 m (165 to 650 ft) that are subject to impact of large ice features [29]. In deeper waters, vertical-sided structures require large quantities of structural materials, the draft is deep, and the maximum ice forces are large. Conical structures, while reducing the impact forces by causing the ice to ride up, may be difficult to construct and deploy in deeper water, resulting in higher costs. Gerwick et al. [29] report that the stepped geometry enables a more efficient utilization of materials than a vertical-sided gravity structure. Additionally, they report that this concept will result in reduced ice impact forces by creating a multi-modal failure of the ice. It is reported that global ice loads would be reduced by 50% or more when compared to those developed by a vertical-sided structure [29]. However, high local ice pressures would continue to be a problem that would need to

be addressed in the design.

3.2.3 FLOATING STRUCTURES

Floating structures (Figure 3f) have been reported [23] as being the most realistic approach for exploration and production in water depths of 150 m (500 ft) or greater. Floating structures have a limited capability to resist ice forces, but they may be moved to avoid large ice features. Cone configurations may be incorporated into the floating structure to create flexural failure in the ice. Induced vertical motions may also be used to achieve the same result [23]. Drill ships have been suggested for drilling in very deep waters [23].

3.3 REVIEW OF PROPOSED DESIGNS

A brief discussion of some of the published work on specific proposals for Arctic offshore structures is presented.

1. Schlechten et al. [25], 1984, SOHIO Arctic Mobile Structure (SAMS):

The SAMS structure consists of a 345 ft wide octagonally shaped concrete base with a plan view as shown in Figure 4a. The height of the exterior wall of the structure is 70 ft. Approximate dimensions of the exterior wall are presented in Figure 4b. Design of the exterior wall was controlled by local ice pressure. The arch profile on the interior face of the wall was used to help resist the ice loads in direct compression, thereby minimizing principal tension in the concrete. Additionally, orthogonal post-tensioning was used to create a biaxial compression state to further reduce principal tension. Ice pressure intensities of 590 to 670 psi (unfactored) over respective areas of 310 to 200 ft^2 controlled the design of the ice wall by creating limiting compressive stresses at the crown of the arch. Higher intensity pressures over smaller areas leading to a punching type of failure did not control the design

because of the arched inner surface and post-tensioned induced state of biaxial compression. Other relevant design details included:

- a semi-lightweight[1], high-strength concrete was used with a unit weight of 133 pcf and a design compressive strength of 7000 psi at 90 days;
- load factor for ice = 1.3; capacity reduction factor = 0.7 (which reflects the compressive type failure mode expected);
- a 15% increase in effective compressive strength was allowed, based on the expected triaxial state of stress in the concrete;
- in designing the exterior wall, a temperature gradient of +34°F (inside) to -50°F (outside) was considered. Tension created by this gradient was compensated for by prestressing the concrete;
- a tension reinforcement ratio of 1% was used in the exterior wall;
- prestressing in the exterior wall varied from 500 to 1000 psi, depending on location; and
- analysis for the design consisted of three-dimensional linear analyses of a segment of the exterior ice wall followed by two-dimensional nonlinear finite element analyses to check the ultimate capacity of the wall. Shear reinforcement and confinement steel requirements were determined from the two-dimensional analyses based on the location and magnitude of the principal stresses.

One final comment on this concept is that the shear design requirements were not based on conventional code formulae. The

---

[1]For this report, lightweight concrete is defined as concrete with a unit weight of 120 pcf or less, semi-lightweight as concrete with a unit weight of 121 to 140 pcf, and regular-weight as concrete with a unit weight of 141 pcf or greater.

designers noted that this would have resulted in excessively thick plates due to the presence of extremely high ice pressures and the relatively low shear (tensile) strength of the concrete. To account for the arch action within the plate, the designers used Section 11.4.2.2 of ACI 318-77 [30] which allows the determination of shear strength to be "computed as the shear force corresponding to dead load plus live load that results in a principal tensile stress of $4\sqrt{f'_c}$ at the centroidal axis of a member." The designers used two-dimensional finite element analyses to demonstrate that the ice wall successfully limits principal tension through arch action to resist loads in compression.

2. Bhula et al. [31], 1984, Brian Watt Associates Caisson System (BWACS):

BWACS is a vertical-sided caisson gravity structure. A perspective view of the BWACS structure is shown in Figure 5a. The exterior ice wall is 90 ft high. A detail showing typical dimensions is given in Figure 5b. Design of the outer wall is controlled by flexure and out-of-plane shear forces. The arched outer wall induces compression which enhances its out-of-plane shear resistance. The external walls were designed for out-of-plane shear in accordance with ACI 318-83 [32]. The ice pressure curves proposed by Bruen et al. [28], shown in Figure 2a, were used in the design. Other relevant design details:

- BWACS is to be a monolithic structure constructed of lightweight, high-strength concrete (compressive strength at 28 days = 7000 psi);
- the structure is to be post-tensioned but no stressing values are given;
- a mild steel reinforcing ratio of 2% was used with a steel yield strength of 60,000 psi;
- load factor for ice = 1.3; shear reduction factor for lightweight concrete = 0.8; and
- the analysis for the design was carried out using finite element techniques. Some of the ice loading patterns

considered on the finite element mesh are shown in Figure 5c.

Brian Watt Associates Inc. conducted an experimental investigation into the punching shear capacity of thick, heavily reinforced regular-weight concrete shells [34] with apparent applications to the BWACS design.

3. Byrd et al. [26], 1984, Arctic Cone Exploration Structure (ACES):

A perspective cut-away of ACES is given in Figure 6. The hull has a conical shape in order to induce a bending failure mode in the ice, resulting in reduced forces on the structure. The authors feel the concept introduced in the ACES design will be used as a prototype for heavy duty, bottom-founded mobile rigs for Arctic offshore drilling. Some typical dimensions of the exterior wall are shown in Figure 7. Local ice pressures determined the configuration and sizes of the principal structural components in the ACES design. The relationship between local ice pressure and loaded area used in the design is given in Figure 2b. Other relevant design details:

- a lightweight, high-strength concrete was used in the design (UW = 115 pcf, 28 day compressive strength = 7000 psi);
- the outer shell contained meridional and circumferential prestressing; and
- load factor for ice = 1.3.

4. Wetmore [27], 1984, The Concrete Island Drilling System: Super Series (Super CIDS):

This structure is one of the few proposed offshore structures for the Arctic that has been built. The general concept of the Super CIDS system is shown in Figure 8. The use of large "brick" units allows the system to be adapted to different locations, i.e. the bricks can be stacked to accommodate varying water depths. A plan view of a typical brick is shown in Figure 9. Relevant design details are:

- design local ice load was 900 psi on an area of 5 ft X 5 ft;
- all of the elements of the "brick", except the interior wall and shear walls, are constructed of lightweight (115 pcf), high-strength (28 day compressive strength = 6500 psi) concrete. The interior wall and shear walls use normal-weight concrete with a design strength of 8000 psi;
- the outer wall is post-tensioned to 500 psi in the horizontal direction and 300 psi in the vertical direction; and
- the load factor for ice is 1.3.

5. Fitzpatrick and Stenning [35], 1983, Tarsiut Island:
Tarsiut Island was constructed of four concrete caissons, arranged in a square, backfilled and placed atop a submerged sand berm. The general arrangement is shown in Figure 10. Thickness of the caisson walls was approximately 250 mm. A lightweight concrete with a density of 120 pcf was used in the construction. The final reinforced concrete density, the weight of the steel and post-tensioning included, was 140 pcf. The concrete had a 28 day compressive strength of 6000 psi.

6. Bruce and Roggensack [1], 1984:
Only a general discussion on designing Arctic platforms is presented in this paper. It is recommended that arch action be built into the design of the exterior ice wall of the offshore structures in order to enhance the capacity of the system. An arrangement for doing this is shown in Figure 11. Even with the arch action, shear stresses can still be large, requiring a significant amount of shear reinforcement. To reduce the shear stresses, transverse prestressing has been suggested, the potential advantages being:
- the load at which inclined cracking first occurs is increased;
- ultimate strength is increased; and
- the congestion of shear reinforcement in the cross section

is reduced.

The practicality of using short tendons to post-tension the section can be questioned, however. The authors also add that the shear lag effects of thick concrete members will ease the problems associated with high local ice impact pressures.

4.0 PUNCHING SHEAR BEHAVIOR OF CONCRETE SLABS AND SHELLS

4.1 INTRODUCTION

The mechanism by which failure will occur in a structure must be considered in the design in order to insure an adequate level of safety. It is important that the structure behave in a ductile manner as it approaches failure rather than failing in a brittle fashion. Flexural failures in properly designed reinforced concrete members are accompanied by a gradual yielding of the flexural steel, and relatively large deflections will occur before failure. The large deflections provide warning prior to the collapse of the structure, and the ductile behavior allows load redistribution to occur thus maintaining the load carrying capacity of the structure even though it has been locally overloaded. A shear failure, in contrast, is undesirable in a concrete structure because of the sudden and catastrophic nature of the failure. The designer must recognize the possible modes of failure and insure that at ultimate loads the structure will behave in a ductile manner.

In many conventional applications of reinforced concrete slabs and shells, the design will be governed by flexural effects or deflection limitations. This is normally the case for slabs or shells supported on beams or walls that are subjected to distributed pressures. For this type of situation, the magnitude of the shear stresses is small relative to the flexural stresses. However, shear stresses can govern the design of slabs and shells when concentrated loads are present. Shear forces can also become critical when the span-to-depth ratio becomes relatively small and large amounts of flexural reinforcement are present.

Shear failures in a slab or shell can occur as a result of a failure across the width of the section (one-way action) or as the result of a local shear failure around a concentrated load

(two-way action). When the slab or shell fails by one-way action, it acts as a wide beam with the shear failure surface extending across the entire width. Failure in shear of a slab or shell by two-way action can be caused by a concentrated load when a shear failure surface develops around the perimeter of the load, i.e. the concentrated load "punches" through the slab or shell. Situations in which two-way shear action is critical can arise from: (1) the transfer of forces from slabs to columns, (2) the transfer of forces from columns to footings, and (3) when a concentrated load is applied to the slab or shell [36]. Both beam shear and punching shear must be evaluated to determine the shear strength of the slab or shell.

It should be noted that shear stress is normally computed by dividing the shear force on the critical section by the length and depth of that section. The resulting shear stress is a nominal stress. It is neither indicative of the actual shear stresses nor their distribution. Further, the nominal shear stress is particularly sensitive to the assumed location and shape of the critical section [37]. Nominal shear stresses are used to provide a reference stress when designing concrete members.

4.2 COMPARISON OF BEAM AND PUNCHING SHEAR

A reinforced concrete slab or shell resists shear forces in many ways analogous to that of a beam. After the formation of a crack, shear forces are carried by the following mechanisms, as shown in Figure 12 [39]:

1. shear resistance of the uncracked concrete or by the concrete lying beyond the inclined crack, V_{cz};
2. aggregate interlock (or interface frictional force transfer) across the inclined cracks, V_a;
3. dowel action of the longitudinal reinforcement crossing the inclined cracks, V_d;

4. contribution of any shear reinforcement present, V_s; and
5. possible arch action from membrane forces.

The mechanism of shear failure in a slab or shell is less well understood than that of shear failure in a beam. This is a result of the three-dimensional nature of shear in slabs and shells and the associated conceptual and observational complications. The developing shear failure mechanism in beams is comparatively easy to observe and identify, whereas in slabs and shells the inclined shear cracks initiate within the member and may not be visible on an exposed surface [37]. A complete understanding of the mechanism of shear failure in slabs and shells has yet to be achieved.

The nominal ultimate punching shear stress that can be developed is usually greater in a slab or shell than in a beam. Criswell and Hawkins [37] have attributed this difference to six factors:

1. Restricted inclined crack location - The inclined crack forming the failure surface is confined to the perimeter of the loaded area because the area resisting shear increases with the distance from the loaded area. Thus the crack is less free to develop at the weakest section than in a beam.
2. State of stress at the apex of the inclined crack - Bending moments in a slab create compressive stresses in the plane of the slab or shell, and the concentrated load causes local compressive stresses, resulting in a complex state of triaxial stress conditions. This favorable state of triaxial compressive stresses is often cited as the main reason higher ultimate shear stresses are obtainable in slabs and shells than in beams. A transition from slab to beam behavior will occur because of a diminished ability to resist these higher shear stresses as the size of the loaded area increases relative to the slab thickness.
3. Lack of symmetry - A lack of axial symmetry results in

variations in the loads for cracking and inelasticity to develop at different locations around the loaded area.

4. Distribution of moments - The relative magnitudes of the moments in a slab or shell vary with the pattern of cracking of the concrete and yielding of the reinforcing steel. This in turn affects the subsequent formation and opening of the inclined shear cracks.
5. Dowel forces - A greater number of bars will cross the shear failure surface in a slab than in a beam, and thus proportionately greater dowel forces may develop in slabs and shells than in beams.
6. Lack of a simple static analysis - Equilibrium requirements alone provide basic knowledge on the forces in a diagonally cracked beam. However, in a slab or shell a simple static analysis is inadequate for accurately predicting the forces. This is because a slab or shell can redistribute forces prior to failure. Further, the in-plane forces generated by restraints provided by the supports and non-yielding portions of the slab or shell cause complications not usually associated with the behavior of beams.

4.3 MECHANISM OF PUNCHING SHEAR

A concentrated load acting on a slab or shell can cause diagonal tension cracking around the perimeter of the loaded area leading to a punching shear failure in the slab or shell. The diagonal failure cracks form a truncated cone or pyramid shaped surface, depending on the shape of the loaded area. The cracks forming the failure surface extend from the edge of the concentrated load at the compressive surface of the slab to distances away of about one to two times the slab depth. When the cracks intersect the flexural reinforcement they may flatten out or even extend horizontally along the level of the steel. The angle of inclination of the truncated cone or pyramid with respect to the plane of the slab varies from 20^{o} to 45^{o}, depending on many

factors including the amount and nature of the reinforcement in the slab [38].

Drawing upon the discussion presented in a comprehensive report on the shear strength of reinforced concrete members by ASCE-ACI Committee 426 [40], a summary of the mechanism by which a punching shear failure occurs can be given as follows. The dominant crack patterns for an axisymmetric loading situation are shown in Figure 13. First, a roughly circular tangential crack forms around the perimeter of the loaded area due to negative bending moments in the radial direction. Radial cracks then form extending away from the loaded area. Because of the rapid rate at which the radial moment decreases with distance from the loaded area, significant increases in load are needed for further cracking to occur. Inclined cracks originating near middepth then form and intersect the radial cracks at right angles. The inclined cracks that form are not likely to be initiated by flexural cracks, and thus the characteristics of inclined cracks in slabs or shells is more similar to the web-shear rather than the flexure-shear cracks of beams[2]. The tangential stiffness of the slab surrounding the cracked region helps to control the opening of the diagonal tension cracks. This preserves the shear transfer by aggregate interlock at higher loads than would occur in beams.

Yielding of the slab or shell reinforcement may develop first at the perimeter of the loaded area because of the high radial

---

[2]Flexure-shear cracks are cracks that start as a flexural crack on the tension face of a beam, and then spread diagonally upward (under the influence of diagonal tension) toward the compression face. Web-shear cracks start in the web section of a beam due to high diagonal tension, then spread both upward and downward. Web-shear cracks in beams are rare except in beams with relatively thin web sections or heavy prestressing [38].

moments present. However, until general yielding of the slab reinforcement in the area of the concentrated load occurs, rotation at the inclined crack will be restrained by increased tangential moments. Thus, a punching shear failure will not normally occur until yielding of the reinforcement in both the radial and tangential direction has occurred. Yielding of the reinforcement, however, is not necessary for failure to occur, nor does yielding of the reinforcement necessarily result in a shear failure.

4.4 FACTORS AFFECTING PUNCHING SHEAR STRENGTH

Based on a review of existing literature on the subject [36-41], a discussion of the factors that influence the punching shear strength of slabs and shells is presented. The factors are listed in no particular order.

1. Concrete strength: The compressive strength of the concrete influences the punching shear strength because the tensile strength of the concrete is related to the compressive strength, and shear failures are controlled primarily by the concrete tensile strength. Current ACI code provisions assume that the nominal shear strength of the concrete is proportional to the square root of the compressive cylinder strength. However, recent research by Carino and Lew [42] has indicated that the current ACI formula for splitting tensile strength underestimates the actual splitting strength of concrete with high compressive strengths. Thus, if shear strength is correlated to the splitting tensile strength, then it is likely that current ACI formulas also underestimate the shear strength of high-strength concretes. However, other research conducted by Elstner and Hognestad [43] suggests just the opposite. The investigators found that equations dependent on the square root of the compressive strength predict too rapid an increase in shear strength with increasing f'_c. Hawkins, Criswell and Roll [41] concluded that the shear strength can be said to be dependent on

the square root of the compressive strength for compressive cylinder strengths less than 4000 psi (28 MPa); any application to higher strength concretes should be made with caution. The shear behavior of high-strength concretes is an area that requires further research.

2. Type of aggregate: Most shear studies have been performed using normal weight concrete. However, lightweight concrete is used extensively in construction because it reduces dead weight. The use of lightweight concrete generally lowers the shear strength because lightweight concrete has a lower splitting tensile strength than does normal weight concrete. Also, the use of lightweight aggregate in the concrete will result in less shear force being transferred through aggregate interlock than when normal weight aggregate is used.

Ivy, Ivey, and Buth [44] tested fourteen concrete slabs made with three different lightweight aggregates. Comparisons were made with previous work on normal weight concrete slabs, and existing and proposed design methods were evaluated. They recommended that the limiting stresses calculated for normal weight concretes be multiplied by 0.75 for all lightweight and 0.85 for sanded lightweight concretes. Results from this study are currently used in the ACI code. Hawkins, Criswell and Roll [41] have suggested that there appears to be no need to differentiate between all lightweight and sand-lightweight concretes, and that the shear strength of a lightweight concrete slab should be taken as 0.85 times the shear strength of a normal weight concrete slab (concrete compressive strengths being constant).

Compared with the data that have been collected on the shear behavior of normal weight concrete slabs, there is an inadequate amount of information on the shear behavior of lightweight concrete. Further, it appears that most of the work completed to date on the shear behavior of lightweight concrete slabs has been performed using moderate strength concrete (compressive cylinder

strengths of 5000 psi (34.5 MPa) or less). Because of the widespread use of lightweight and increasingly high-strength concrete, further research in this area is needed.

3. Amount of flexural reinforcement: Dowel forces develop as a result of the flexural reinforcement crossing the inclined shear cracks, and may be responsible for a larger percentage of the shear resistance in slabs than in beams. This is because of the shape of the failure surfaces, resulting in a larger number of bars crossing the failure surface in a slab than in a beam. Kinnunen [45] and Anis [46] concluded that dowel forces carry about 30 percent of the total shear in a slab. However, Moe [47] found that the contribution of dowel forces was insignificant. It would be reasonable to expect that an increase in the amount of flexural reinforcement would result in an increase in the shear force carried by dowel action. This was observed in tests by Elstner and Hognestad [43] in which the punching shear strength increased as the reinforcing ratio increased. However, dowel action is complex and not totally understood. Dowel action is influenced by the size and distribution of the flexural reinforcing bars, and the amount of concrete cover over the bars. In a recent study conducted by Brian Watt Associates Inc. [34] on the punching shear resistance of shells, the investigators found that an increase of 43 percent in the amount of flexural reinforcement resulted in only a 2 percent difference in shear capacity. Dowel action will be strongly influenced by the manner in which cracking of the slab or shell occurs, because dowel forces cannot be mobilized prior to some type of displacement that reacts against the dowel stiffness. This may be one of the main reasons why the percentage of the total shear force carried by dowel action varies from one experiment to another. Dowel forces will be very small prior to cracking, and if failure occurs soon after cracking commences, without any transverse displacements to mobilize the stiffness of the dowel bars, then dowel forces will also be small.

4. Thickness of the slab or shell: It has been observed that, in general, the relative strength of a structural element decreases as the size of the specimen increases. This phenomenon is commonly referred to as size effect. In conducting laboratory tests on scaled models of prototype structures, size effects may result in higher strengths being observed in the scaled models than in the prototype structures. In addition, test results that were successfully applied to typically dimensioned members may not be valid for applications to members with significantly increased dimensions.

Roll et al. [48] built 1/2.5-scale models of specimens tested by Moe [47] and Elstner and Hognestad [43] and found excellent agreement between the model and prototype shear strengths. Batchelor and Tissington [49] tested 1/6- to 1/15-scale models of a hypothetical prototype bridge deck and found no significant effect of scale on the punching strength of the slabs. However, Malhotra [50] found that the tensile strength, and therefore by extension possibly the shear strength, of concrete increased as the size of the specimen decreased. In experimental tests conducted at Delft University, Walraven [51] investigated the influence of depth on the shear strength of both normal- and lightweight concrete beams without shear reinforcement. He found that the nominal shear stress that developed at failure decreased approximately 45 percent in both the normal- and lightweight beams when the depth was increased from 0.1 m to 0.7 m (4 in. to 28 in.). Bazant [52] applied the theory of fracture mechanics to diagonal shear failures of concrete beams without shear reinforcement and concluded that significant size effects exist with increasing beam depth.

Size effects in the punching shear strength of slabs due to increased thickness have been reported by Kinnunen, Nylander and Tolf [53]. They found that the nominal punching shear strength decreased with increasing effective depth of the slab if the other parameters were kept constant. They reported a reduction

in shear strength of up to 10 percent for slabs with shear reinforcement and up to 40 percent for slabs without reinforcement when the depth of the slab was increased from 0.1 m to 0.62 m (4 in. to 24 in.). Several European codes specify reductions in allowable shear stresses with increasing thickness, but the current ACI code does not recognize any effect of concrete thickness.

5. Size of the loaded area relative to the slab thickness: The ability of a slab to resist higher shear stresses diminishes as the size of the loaded area increases relative to the slab thickness. Tests have shown that the rate of decrease is a function of the shape and size of the loaded area and the relative magnitude of the principal moments in the slab [37]. Moe [47] was the first to recognize that the ratio of the characteristic dimension, c, of the loaded area to the effective slab thickness, d, affected the shear strength. Moe examined test data for c/d ratios between 0.75 and 3.0 and proposed equations for predicting the punching shear strength of slabs with c/d ratios in this range. Moe recommended that a critical section for punching shear be assumed at a distance of d/2 away from the perimeter of the loaded area, resulting in the shear strength equations proposed by Moe becoming independent of the c/d ratio. Thus, the effect of the size of the loaded area relative to the thickness is addressed by Moe in an indirect manner. This work by Moe was used in the development of the provisions in the ACI code. For larger c/d ratios, these equations will overestimate the shear strength; new equations for predicting the punching shear strength of slabs with c/d ratios higher than 3.0 have been proposed [41]. Another problem that has been associated with high c/d ratios is the possibility of a flexurally-influenced shear failure, termed a flexural-shear failure, at lower loads than would be predicted based on punching shear considerations or flexural considerations alone [54].

6. Shape of the loaded area: The shape of the loaded area

affects the deformations that will develop in a loaded slab or shell. This in turn will influence the distribution of the shear forces around the loaded area. In general, for the same c/d ratios, slabs loaded by a circular area are stronger in shear than those loaded by a square area [40]. Vanderbilt [55] found that the shear strengths of slabs with circular columns were consistently higher than slabs with square columns, reaching a maximum of about 35 percent difference for a c/d ratio of 4. However, Nightingale [56] and Plisga [57] found that with a c/d ratio of 2.5 strengths for slabs with square columns were 16 percent higher than strengths for slabs with circular columns. The conflicting results are apparently because the shear strengths are influenced by the c/d ratio, the reinforcement pattern, and the method of support, all of which were not held constant in the tests [40].

There is, however, clear evidence that the limiting shear stress decreases with increasing rectangularity of the loaded area [40]. There are two reasons for this. In tests [58] in which the length of the column perimeter was held constant as the aspect ratio of the sides of the column were varied, the shear strength decreased because one-way bending became more predominant resulting in increasing beam shear action developing along the sides of the column. Criswell [54] notes that a second reason for a reduction in shear strength is that shear forces tend to concentrate at the corners of rectangular columns. Shear distress occurs at the corners before the column faces, and the failure is sequential resulting in the decrease in strength. He also notes that this effect decreases for very large or very small c/d ratios.

7. Interaction of shear and flexural effects: In a slab or shell subjected to a concentrated load, the critical sections for maximum moment and shear both coincide with the perimeter of the loaded area, resulting in an interaction between the shear and flexural forces. This makes it almost impossible to visually

classify the failure as being totally flexural or totally shear in nature. The effects of in-plane forces also complicate this classification. Hawkins [59] found that, in general, even lightly reinforced slabs eventually fail by punching unless shear reinforcement is provided well in excess of the amount needed to carry the shearing force at the theoretical ultimate flexural strength of the slab. The transition between a shear failure and the attainment of the ductilities normally associated with flexural failures is a gradual change as the flexural strength of the region is decreased [54]. While it is accepted that the shearing stress for failure decreases as the intensity of the flexural loading increases [40], this relationship has not been fully investigated. Moe [47] has proposed an interaction equation for slabs subjected to combined flexure and shear. However, Moe also notes that the shear failure mechanism need not always be related physically to the flexural failure mechanism.

8. Rate of loading: Criswell [60] tested duplicate sets of specimens, with one group being subjected to static loading and the other to dynamic loading. In specimens where the load was applied with a rise time of 20 to 40 milliseconds, an increase in strength of about 26 percent resulted for specimens failing in shear and an increase of about 18 percent resulted for specimens failing primarily in flexure when compared to static tests on similar specimens. Criswell attributed these increases in strength to the increase in material strength properties at the rapid strain rates of the dynamic loading. Investigations into the effect of the rate of loading on the punching shear strength have also been conducted for nuclear reactor structures subjected to impact loads. Some of these investigations are discussed in Section 5.2.

9. In-plane forces: Many investigators have recognized that both the flexural and shear strengths of slabs and shells are influenced by the presence of in-plane forces. Compressive in-

plane forces can significantly increase the strengths, while tensile in-plane forces may have the tendency to reduce the strengths. Compressive in-plane forces can be introduced into a slab or shell by lateral restraint provided by the supports or by the elastic portions of the structure surrounding the yielded region in the immediate vicinity of the concentrated load. The supports may be fixed against horizontal movement or they may provide partial restraint because of increased stiffness around the perimeter, as is the case for a slab with edge beams. In-plane forces may develop because of the geometry of the structure, such as in an arched shell, and can also be introduced by the presence of prestressing. While compressive in-plane forces can enhance the flexural and shear capacities of slabs and shells, the compressive forces also tend to reduce the ductility of the section and brittle failure modes may result.

For a slab subjected to a concentrated load and supported around its perimeter, outward displacements will occur with yielding of the slab surrounding the load. Since the region away from the yielded area will remain elastic, the displacements are restrained and axial forces develop. The elastic region surrounding the concentrated load acts as an external frame that will enhance the flexural and shear capacities of the slab [37]. The magnitude of the compressive forces that can develop will increase as the stiffness of the elastic region increases relative to the stiffness of the yielded region, and the magnitude of the forces will decrease as the reinforcing ratio increases [37]. Horizontal restraint provided by supports results in similar behavior.

Criswell and Hawkins [37] have suggested that the jamming action that occurs in slabs with horizontal restraint can be compared to the difficulty that is encountered in opening a pair of doors when the gap between them is insufficient. The mechanism by which restraining forces at the slab boundaries can result in compressive membrane (arch) action is illustrated in Figure 14.

Based on experimental results for uniformly loaded laterally restrained reinforced concrete slabs, Moll [61] obtained the typical deflection and restraining force versus load curves shown in Figure 15. Moll identified three distinct phases in the curves:

Phase A, Loading: Due to changes in geometry and cracking, the edges of the slab tend to move outward and as a result a compressive membrane force can develop.

Phase B, Unloading: At some point, the membrane force will begin to contribute to, rather than reduce, the deformation of the slab. Once this point is reached, the membrane force begins to decrease. In the results that Moll examined, he found that the transition from phase A to phase B occurs when the deflection is approximately equal to half the slab thickness.

Phase C, Reloading: After substantial deformations occur, the edges of the slab tend to move inward and a tensile membrane force may develop.

For unreinforced slabs, only phases A and B can occur.

The beneficial effect of lateral restraint provided by arching action in slabs increases with decreasing span-to-depth ratios. Brotchie and Holley [62] tested square slabs with different span-to-depth ratios and variable amounts of flexural steel. For slabs with lateral restraint provided at the supports, decreasing the span-to-depth ratio from 20 to 5 resulted in more arch action and significantly higher capacities. As the amount of flexural steel was increased, the improvement in capacities was less marked.

Taylor and Hayes [63] tested plain and reinforced slabs failing in punching shear. Two duplicate specimens were made of each test slab, one simply supported along the edge and the other similarly supported but confined horizontally within a steel frame. Three reinforcing ratios of 0.0, 1.57 and 3.14 percent and a variable loaded area were studied. Results of their tests are shown in Figure 16. They found that increases in the

punching shear capacity caused by the horizontal restraint were greater with smaller reinforcing ratios. The increase was 24-60 percent when the corresponding simply supported slabs were near flexural failure at collapse, but only 0-16 percent when the corresponding simply supported slabs were not near flexural failure at collapse.

Aoki and Seki [64] tested fourteen square slabs supported around the perimeter with edge beams of varying dimensions. The investigators found that arch action was more effective in slabs with high concrete compressive strength and lower steel ratios, however the magnitude of the arch action was difficult to measure. Their test results indicated that the flexural collapse load was 2.1 times that calculated without considering the membrane force, and improvements in shear capacity of up to 67 percent were measured. Equations for predicting the enhancement resulting from edge restraint are presented, however it has been noted by Hewitt and Batchelor [65] that the equations suggested by Aoki and Seki are valid only for the relative restraint provided by their configuration and should not be applied to other slab systems.

Tong and Batchelor [66] tested 1/15-scale models of a three span bridge subjected to concentrated loads. They proposed a method for predicting the ultimate capacity of the slabs taking into account the enhancement in strength due to compressive membrane action. They assumed that the compressive in-plane forces could be represented by a membrane moment which helped to carry the applied load. Their proposed method for including in-plane effects was applied to the tests conducted on the models of the bridge, and good correlation was obtained. The investigators concluded that recognizing the compressive membrane enhancement in slabs would result in significant savings in the reinforcement required for two-way bridge slabs. However, Masterson and Long [67] note that the particular approach suggested by Tong and Batchelor would not be widely applicable until further tests are

done on different slab configurations. Hewitt and Batchelor [65] have proposed an idealized rational model for predicting the punching strength of slabs with unknown restraints by extending the theory of Kinnunen and Nylander [68] (the basics of the theory suggested by Kinnunen and Nylander are discussed in Section 4.5). Hewitt and Batchelor suggested that it would be possible to evaluate limits on the range of the restraint effects and use this information for design purposes. However, they also note that more tests are needed.

Many investigators [69-71] have studied the effects of in-plane forces caused by prestressing on punching shear strength, with the level of prestressing in the tests varying from zero to as high as 650 psi. Both normal weight and lightweight concrete slabs subjected to prestress have been investigated. All investigators reported increases in punching shear strength resulting from the prestress, with the ultimate shear strength increasing approximately linearly with increasing prestress. ACI-ASCE Committee 423 [72] has recommended a lower bound expression, shown in Fig. 17, for predicting the punching shear strength of prestressed two-way slabs. This expression is included in the current ACI building code [32] and is discussed in more detail in Section 4.6.1 of this report.

An example of a structure in which tensile in-plane forces can develop is a reinforced concrete containment vessel when subjected to combined internal pressure and punching shear loads normal to the containment wall. Tensile in-plane forces may have the effect of reducing the capacity of a concrete slab section, but only a limited number of tests have been conducted. Researchers at the University of Maine [56,57] reported that tensile forces on uniformly loaded slabs supported by columns caused the measured loads for a general flexural failure to be about 20 percent less than the loads predicted using the moments for pure bending. Researchers at Cornell University [73,74] found that the punching shear capacity of slabs was only slightly

related to the level of biaxial tension. Johnson and Arnouti [75] also found that little reduction in shear strength occurred. The limited amount of work that has been done on the effects of tensile in-plane forces has not led to a comprehensive understanding of the relationship, and more work is needed.

It is clear from the research that has been conducted that compressive in-plane forces can enhance both the flexural and shear capacities of slabs and shells, particularly for low reinforcing ratios and high strength concrete. However, the magnitude of the in-plane forces, and thus the degree of enhancement, is difficult to calculate since it depends on the complex interaction of the slab, supports and the surrounding structure. More work is needed in this area before economies resulting from the enhancement can be realized.

4.5 PREDICTING PUNCHING SHEAR RESISTANCE

Many equations have been proposed for predicting the punching shear resistance of concrete slabs, and the strengths predicted by the different equations vary considerably. Criswell and Hawkins [37] provide a comprehensive review of the methods and equations that have been proposed. Two general design approaches have developed. The first approach is the use of primarily empirical equations suitable for codification to predict the punching strength, and the second is the development of an idealized model that will capture the dominant behavior of the punching shear mechanism.

Empirical equations that have been proposed can be classified into two broad groups, those in which the expressions are mainly dependent on the concrete strength and those in which the flexural strength or amount of flexural reinforcement is the main factor. A summary of the equations that have been proposed is given in Table 2. Development of the equations is discussed in Reference 37.

While most North American efforts have been directed towards empirical equations to fit test data that would be suitable for codification, the European approach has been to develop idealized models that will provide a realistic conceptualization of the mechanism of failure [37]. The most complete model for punching shear in a slab is that developed by Kinnunen and Nylander [68]. The basic model has been modified by Kinnunen [45] to include effects of dowel forces, and also by Anderson [85] to extend the model to slabs with shear reinforcement. The idealized axisymmetric model of the slab developed by Kinnunen and Nylander is shown in Figure 18. The slab outside the inclined crack is divided into sectors bounded by radial cracks, the perimeter of the slab, and the inclined crack. Each sector is assumed to rotate as a rigid body about the apex of the inclined crack and to be supported on an imaginary conical shell which is in turn supported on the column. Forces on each sector, except for the load and the reaction, are proportional to the rotation of the slab. The shear strength is calculated from the equilibrium conditions at failure, and collapse is assumed to occur when tangential compressive concrete strain under the root of the crack reaches limiting values obtained from tests. Hewitt and Batchelor [65] evaluated the model developed by Kinnunen and Nylander by comparing results of the model with previous tests.

They examined 137 slab tests reported in literature, and found a very good comparison of the test load and the theoretical load predicted by the Kinnunen and Nylander model. They also reported that the comparison was better than that obtained by evaluating the punching shear equations suggested by Moe [47].

A different approach in which the classical theory of plasticity is applied to the problem of shear in concrete structures has been suggested by Nielsen et al. [86] and Braestrup et al. [87,88]. To calculate the ultimate punching load, the external work done by the punching force is equated with the internal work

dissipated along the failure surface. The load found is an upper bound solution for the ultimate punching load. The concrete is assumed to behave as a rigid, perfectly plastic material with the modified Coulomb failure criterion as the yield condition and the deformations are governed by the associated flow rule (normality rule). These assumptions about the constitutive model for the concrete enable the strength and failure deformations of the concrete to be described by three parameters: the compressive strength, the tensile strength, and the angle of internal friction. Elastic deformations are neglected and unlimited ductility at failure occurs using these assumptions, resulting in a modification factor needing to be applied to the theory in order to obtain a better fit of the predicted strengths with test data. Also, for the theory to work, the tensile strength of the concrete is taken as essentially zero, a departure from realistic conditions. In comparisons of the proposed method with both punching shear tests and pull-out tests, a good prediction of the failure surface is obtained. However, different modification factors must be used with different test series in order to obtain a good fit of the theoretical strengths with the test strengths. Further, no method is suggested to account for variations in the amount of flexural and shear reinforcement.

4.6 CODE PROVISIONS ON PUNCHING SHEAR STRENGTH

A review and comparison is presented of the provisions for the punching shear resistance of slabs and shells in three major codes of practice for concrete design: the American ACI 318-83 code [32,33], the European CEB-FIP code [89], and the British Code of Practice CP110 [90]. In all the codes that are reviewed, the punching shear resistance is calculated as an allowable nominal shear stress multiplied by a specified critical surface. However, the provisions in the codes differ considerably in the value of the nominal shear stress that is to be used, and also in the definition of the critical surface. Treatment by the codes of the various factors discussed in Section 4.4 affecting the

punching shear resistance also differs.

4.6.1 ACI 318-83

The ACI code provisions for punching shear are based on equations that use the strength of the concrete as the primary variable. The amount of flexural reinforcement is not recognized as having an effect on the punching shear resistance. The shear strength, V_c, of nonprestressed slabs is [Reference 32, Section 11.11.2.1]:

$$V_c = (2 + 4/\beta_c)\sqrt{f'_c}\, b_o\, d \leq 4\sqrt{f'_c}\, b_o\, d \qquad (4\text{-}1)$$

where β_c = the ratio of the long side to the short side of the loaded area;

b_o = the perimeter of the critical section located at a distance of d/2 away from the perimeter of the loaded area (in);

f'_c = the compressive cylinder strength of the concrete (psi); and

d = the distance from the extreme compression fiber to the centroid of the tension reinforcement (in).

For two-way prestressed slabs, an alternate expression is given [Reference 32, Section 11.11.2.2]:

$$V_c = (3.5\sqrt{f'_c} + 0.3\, f_{pc})\, b_o\, d + V_p \qquad (4\text{-}2)$$

where f_{pc} = the average value of the compressive stress in the concrete (after allowance for all prestress loss) for the two directions (psi); the value shall not be less than 125 psi, nor taken as greater than 500 psi;

V_p = the vertical component of all effective prestress forces crossing the critical section; and

f'_c shall not be taken as greater than 5000 psi because of limited test data.

The ACI building code commentary [33] notes that the shear strength predicted by the equation for nonprestressed slabs corresponds to a diagonal tension failure of the concrete initiating at the critical section, while the second equation for two-way prestressed slabs predicts a punching shear failure of the concrete compression zone around the perimeter of the loaded area. Consequently, the code includes the term β_c only in the first equation for nonprestressed slabs.

To determine the punching shear resistance of slabs and shells made with lightweight aggregate concrete, the ACI code gives two alternative procedures that can be used to modify the shear strength as calculated by the equations discussed above. One method is based on laboratory tests which determine the relationship between the splitting tensile strength and the compressive strength for the particular lightweight concrete being used [Reference 32, Section 11.2.1.1]. As a simplification, a second method recommends the use of reduction factors which have been established based on the assumption that, for a given compressive strength of concrete, the tensile strength of lightweight concrete is a fixed proportion of the tensile strength of normal weight concrete [Reference 32, Section 11.2.1.2]. Specified reduction factors are 0.75 for all-lightweight concrete and 0.85 for sand-lightweight concrete. A summary of the ACI code equations and provisions is given in Table 3.

4.6.2 CEB-FIP

Punching shear provisions in the CEB-FIP model code include factors to account for the reduction in shear strength with increasing slab or shell thickness, the beneficial effect of higher amounts of flexural reinforcement, and the beneficial effect of axial compression, in addition to the usual term that

relates the concrete compressive strength to the shear strength. The shear strength, V_{Rd1}, of slabs without significant longitudinal forces is [Reference 89, Section 13.4.1]:

$$V_{Rd1} = 1.6 \tau_{Rd} K (1 + 50 \rho_{\ell}) u d \qquad (4\text{-}3)$$

where τ_{Rd} = the shear stress which is based on the cylinder compressive strength and is given in tables [MPa];

K = a depth factor, $K = 1.6 - d \geq 1.0$;

ρ_{ℓ} = the flexural reinforcement ratio, ≤ 0.008;

u = the perimeter of the critical section located at a distance of d/2 away from the loaded area (m); special provisions are given for loaded areas with aspect ratios greater than 2; and

d = the distance from the extreme compression fiber to the centroid of the tension reinforcement (m).

For members subjected to significant axial compression, including prestress, the shear strength obtained from the above equation may be increased by multiplication with the following factor [Reference 89, Section 11.1.2.2]:

$$\beta_1 = 1 + (M_o/M_{sdu}) \leq 2$$

where M_{sdu} = the maximum design moment in the shear region under consideration; and

M_o = the decompression moment for the section where M_{sdu} is acting.

For lightweight aggregate concrete, the above provisions apply except that the factor K is set equal to 1.0 independent of the value of d [Reference 89, Section 20.11.1]. Thus, for slabs with an effective depth greater than or equal to 0.6 m, no reduction

in the nominal punching strength is required by the code when lightweight aggregates are used. A summary of the provisions on punching shear of the CEB-FIP code is given in Table 3.

4.6.3 CP110

The British CP110 code also includes provisions to account for the reduction in shear strength with increasing slab thickness and for the beneficial effect of higher amounts of flexural reinforcement, in addition to relating the concrete compressive strength to the shear strength. However it differs from the ACI and CEB-FIP codes in two major ways. First, the concrete compressive strength is determined using compressive tests on cubes of concrete, whereas ACI and CEB-FIP use standard cylinders. The apparent strength of cubes is approximately 1.25 times higher than that of cylinders due to the state of stress that exists in a cube under compressive loading. The second major difference is that the critical perimeter is assumed to be located at a distance of 1.5 times the total thickness of the slab away from the perimeter of the loaded area, rather than at half the effective depth away as in the ACI and CEB-FIP codes. Part of the motivation for selecting this perimeter as the critical section is to enable both beam and two-way punching shear to be calulated using the same nominal shear stress values.

According to the British code, the shear strength, V, of slabs is given by [Reference 90, Section 3.4.5]:

$$V = v\, u_{crit}\, d \qquad (4\text{-}4)$$

where v = the nominal shear stress (N/mm^2) = $\varepsilon_o\, v_o$

ε_o = depth factor given in tables; a 20 percent increase in the shear capacity is permitted as the slab depth decreases from 300 mm to 150 mm;

v_o = the ultimate shear stress (N/mm^2), which

is determined from the characteristic concrete compressive strength and from the longitudinal tension reinforcement ratio and is given in tables;

u_{crit} = the perimeter of the critical section located at a distance of 1.5 h (h = the total thickness of the slab) away from the loaded area (mm);

d = the distance from the extreme compression fiber to the centroid of the tension reinforcement (mm).

Special provisions apply for prestressed slabs. For lightweight aggregate concrete the above equation applies except that the specified ultimate shear stresses are multiplied by 0.80 [Reference 90, Section 3.12.7]. The punching shear provisions of CP110 are summarized in Table 3.

4.6.4 COMPARISON OF THE CODES

Braestrup [87] performed a comparison of the various punching shear code provisions by making plots of the ratio of the predicted punching strength versus the calculated punching strength for four test series: Elstner and Hognestad [43], Kinnunen and Nylander [68], Taylor and Hayes [63] and Base [91]. The results of his comparison are shown in Figure 19. Braestrup noted that while the ACI 318-71, CEB-FIP, and British CP110 code were all rather conservative, the ACI and CEB-FIP were both, in general, more conservative than the CP110 code. Regan [92] examined the way various factors affecting punching shear strength are treated in the ACI 318-71 code and the British CP110 code. Regan showed that the relative strengths predicted by the two codes will vary depending on the specific parameters being studied. Under some circumstances the ACI code will be more conservative, while under others the CP110 code will be more conservative. However, he concludes that the treatment of

several of the factors is superior in the CP110 code.

Numerical comparisons of ACI, CEB-FIP, and CP110 punching shear provisions, for selected values of slab depth, flexural reinforcing ratio, and loaded area, as a function of concrete strength are shown in Figures 20 and 21. These comparisons are for nominal punching shear strength as material reduction factors have been included. It should be noted that the different load factors used by the various codes are not incorporated in the comparison. Since CP110 provisions are based on characteristic compressive strengths obtained from cube tests instead of the standard cylinder tests used by ACI and CEB-FIP, the approximate relationship that the cube strength is 1.25 times the cylinder strength was used to convert cube strengths to equivalent cylinder strengths. Based on an examination of the selected parameters, punching shear strengths predicted by the CEB-FIP model code are more conservative than those predicted by the ACI code, particularly for lower reinforcement ratios and thicker slabs. However, the CEB-FIP code becomes less conservative relative to the ACI code as the compressive strength of the concrete increases. The punching shear strengths predicted by the CP110 code for the selected parameters also tend to be more conservative than those predicted by the ACI code. However, the ACI code provisions become more conservative than the CP110 provisions for larger reinforcement ratios and thicker slabs. It is also interesting to note that, with increasing concrete strength, the CP110 code becomes more conservative relative to the ACI code, just the opposite of what was observed in the comparison of the ACI code and the CEB-FIP model code.

4.6.5 LIMITATIONS OF CODE PROVISIONS ON PUNCHING SHEAR

Current punching shear design provisions are based on data obtained from experimental and analytical studies of relatively thin and lightly reinforced members, such as building slabs, roof shells and footings. Although these provisions have been proven

to be adequate for conventional construction, their applicability to the design of thick, heavily reinforced, lightweight high-strength concrete offshore structures can be questioned for many reasons.

Failure modes in the thick, heavily reinforced walls of the offshore structures will involve both flexural and shear mechanisms, and design formulas will need to incorporate both effects. Such interaction formulas have been proposed for thick, prestressed nuclear reactor vessel end slabs subjected to pressure loadings and are discussed in Section 5.2.

Insufficient data exists concerning the shear strength behavior of high-strength concretes. Current ACI design formulas base the shear strength of the concrete on the square root of the compressive strength. This relationship was proposed before the widespread use of high-strength concrete and, as discussed previously, this relationship may not be valid at higher strengths. In addition, there is the question concerning the shear strength of high-strength concretes made with lightweight aggregates. It does not seem probable that the reduction factors specified for lightweight aggregates typically used in normal strength concretes will apply.

There will clearly be a beneficial effect if in-plane compressive forces are present. However, with the exception of the CEB-FIP model code, no provisions are made to take this into account in calculating the punching strength (other than for prestressed slabs). Further testing is needed to quantify what effect in-plane restraint will have in both slabs and shells in order to be able to take advantage of this beneficial effect in design.

The current ACI code does not recognize any effect on the punching shear strength of the amount of flexural reinforcement or the thickness of the slab or shell. Because of the large amounts of reinforcement that will be present in the walls of

Arctic offshore structures, and because of the very large relative thicknesses that will be used, it seems likely that neglecting these factors will be more significant in the design of concrete offshore structures than in the design of conventional concrete structures. A better understanding of shear transfer mechanisms in thick, heavily reinforced, possibly prestressed, lightweight high-strength concrete slabs and shells is essential.

5.0 RECENT RESEARCH IN PUNCHING SHEAR

5.1 PUNCHING SHEAR IN THICK SLABS

The punching shear behavior of thick concrete slabs was studied by Kinnunen, Nylander and Tolf [53] at the Royal Institute of Technology in Stockholm, Sweden. Static punching shear tests were performed on five rectangular concrete slabs supported on circular center columns. Both prestressed and nonprestressed slabs were investigated. The thicknesses of the test slabs were approximately those of typical full size bridge decks. The main objective of the investigation was to study the influence of slab thickness on the punching shear strength of slabs with and without shear reinforcement.

In the series conducted on nonprestressed slabs, three 0.73 m (29 in.) thick slabs reinforced with high-strength deformed bars were tested. Two of these slabs were provided with shear reinforcement in accordance with the Swedish concrete code. The results of these tests were compared with results obtained in a previous investigation conducted by Nylander and Sundquist [93] on similar but smaller scale slabs. When the punching failure loads were compared, it was found that the ratio between the measured and calculated failure load decreased as the effective slab thickness increased. For the slabs without shear reinforcement, the reduction in shear strength was 25 percent and 45 percent for effective slab depths of 0.2 m (8 in.) and 0.62 m (24 in.), respectively, than for an effective slab depth of 0.1 m (4 in.). For the slabs with shear reinforcement, the reduction in strength was considerably less, approximately 10 percent.

In the series conducted on prestressed slabs, two 0.55 m (22 in.) thick slabs with prestressing running in one direction were tested. The prestressing resulted in a mean compressive stress in the concrete of 5.36 MPa (777 psi) in the prestressed

direction. One of the prestressed slabs was provided with shear reinforcement in accordance with the Swedish concrete code. The results of these tests were also compared with results obtained in a previous investigation conducted by Nylander, Kinnunen and Ingvarsson [94] on similar but smaller scale prestressed slabs. For the prestressed slabs without shear reinforcement, the shear strength was 30 percent lower for an effective slab depth of 0.471 m (19 in.) than for an effective slab depth of 0.207 m (8 in.). For the prestressed slabs with shear reinforcement, the reduction in strength with the larger depth was only 5 percent.

To monitor the progression of shear cracks within the slabs, four vertical brass tubes, with a diameter of 10 mm (0.40 in.) and a wall thickness of 1 mm (0.04 in.), were placed in each specimen at a distance of half the effective slab depth away from the periphery of the column on each of the four major axes. The brass tubes were smooth and equipped with anchor plates at each end, and strain gages were mounted at the midheight of the tubes. In the slabs with shear reinforcement, gages were placed on the shear reinforcement at the middepth of the slab. Close agreement was observed between the predictions of crack progression based on results obtained from gages on the tubes and the predictions based on results obtained from gages on the shear reinforcement. It was observed that the load level at which shear cracking first occurred was approximately the same for the shear-reinforced slabs as for the slabs without shear reinforcement. However, the load at which failure occurred was greater relative to the first cracking load in the slabs with shear reinforcement. In the prestressed slabs, the load level at which shear cracking first occurred was higher than that in the nonprestressed slabs, and also the first cracking load was closer to the ultimate load. It was also noted by the investigators that shear cracking did not develop uniformly around the column, but rather cracking progressed around the column as the load increased.

The shape of the shear cracks was examined after failure. The angle of the failure surfaces with respect to the plane of the slab varied from 29° to 42° in the nonprestressed slabs, although in some cases it was noted that the cracks followed along the flexural reinforcement layer towards the periphery. The flatter cracks were observed in the slab without shear reinforcement. In the prestressed slabs, the crack inclinations were strongly influenced by the presence of prestress. Shear cracks that formed perpendicular to the direction of prestressing were very steep, developing at approximately an angle of 45°. In contrast, shear cracks that developed in the prestressed direction were very flat, ranging from 14° to 18°. In none of the tests on prestressed slabs did the shear cracks parallel to the prestressing direction penetrate through the thickness of the slab.

Based on this study, the investigators concluded that size effect has a significant influence on punching shear strength and must be considered when evaluating the results of model tests and drawing conclusions about prototype behavior. They also concluded that size effect is highly decreased if the slab is provided with shear reinforcement. The results of this investigation and the previous investigations on thinner slabs were incorporated into the Swedish code for concrete structures, BBK 79, and the CEB-FIP Model Code for Concrete Structures, by introducing a depth factor into the punching shear design equations.

5.2 PUNCHING SHEAR IN NUCLEAR REACTOR STRUCTURES

The behavior of nuclear reactor containment structures under extreme load has been studied extensively in the last 20 years. Thick, heavily reinforced and prestressed concrete walls are normally used in the construction of the containment vessels. Many experimental and analytical investigations have been carried out in order to obtain a better understanding of the complex

failure mechanisms that can occur in these vessels. Punching shear failures may occur in a reactor structure in at least two ways: (1) the punching out, under internal pressure, of the end caps on the reactor vessel, and (2) the local punching failure of the reactor walls under impact of missiles (projectiles). A review of some of the investigations conducted in this area is presented.

5.2.1 REACTOR VESSEL END SLABS UNDER PRESSURE LOADING

The configuration of a prestressed concrete reactor vessel (PCRV) is typically that of a cylindrical barrel with flat end slabs. The behavior of the barrel section under pressure loading is relatively well defined, however the behavior of the PCRV end slabs is more complex [95]. The end slabs are significantly thicker than would be encountered in conventional slab construction, with span-to-depth ratios typically in the range of 2 to 3.5 [96]. Under internal pressure, the end slabs are subjected to high flexural and shear stresses. Although flexural failures in PCRV end slabs have been reported in model investigations conducted at the University of Illinois [97], most end slabs of conventional design would fail in shear [96].

Observed modes of failure in PCRV end slabs are similar to the shear failures occurring in slabs at column intersections. Cracking occurs first in the negative moment region near the connection of the end slab to the barrel section and in the postive moment region on the exterior surface of the end slab opposite the applied load, as shown in Figure 22 [98]. As loading progresses, the radial cracks spread toward the edge of the slab and a compression zone develops due to flexural distortion. At some point an inclined tensile crack forms near the middepth of the end slab at approximately 45 degrees. This inclined crack propagates outward to the unloaded surface of the slab and inward to the compression zone. Thus the load is resisted by a dome carved out of the end slab, as shown in Figure

22. This dome will fail by shear-compression (failure of the compression zone) or by punching shear when a plug of concrete in the form of a truncated cone is extruded [95].

A study of the behavior of 20 model PCRV end slabs was conducted by Langan and Garas at Taylor Woodrow Construction Ltd. [96]. Some of the conclusions from their study may be relevant to punching shear in offshore structures. An increase in the thickness in relation to the span had the effect of increasing the shear strength in the end slabs. Reducing the span-to-depth ratio from 2.5 to 2.0 in otherwise identical models increased the shear strength by 20 percent. The effect of concrete strength on the shear strength was examined in similar models where the compressive cylinder strength of the concrete varied from 3000 to 8000 psi (20.7 to 55.2 MPa). The ultimate shear strength was found to be approximately proportional to the square root of the compressive strength for the range of concrete strengths tested. The presence of hoop prestress provided lateral restraint which resulted in an increase in the ultimate shear strength, but the rate of increase in shear strength progressively fell. Beyond a prestress level of 1200 psi (8.3 MPa), the restraint provided had no significant effect on the shear strength. The investigators noted that while restraint provided by the supports will have a beneficial effect on the shear strength, beyond a certain level the beneficial effects will be negligible, as they found in the slabs with hoop prestressing. The researchers concluded that the contribution of dowel effects is very small in slabs of this nature when subjected to punching shear.

The researchers developed an empirical equation for predicting the shear capacity of end slabs, taking into account the effect of lateral prestress, depth-to-span ratio and the strength of the concrete:

$$P = 77\ d/D\sqrt{f'_c} + 10\ \sqrt{1 - D/\Phi}\ \sqrt{f_h} \qquad (5\text{-}1)$$

where P = the pressure resulting in failure, psi;
d = the depth of the end slab;
D = the diameter of the loaded area;
f'_c = the compressive cylinder strength, psi;
Φ = the total diameter of the end slab; and
f_h = the average compressive stress from the lateral prestress, psi.

The researchers noted that this equation is based on a limited number of tests on a specific structural configuration, and additional data is needed before a more generally applicable expression can be developed.

Cheung, Gotschall and Liu [95] examined results from 69 model tests on PCRV end slabs in which the effects of major parameters on the ultimate strength were investigated. Recognizing the similarity of the failure mechanism in end slabs to that of the shear failure that can occur at slab and column intersections, and drawing upon previous investigations on slabs, notably that of Elstner and Hognestad [99] and Moe [47], Cheung et al. developed a shear-flexure interaction expression for end slabs. The proposed interaction expression was based on yield line theory and had the following general expression:

$$\frac{P}{P_S} + C\,\frac{P}{P_F} = 1 \qquad (5\text{-}2)$$

where P = the failure load = $\pi R^2 \sigma_g$;
P_S = the ultimate shear load = $K\ 2\pi R\ D\sqrt{f'_c}$;
P_F = the ultimate flexural load = $\pi R^2 \sigma_F$;
R = the radius of the critical section;
D = the depth of the head (end slab);
σ_g = the failure pressure of the head;
σ_F = the pressure corresponding to the flexural failure of the head; and
C,K = constants which are determined by minimizing the

standard deviation between theoretical and experimental results.

By substituting the values of P, P_s and P_F into the equation and solving for σ_g, the following expression was obtained for the failure pressure of the head:

$$\sigma_g = \frac{2\ K\ D\sqrt{f'_c}}{R + \frac{C\ 2\ K\ D\sqrt{f'_c}}{\sigma_F}} \qquad (5\text{-}3)$$

The constants K and C were determined for end slab designs of practical interest and then modified to take into account the contribution of bonded reinforcement, the effects of compression in the concrete, and the strain capacity of the prestressing elements. As a result, the following equation for predicting the ultimate strength of end slabs was obtained:

$$\sigma_g = \frac{70\ D\sqrt{f'_c}}{R + \frac{60\ D\sqrt{f'_c}}{\sigma_F}} \qquad (5\text{-}4)$$

A comparison of the proposed shear-flexure interaction equation (equation 5-4) with experimental results is shown in Figure 23. While Arctic offshore structures will not have as high span-to-depth ratios as the PCRV end slabs, the procedure used in the development of the shear-flexure expression may be useful in developing a similar expression for Arctic structures.

5.2.2 IMPACT LOADING ON NUCLEAR REACTOR CONTAINMENT STRUCTURES

Under hypothetical accident conditions, a nuclear power plant may be subjected to impact loads from high velocity missiles, such as turbine blades, aircraft and free falling weights. The impact

loads are of a very short duration, 10 to 400 milliseconds, and may have impact velocities of as high as 1500 fps (450 mps). Protection against a punching type of failure due to these impacts is an important consideration in nuclear power plant design, and considerable effort has been made to develop impact design criteria for nuclear reactor containment structures.

Experimental programs [100-119] have been conducted to study the failure mechanisms due to impact loads, obtain load-time functions of missile penetrations, establish performance criteria, and develop design formulas to predict the capacity of the reactor structures under impact loads. Both full- and small-scale model tests have been performed, and in most cases satisfactory agreement was obtained between the model and full-scale tests when careful attention was given to the modeling requirements. The investigations found that the high velocity impact of a missile on a reinforced concrete slab or shell was a localized phenomenon as large deformations and damage occurred only in the immediate zone of the impact.

Several factors limit the applicability of these experimental results to offshore structures. First, the loading conditions and the structural response of the reactor structures when subjected to impact loads are dynamic. A considerable increase in punching strength occurs due to the increased strain rate [116], with the increase in strength with increasing rate of loading possibly being described by a power law function [101]. These results would not be applicable to offshore structures subjected to long duration impact loads by slowly moving ice masses. A second factor limiting the applicability of the reactor structure results is that the ultimate state behavior of the specimens in the tests was highly sensitive to the loading conditions selected for use in the experiments. The material used to model the missile (deformable, hard or semi-hard), the size and shape of the missile, and the impact velocity used in the tests all strongly influenced the behavior, resulting in wide

variation and often conflicting results being reported.

Analytical studies have been performed in an attempty to predict the behavior of reactor structures to impact loads [120-133]. These analytical studies have been conducted both in conjunction with and separate from the previously discussed experimental studies. The analytical models used were based on finite difference and, more commonly, finite element methods. The models typically incorporate geometric or material nonlinearities or both, as well as various failure criteria for the concrete and steel. The techniques used to study the behavior of the reactor structures under impact, particularly the techniques for simulating the nonlinear response of the reinforced concrete structures, are of interest and may be applicable to offshore structures under ice loading.

5.3 FIBER REINFORCED CONCRETE SUBJECTED TO PUNCHING AND IMPACT LOADS

The use of steel fiber reinforcement in a concrete structure can significantly improve the performance of the structure under loads. In fiber reinforced concrete, cracks can propagate only by stretching and debonding the fibers. As a result, large amounts of energy must be input to the structure before a complete fracture of the composite material can occur. Tests have shown that the toughness of fiber reinforced concrete can be an order of magnitude higher than that of plain concrete [134,135]. Kormeling [136] found that the increased energy-absorbing characteristics of fiber reinforced concrete is present over a wide range of temperatures. The greater ductility exhibited by fiber reinforced concrete can result in a greater level of safety in a structure by increasing the structure's capacity for internal redistribution of forces when overloaded. Fiber reinforcement can also prevent the total disintegration and shattering of concrete that is often associated with impact loads. In marine environments, fiber reinforced concrete

structures may be advantageous because of their high resistance to crack formation, fatigue and seawater corrosion, and also their improved freeze-thaw and abrasion characteristics [137,138]. A guideline for specifying, mixing, placing and finishing fiber reinforced concrete has been developed by ACI Committee 544 [139].

Swamy and Ali [140] investigated the behavior of reinforced slab-column connections made with steel fiber concrete and subjected to static loadings. The addition of steel fibers delayed the formation of diagonal cracks within the slab, reduced deformations at all stages (particularly after initial cracking), and transformed brittle-type shear failures into gradual and ductile shear failures and in some instances into flexural failures. The addition of fibers also increased the ultimate punching shear capacity. As the volume of fiber reinforcement was changed from 0.6 to 1.2 percent, the ultimate punching load increased from 23 to 46 percent with respect to an unreinforced slab.

Walraven [141] conducted a series of tests to determine if steel fibers were suitable as a substitute for traditional punching shear reinforcement. The tests were carried out on circular slabs supported along the edge and loaded in the center. Both normal weight and lightweight concrete specimens were included in the test series. The amount of steel fibers added to the slabs ranged from 0 to 1 percent by volume. Walraven found that the addition of steel fibers increased the ultimate punching capacity of both the normal weight and lightweight slabs, with the increase being more pronounced in the specimens made with lightweight concrete. The increase was found to be approximately proportional to the increase of the concrete strength measured on the control specimens. In addition to the increased punching resistance, the use of steel fibers also considerably enhanced the post-failure behavior of the slabs.

The behavior of reinforced and prestressed slabs made with steel fiber reinforced concrete and subject to impact loadings also shows significant improvements over the behavior of slabs made with conventional reinforced concrete [134,142-145]. In some of the tests, the addition of fibers increased the tensile strength of the concrete sufficiently to prevent a punching type of failure without the addition of shear reinforcement. Impact tests were conducted on lightweight concrete specimens and increased strength and impact resistance were reported [134,146]. Arockiasamy et al. [137,147] conducted impact tests on normal and fiber reinforced cylindrical panels representative of offshore structures and found that the fiber reinforced concrete panels were 1.65 to 1.70 times stronger than those of normal reinforced concrete. The investigators also developed a three-dimensional nonlinear finite element program to predict the behavior of the fiber reinforced panels. Nonlinear material properties for the fiber reinforced concrete were determined by testing fiber reinforced concrete cylinders.

Gerwick, Litton and Reimer [148] have suggested that the use of steel fibers in practical proportions for the reinforcement of offshore structures will not result in adequate ultimate capacity for the extreme ice loading conditions associated with the Arctic. However, steel fibers may be added to the structure to supplement the conventional reinforcement, resulting in improved performance of the structure and reduced amounts of conventional reinforcement, particularly shear reinforcement. Combining fiber and conventional reinforcement may offer significant advantages over the use of either type of reinforcement alone [140].

5.4 PUNCHING SHEAR IN OFFSHORE STRUCTURES

Only a limited amount of research has been performed to date on the punching shear behavior of thick slabs and shells that are representative of offshore structures. Further, results from many of the investigations that have been conducted are currently

proprietary information. The experimental study by Brian Watt Associates, Inc. (BWA) [34] represents the only major investigation into the punching shear resistance of offshore structures for the Arctic in which results are currently in the public domain. Because of the significance of this investigation with respect to the current study of punching shear in lightweight concrete offshore structures for the Arctic, the BWA investigation is reviewed in depth. Much of the other work that has been conducted to date has been directed primarily towards the behavior of North Sea offshore structures subject to ship collisions. Colbjornsen and Lenschow [149] studied punching shear in models representative of Norwegian North Sea structures, and their report is reviewed in some detail. Some other work on punching shear in North Sea structures is also briefly reviewed.

5.4.1 BWA PUNCHING SHEAR STUDY

The punching shear resistance of thick slab and shell sections representative of Arctic offshore structures was investigated by Brian Watt Associates, Inc. (BWA) [34]. The project is listed by the Alaska Oil and Gas Association (AOGA) as Project No. 152, and was undertaken on the behalf of eight oil companies.

Ten model specimens were subjected to punching loads: one slab, one arch and eight cylindrical shells. All of the specimens were supported along two opposite edges and a concentrated load was applied at the center of the specimens. The general dimensions and loading arrangements for a typical specimen are shown in Figure 24. The main variables investigated in the study as having a possible effect on the punching resistance were:

1. flexural reinforcement ratios;
2. shear reinforcement ratios;
3. ratio of shell radius-to-thickness (R/t); and
4. cyclic loading.

The investigators identified radius-to-thickness ratios in the range of 16 to 42 as being representative of proposed concrete structures for the Arctic. For the shell specimens, two radius-to-thickness ratios of 12 and 36 were selected as being reasonably representative. Specimens with these ratios would also be expected to respond differently to the punching loads because of the significantly different moment-to-thrust ratios that would develop in each. Five of the shell specimens were cast with radius-to-thickness ratios of 12 and three shell specimens were cast with radius-to-thickness ratios of 36. One of the shell specimens was subjected to cyclic loading.

The concrete used in the study had an average cylinder compressive strength at 28 days of 7000 psi (48 MPa), and in none of the specimens did the strength vary from this value by more than 7 percent. Regular weight aggregate with a maximum size of 0.4 in. (10 mm) was used which resulted in an average density of the concrete of 146 pcf (22.9 kN/m^3). Even though air entrainment is expected to be used for concrete structures in the Arctic because of the resulting improved freeze-thaw characteristics, air entrainment was not used in the model concrete because of an adverse interaction with a superplasticizer being used in the model concrete mix to provide needed flow characteristics.

Two flexural reinforcing ratios of 2.33 percent and 1.67 percent were used in the test specimens, with all but one specimen having a ratio of 2.33 percent. These reinforcing ratios represented the amount of flexural steel on each face and in each direction. These ratios were selected as being representative of the level of flexural reinforcement likely to be used in offshore structures of this type. The average yield strength of the bars used in the models was 75 ksi (518 MPa).

Determining the effect of different amounts of shear

reinforcement on punching shear resistance was one of the main objectives of the test program. Three shear reinforcing ratios were investigated: 0, 0.22 and 0.49 percent. Shear reinforcement was provided in the specimens using conventional shear stirrups. The yield strength of the shear reinforcement actually used in the test program was substantially higher than the targeted yield strength of 40 ksi (276 MPa). The shear reinforcement used in the models had yield strengths of 53 ksi (366 MPa) and 106 ksi (731 MPa), depending on the size of bar being used to provide the shear reinforcement. To account for the difference in yield strength, an effective shear reinforcement ratio was used in all calculations. The effective shear reinforcement ratio was defined as the actual shear reinforcement ratio multiplied by the ratio of the actual yield strength to 40 ksi (276 MPa).

The radius-to-thickness ratios of the shell specimens, the rebar size and spacing, and the material strengths were prescribed in order to be representive of those proposed for Arctic structures. The thickness of the specimens was chosen as 6 in. (15 mm) in order to allow normal concrete to be used instead of microconcrete. The investigators noted that this thickness would probably allow for a good representation of aggregate interlock, dowel effects, etc. A span length and transverse length of 7.5 ft (2.3 m) were selected for the slab and shell specimens in order to eliminate any support and edge effects on the stresses and deflections in the vicinity around the applied load. However, these conclusions were based on linear elastic analyses and were therefore valid only in the linear elastic response range of the specimens. Upon completion of the tests, the investigators observed that the amount of support rotations and displacements was not constant from specimen to specimen, and they noted that this may have had an effect on the behavior of some of the specimens. It is not clear that the investigators attempted to satisfy modeling similitude requirements in choosing the thickness, span and transverse dimension, and perhaps other

parameters used in their study. Further, the span-to-depth ratio of their specimens was 15, which may be unrepresentatively high for proposed Arctic offshore structures.

The investigators recognized that it would not be possible in the test program to duplicate the actual distribution of ice contact pressures. Therefore they decided to apply the loads on the models as a uniform pressure acting over a circularly-shaped area. This method of applying the loads was chosen as being the most reasonable loading that could be practically achieved in the model investigation. This type of loading is also advantageous in that a uniform pressure is easily applied to a structure in an analytical model.

Conventional means of applying the loads through a stiff platen were rejected by the researchers since this would have resulted in stress concentrations around the edge of the platen. The loading system shown in Figure 25 was developed to apply a nearly uniform distribution of pressure on the specimens. Load is applied through a steel piston acting on a layer of natural rubber constrained by a steel cylinder. Under pressure, the rubber will flow, closely simulating fluid behavior. Extrusion of the rubber is prevented by leather discs. Friction between the rubber and cylinder is limited by applying silicon grease along this interface. A somewhat similar loading system was used in punching tests on PCRV end slabs conducted by Langan and Garas [96].

In selecting the area of loading to be used in the test program, it was desired that the applied pressure on the specimens at failure be representative of the ice contact pressures that might be experienced by structures in the Arctic, i.e. pressures in the range of 2000 to 2500 psi (13.8 to 17.3 MPa). Using this range for the applied pressures and estimating the nominal shear stress that might be expected to develop in the specimens at failure, the investigators selected a load diameter of 18 in. (0.46 m) for

the shell specimens. Recognizing that the flexural capacity of the slab specimen would be less than that for the shell specimens, a load diameter of 6 in. (0.15 m) was chosen for the slab specimen in order to prevent a premature bending failure of the specimen before a punching failure could develop.

A special test rig was designed and built for testing the specimens. Steel end beams were used to transfer the reaction loads from the specimens into a prestressed concrete base. A cementitious grout was injected into the interface between the shell specimens and the steel support beams. This reportedly produced a fixed support condition, although it is more likely that the actual support condition was somewhere between fully fixed and pinned. The supported edges of the slab specimen were held down by beams which were prestressed to the test rig and which also provided support conditions somewhere between perfectly fixed and pinned.

To try to insure that a punching failure rather than a flexural failure developed first, both the shear and flexural capacities of the specimens were calculated prior to the beginning of the testing program. To determine the flexural capacity, a method was developed to account for force redistribution in the slab and shells by averaging the moments obtained from elastic analyses. In the test on the slab specimen, the load which resulted in failure was much higher than the predicted flexural load capacity of the slab. However, even though yielding of the flexural steel did occur, the slab failed in punching and not in flexure, indicating that the approximate method developed for predicting flexural capacity was conservative.

As a means to predict, and also to later evaluate, the punching shear performance of the specimens, the shear provisions of four codes were examined:

- ACI 318-77 (American) [30]

- CEB-FIP Model Code (European) [89]
- CP110 (British) [90]
- DnV Rules (Norwegian) [150]

Three approaches were used in calculating the punching shear resistance of the specimens. In the first approach, the shear resistance was calculated using the conventional punching shear provisions in the four codes. The ACI and CP110 codes do not account for any beneficial effects due to compressive inplane forces (other than for prestressed slabs, see the discussion in Section 4.6). The CEB-FIP code does contain provisions to account for membrane compression. The ACI, CEB-FIP and CP110 codes severely limit the maximum permitted shear stresses. The DnV code does not distinguish between slabs and other elements.

Recognizing that compressive inplane forces would have a significant effect on the punching resistance of the shell specimens, the investigators considered a "modified punching shear method" as a second approach. Slab provisions on punching shear recommended by the codes were used but beam provisions on membrane compression effects were incorporated. In addition, the higher limits allowed for beams were used for the maximum permissible shear stresses. A third approach using beam provisions on a critical section at a distance of the effective depth of the specimen away from the perimeter of the load was also considered.

The slab and all shell specimens failed in punching shear when subjected to the local loading. Cracking of the specimens primarily occurred only in the vicinity around the load. Observed crack inclinations in the failed specimens ranged from 24^{o} to 53^{o} with respect to the plane of the specimen, the flatter crack inclinations occurring in the transverse direction of the specimens. Failure in the specimens was relatively ductile in that there was no significant sudden loss of load and the specimens were capable of sustaining at least 60 percent of the

ultimate capacity at deformations substantially greater than those at the ultimate loads. This was true even for the case of the shell specimen with no shear reinforcement.

The nominal shear stresses at failure in the test specimens, defined on a critical section at a distance equal to half the effective depth away from the edge of the loaded area, were:

$v_u = 13.5\sqrt{f'_c}$ slab;
$v_u = (11.0 \text{ to } 14.0)\sqrt{f'_c}$ shells with R/t = 36; and
$v_u = (15.0 \text{ to } 18.0)\sqrt{f'_c}$ shells with R/t = 12.

These nominal shear stresses are considerably higher than the upper limits on shear stresses allowed by the four codes examined. It is worth pointing out that the nominal shear stresses that will develop will be influenced by the size of the loaded area relative to the thickness (see Section 4.4). Thus, it may not be appropriate to compare the slab failure stresses, obtained with a load diameter of 6 in. (0.15 m), to the shell failure stresses, obtained with a load diameter of 18 in. (0.46 m).

Shear cracking initiated in the specimens when the nominal shear stresses, defined on a critical section at a distance equal to half the effective depth of the specimen away from the perimeter of the loaded area, reached the following levels:

$v_{cr} = (3.5 \text{ to } 5.0)\sqrt{f'_c}$ slab, shells with R/t = 36; and
$v_{cr} = (9.0 \text{ to } 10.5)\sqrt{f'_c}$ shells with R/t = 12.

The reason that the load at which shear cracks first occurred is higher in the shell specimens with greater curvature is due to the higher levels of membrane compression generated in these shells.

Approximately 78 to 89 percent of the ultimate shear capacity of

the shear reinforced specimens was found to be provided by the concrete. The remaining 11 to 22 percent of the ultimate capacity was carried by the shear reinforcement. Increasing the amount of shear reinforcement had a greater effect on the shallower shells. Average gains in the ultimate punching strength of 6 percent and 12 percent were realized for every 0.001 increase in the shear reinforcement ratio for the shell specimens with radius-to-thickness ratios of 12 and 36, respectively. The effect of increasing the amount of shear reinforcement on the ultimate capacity is shown in Figure 26. Increasing the shear reinforcement ratio also resulted in an increase in the load at which shear cracking first occurred.

Two identical shell specimens were tested except that one shell had 43 percent more flexural reinforcement than the other. No significant difference in ultimate capacity or general failure mode was observed in the tests on the two specimens.

The specimen subjected to cyclic loading underwent 100 cycles of loading at different load levels prior to progressing to failure. When the cycled loads were below that which caused the initiation of shear cracking, no significant difference in performance was observed from the specimen loaded to a similar load level monotonically. However, when the load cycles extended above the level at which shear cracking initiated, progressive development of the shear cracks occurred with each cycle. This would be expected to result in a degradation of the shear capacity. However, the specimen subjected to the cyclic loads failed at a higher load than did the comparable specimen loaded monotonically, suggesting that further tests on the effects of cyclic loading are needed.

The investigators found that the conventional punching shear provisions of all four codes examined were highly conservative in predicting the capacity of the test specimens. This was particularly true for the ACI code provisions where the measured-

to-predicted capacity ratios were between 3.3 and 6.5. Comparisons of the test results with the predicted capacities are shown in Figures 27 and 28. Use of the modified punching shear method suggested by the investigators, which allows for membrane compression effects, resulted in closer agreement between the measured and predicted capacities. The "ACI Modified Punching Shear Method" resulted in measured-to-predicted capacity ratios between 2.01 and 2.26 (see Figure 29). Punching shear resistances predicted using the beam shear provisions in the codes resulted in the closest agreement with the measured resistances, however the investigators suggested that use of this third method to predict the punching shear capacity may not provide an adequate factor of safety for design. Based on the limited number of tests conducted, the investigators recommended their suggested "ACI Modified Punching Shear Method" as being the most appropriate for designing Arctic offshore structures to resist punching shear.

A conclusion of the BWA study was that linear elastic analyses could be used to adequately predict the ultimate punching shear capacities of the slab and shell sections of offshore structures. However, large safety factors would have to be used in the design in order for this analysis tool to be used with any measure of confidence. Further, results from the investigation point out the inability of the elastic analysis techniques to describe the ultimate state response of the slab and shell specimens when subjected to punching loads.

Upon the completion of their testing program, the investigators identified several areas where further work was needed in order to improve the understanding of shear behavior in arctic offshore structures. These include investigations into:

- the effect of support flexibility on punching shear resistance;
- the strength of repaired members;

- the use of lightweight concrete in the models;
- the effect of longitudinal prestressing;
- the use of headed stirrups for shear reinforcement as rebar congestion with conventional stirrups is a problem; and
- improved analytical methods.

The first two areas that were identified have been investigated under AOGA Project Nos. 152 and 198, the results of which are not yet publicly available. The remaining four areas identified are being addressed by the current research project at the National Bureau of Standards on the punching resistance of lightweight slabs and shells.

5.4.2 PUNCHING IN PRESTRESSED CYLINDRICAL SHELLS: NORWEGIAN WORK

A study was undertaken in Norway to investigate the behavior of marine structures in the North Sea subjected to punching loads resulting from ship collisions [149]. Six 1/10-scale models of cylindrical shells representative of the Condeep structures were tested. The shell models contained conventional reinforcement and were prestressed in the longitudinal direction. To approximate continuity conditions, an edge beam was cast onto each end of the shell specimens. The general geometry and dimensions of the test specimens are shown in Figure 30.

The variables selected for study in the investigation were the size and shape of the loaded area. Two specimens were tested with applied load areas of 5 cm X 5 cm (2 in. X 2 in.), two with areas of 5 cm X 15 cm (2 in. X 6 in.), and two with areas of 5 cm X 25 cm (2 in. X 10 in.). For the tests on specimens with rectangular load areas, the direction of the long dimension of the load was alternated in the two tests between the circular and longitudinal direction. Steel plates were used to apply the loads to the specimens, with a layer of plaster being placed

between the specimens and the steel plate.

The concrete used in the specimens had an average cube strength of 38.8 MPa (5600 psi), corresponding to an approximate compressive cylinder strength of 31 MPa (4500 psi). Mild steel flexural reinforcement was provided in both directions and on both faces, with flexural reinforcing ratios of 3.14 percent in the circumferential direction and 2.00 percent in the longitudinal direction (the reinforcing ratios being based on the total area of steel in both faces). The flexural reinforcement consisted of 6 mm (0.24 in.) diameter bars with a yield strength of approximately 410 MPa (60 ksi). No shear reinforcement was provided in any of the test specimens. Prestressing was provided in the longitudinal direction resulting in an effective centroidal prestress in that direction of 7 MPa (1014 psi).

The ultimate punching capacity of the shells was found to be significantly higher than would be expected based on results of previous tests conducted on slabs. The investigators attributed this increase in strength to the presence of prestressing and the arch action that developed because of the cylindrical shape of the specimens. Increases in load carrying capacity were observed with increasing area of loading, which is to be expected as the failure surface is also increasing. In tests conducted on specimens with the same area of loading, the greater capacity was found to occur in the case where the long dimension of the rectangularly-shaped loaded area was in the circumferential direction rather than in the longitudinal direction of the shell. Crack angles in the failed specimens ranged from 20^{o} to 70^{o} with respect to the plane of the specimen, with the steeper cracks forming in the circucumferential direction and the flatter cracks forming in the prestressed longitudinal direction.

The investigators attempted to accurately estimate the true area of the failure surface in the specimens. Using this area, the investigators then calculated a nominal failure stress on this

surface and found that in all six tests, even though the ultimate capacity varied considerably, the failure stress was almost constant at 1.7 MPa (250 psi). For comparison, the nominal shear stress can be calculated at a critical surface of half the effective depth of the specimen away from the perimeter of the loaded area, as per ACI code provisions. Results from the tests indicate that nominal shear stresses of between 9.0 and 11.0 $\sqrt{f'_c}$ developed, based on an f'_c value of 4500 psi. This is significantly higher than the stresses specified in the current ACI code.

5.4.3 OTHER PUNCHING SHEAR STUDIES ON OFFSHORE STRUCTURES

Sorensen [151] conducted a theoretical and experimental investigation on the impact resistance of tubular structural members of concrete offshore structures. Sorensen noted that punching shear in cylindrical tube walls representative of offshore structures would differ from punching shear in slabs in two major ways. First, the cylindrical shape would result in compressive membrane forces developing which would increase the punching resistance. Compressive membrane forces would also occur if prestressing was provided in the tube walls. The second reason for a difference is that wall thicknesses in the offshore structures will be larger than the thicknesses of previously tested slabs so that possible extrapolation from slab test results, expecially concerning shear failures, may give misleading results.

In discussing the stresses in the specimens, Sorensen notes that the real stress distribution is complex. In a thick tube, inclined cracks will not develop simultaneously in all directions and stress redistribution may occur. Sorensen suggests that the ultimate punching resistance may be calculated using the tensile strength acting on a conical ultimate fracture surface. He suggests the following formula for calculating the punching resistance of thick tubes:

$$P_u = \pi \mu h (d + \mu h) f_c \qquad (5\text{-}5)$$

where P_u = the ultimate load capacity;
h = the thickness of the tube;
d = the diameter of the circular loaded area;
f_c = the tensile strength of the concrete;
$\mu = \sqrt{1 + \sigma_m/f_c}$; and
σ_m = the effective membrane stress.

The magnitude of the effective membrane stress will depend on the radius-to-thickness ratio of the tube and the level of prestress.

Regan and Hamadi [152] conducted tests to investigate the behavior of concrete caisson and tower members subjected to combined bending and shear, including some tests aimed at gathering information on the punching resistance. The specimens tested were hollow cylinders with an external diameter of 0.80 m (31.5 in.) and a wall thickness of 0.04 m (1.57 in.). The concrete used in the specimens had an average cube strength of 50 MPa (7250 psi), corresponding to an approximate compressive cylinder strength of 40 MPa (5800 psi). Both prestressed and nonprestressed specimens were tested. The models used in the investigation provided a reasonable representation of the lower ends of towers of North Sea platforms with a scale factor of approximately 1:20 to 1:25.

Crack angles of approximately 20° in the longitudinal direction and approximately 30° in the circumferential direction were observed on the failure surfaces. Results of this investigation into the punching behavior are summarized in Figure 31. Two lines are shown on the figure. The top line gives a reasonable fit to the test data and corresponds to a nominal shear stress of 4.5 MPa (625 psi) acting on a critical section at a distance of half the depth of the wall away from the perimeter of the load. The bottom line represents the predictions of the ACI code, and

gives shears which are approximately half those of the top line. The investigators identified three factors in addition to the general conservatism of the code that might explain why the experimental strengths were far greater that the predicted values:

1. the presence of prestress in some of the specimens;
2. the curvature of the shells resulting in compressive membrane action; and
3. the effects of scale in the model tests.

While results of these tests are of interest, the investigators noted that further work is needed before conclusions can be drawn about the punching resistance of curved shells.

Kavyrchine [153] conducted statical and low speed dynamic tests on cylindrical concrete shells. The specimens had an exterior diameter of 0.716 m (28 in.) and a wall thickness of 0.058 m (2.28 in.). Reinforcement was provided at the mid-thickness of the specimens. The ultimate strength of the specimens was essentially the same in both the static and dynamic loading tests, and might be attributed to the relatively low speeds used in the dynamic tests. The presence of prestressing in the specimens was found to have a negligible effect on the punching behavior. The investigators used the analytical procedure suggested by Braestrup (see Section 4.5) to predict the capacities of the tested specimens. After some manipulation of the factors in the procedure to account for different loading mechanisms, the investigators obtained experimental-to-predicted capacity ratios in the range of 0.81 to 1.26.

5.5 FINITE ELEMENT PREDICTIONS OF PUNCHING SHEAR STRENGTH

Finite element models of reinforced concrete structures are based on representing the concrete and steel reinforcement by an assembly of finite elements and specifying appropriate

constitutive relationships to govern the behavior of the materials. The problem of predicting the punching shear behavior of reinforced concrete slabs and shells is very complex and has not yet been completely solved for the general case. Consideration must be given to the nonlinear behavior of the concrete and reinforcing steel, possible dowel action and bond failure of the reinforcement, and, most importantly, cracking of the concrete. Further, the stress and strain distributions through the thickness must also be considered, so the problem becomes three-dimensional.

A brief discussion of the problems that are encountered in using finite elements to predict punching shear strength is given, along with a presentation of some of the approaches that have been suggested for solving these problems. For illustrative purposes, three examples of finite element analyses of punching shear in slabs are presented. A comprehensive review of finite element applications to reinforced concrete structures can be found in the ASCE "State-of-the-Art Report on Finite Element Analysis of Reinforced Concrete Structures" [154]. A literature review of finite element techniques for modeling shear in reinforced concrete structures has been performed by Noguchi and Inoue [155].

An accurate description of the nonlinear, multiaxial stress-strain relationship of concrete is very complicated. Three constitutive models have been shown to be promising [154]. Ottosen [156,157] has developed a constitutive model using four parameters to define the material behavior, and the model has been shown to provide a close approximation of experimental results over a wide range of stress states for short-time, monotonic loading of concrete [154]. Another important constitutive model is the Willam-Warnke failure criterion [158] which uses five parameters to numerically represent the failure surface of concrete under three-dimensional states of stress. A third constitutive model for concrete that has been successfully

used is the "endochronic theory of plasticity" proposed by Bazant and Bhat [159]. The endochronic theory uses increments of strain as a measure of intrinsic time (always positive). This intrinsic time is used to measure the extent of change (or damage) of the internal structure of the concrete when it is subjected to deformation histories [154]. Another important aspect in addition to describing the behavior of the material under any state of stress is that the constitutive model must also describe the behavior beyond the peak stress, i.e. tension and compression softening of the the concrete once the peak stresses have been reached.

Material modeling of the steel reinforcement is fairly well defined. The steel can be represented using an elastic-perfectly plastic material model, or if added refinement is needed, it may be modelled as a bilinear material. Reinforcing bars can be represented in the finite element model as truss elements connected at node points, or as beam elements if dowel effects are to be included in the analysis. The reinforcement may also be represented by an equivalent smeared layer of steel. Bond between the reinforcement and the concrete has been modelled using linkage elements (e.g. Scordelis [160]). More recently, fracture mechanics has been used by Ingraffea et al [161] to study and model bond-slip behavior. Fortunately, in many practical applications perfect bond between the concrete and reinforcement may be assumed with little loss in accuracy.

Tensile cracking in concrete has been recognized as the dominant nonlinear effect in reinforced concrete structures [154]. Two approaches have been used for representing cracks: discrete crack modeling and smeared crack modeling. Historically, the first approach used to represent cracks in finite element analyses of reinforced concrete members was to model the cracks as discrete discontinuities along element boundaries (e.g. Ngo and Scordelis [162] and Nilson [163]). This approach suffers from the drawback that the finite element mesh must be updated

after the formation of each crack, and the model also lacks complete generality in possible crack direction [154]. These problems associated with the discrete cracking model have led many investigators to adopt the so-called "smeared" cracking model where instead of one discrete crack forming, many finely spaced (or smeared) cracks form perpendicular to the principal stress direction once the limiting tensile stress has been exceeded. After cracking has occurred, the modulus of elasticity of the material is set to zero for the direction perpendicular to the principal stress. Using the smeared crack approach, the finite element mesh does not need to be updated during the analysis, which is a significant improvement over the discrete crack approach. However, some drawbacks do exist with the smeared crack approach. In some instances, the smeared cracks may be excessively diffused, resulting in an inability to predict dominant crack patterns. In addition, aggregate interlock and dowel effects can be accounted for only indirectly with the smeared crack approach.

Recently, attention has again been given to representing cracks as discrete discontinuities, particularly in combination with using fracture mechanics for the criteria for crack propagation (e.g. Kesler, Naus and Lott [164], Ingraffea and Gerstle [165], and Ingraffea and Saouma [166]). However, it should be noted that there is some question about the practical applicability of fracture mechanics to reinforced concrete, at least at its current state of development [154].

Once cracking occurs in the concrete, shear will be transferred across the crack by aggregate interlock. Relatively simple linkage elements at discrete cracks have been used to model aggregate interlock (e.g. Ngo and Scordelis [162]). More elaborate shear transfer models have also been developed, such as those of Walraven [167], Pruijssers [168], and Bazant and Gambarova [169]. A more common approach to modeling of aggregate interlock has been to assume that some portion of the shear

stiffness of the element remains after the element cracks. Many investigators (e.g. Hand, Pecknold and Schnobrich [170] and Lin and Scordelis [171]) have used this "shear retention factor" to include not only the effects of aggregate interlock, but also to include dowel effects and any remaining shear transfer in the concrete. The shear retention factor has thus become a "catch all" for mechanisms of shear transfer that are otherwise not explicitly incorporated into the analytical model.

Loseth, Slatto and Syvertsen [172] used finite elements to predict the punching shear capacity of the circular slabs tested by Kinnunen and Nylander [68]. Because of the nature of the test slabs, Loseth et al. were able to achieve an accurate formulation of the problem using an axisymmetric finite element model rather than a full three-dimensional model, resulting in a huge reduction in the amount of computational time needed to solve the problem. Moreover, the investigators noted that a full three-dimensional program with the necessary capabilites was not available. A modified version of the endochronic theory was used for the concrete material model. For comparison purposes, a simple elastic-plastic constitutive model was also used. Tension failure in the concrete was modeled by assuming a gradual softening of the material, and tensile cracks were represented using the smeared crack approach. The steel reinforcement was modelled in the slabs as smeared layers. Aggregate interlock, friction and dowel action of the reinforcement were accounted for by applying a shear retention factor. An example of their analyses is shown in Figure 32a. The modified endochronic theory using a shear retention factor of 0.2 provided the best results.

Tao and White [173] used finite elements to predict the punching shear capacity of slabs tested at Cornell University [74]. The slabs were modelled as a layered system of concrete and steel, drawing upon the work of Scanlon [174] and Hand, Pecknold and Schnobrich [170]. The stiffness matrix for an element is obtained by integrating the contribution of each layer. Each

layer is assumed to be in a state of plane stress, and thus a biaxial material model is sufficient to describe the behavior of the concrete. Shear deformation through the thickness of the slabs is approximately accounted for using this method. Cracking was represented using the smeared crack approach. A shear retention factor was incorporated into the program to account for dowel action and aggregate interlock, based on the approach of Lin and Scordelis [171]. An axisymmetric finite element formulation was used in order to simplify the program. An example analysis of a test slab is shown in Figure 32b.

Borst and Nauta [175] used a finite element program to predict the shear strength of reinforced concrete beams and slabs. A modified smeared cracking approach was developed in which the total strain at a point was decomposed into a concrete strain component and a crack strain component, as originally suggested by Litton [176] and Bazant and Gambarova [169]. This decomposition allows for treatment of both concrete nonlinearity and cracking at one integration point. Borst and Nauta's approach also allows cracks to develop at any arbitrary inclination angle and multiple cracks can occur in one integration point. In their study, the investigators assumed that the nonlinear behavior of the reinforced concrete beams and slabs was dominated by tensile cracking, and they therefore used a simple linear elastic material model for the concrete in compression. Axisymmetric finite element analyses were performed of punching shear tests on slabs conducted at Delft University. An example of their analyses, using a shear retention factor of 0.2, is given in Figure 32c.

To date, most of the attempts to predict punching shear strength using finite elements have been performed using an axisymmetric formulation of the problem. Offshore structures, particularly those with cylindrical shapes and one-way prestressing in the ice walls, are not adequately described by an axisymmetric model. Rather, a full three-dimensional model is needed. Gerwick et al.

[148] have performed nonlinear finite element analyses of offshore structures using a two-dimensional plane strain formulation, but this formulation is actually modeling a line load acting on the structure rather than a localized punching load. An important advancement in the ability to analyze offshore structures subjected to punching shear will be the availability of a three-dimensional finite element program incorporating the features that are currently included only in two-dimensional programs. It may be possible to simplify some of the criteria to reduce the computational requirements of the problem and yet retain the dominant behavior, as was done by Borst and Nauta when they used a linear elastic material model for the concrete in compression.

6.0 SUMMARY

The punching shear resistance of lightweight, high strength, heavily reinforced slab and shell sections representative of proposed Arctic structures is being investigated at the National Bureau of Standards. The project is being sponsored by The Minerals Management Service of the U.S. Department of the Interior and five American oil companies. Both analytical and experimental studies are planned. This report reviews current knowledge on punching shear and other subjects relevant to the project.

Arctic offshore structures will be required to withstand tremendous global and local ice pressures. Knowledge of the behavior of ice action on Arctic structures is limited. Current investigations include analytical, experimental, and field measurement studies of ice forces. A coordinated effort using all three approaches is necessary before design values of ice forces for Arctic structures can be selected with any measure of confidence. Design values of ice forces used in proposed designs are based to a considerable extent on engineering judgement. Design curves have been proposed, but the magnitudes of ice pressure vary from curve to curve. The only agreement on local ice pressure design values is that as the contact area gets larger, the pressure should decrease. There is a need for more research into the interaction of Arctic structures with ice.

Proposed structures for the Arctic can generally be classified into three categories: island structures, gravity structures and floating structures. The choice of a particular structural concept will depend upon the location, usage, and depth of operation for which the structure is intended. Only a limited amount of design information is publicly available on existing and proposed Arctic offshore structures.

The basic theory of punching shear and the mechanism by which it occurs were discussed, and a comparison was made of beam and punching shear action. Nine factors that may have an effect on the punching shear resistance of a slab or shell were identified. Most methods to predict punching shear strength have been based on empirical equations, although some conceptual models for predicting punching shear strength have been developed. Code provisions of three major codes of concrete practice, the ACI, CEB-FIP, and CP110 codes, were reviewed and a comparison made. Some limitations of the current code provisions were noted.

Various investigations of punching shear strength relevant to the project were reviewed. Size effects due to increased slab thickness were observed in tests conducted in Sweden. Punching shear tests on nuclear reactor structures due to internal pressure loading and impact loading, while not directly applicable to offshore structures, are useful in that the techniques used to conduct the tests and the approaches used to develop design equations may provide guidance for the testing and design of offshore structures. Further, the analytical tools developed to analyze the reactor structures may also be useful for analyzing offshore structures. Fiber reinforcement has been shown in model tests to significantly improve the punching shear performance of slabs and shells. A limited number of investigations has been conducted on the punching shear resistance of offshore structures, the most notable of which is the study conducted by Brian Watt Associates, Inc. In all of the investigations reviewed, the observed strengths of the test specimens were considerably higher than those predicted by any of the codes. Current finite element approaches for predicting punching shear strength yield good results for particular cases. However, the general, three-dimensional problem of punching shear in a slab or shell has yet to be completely solved.

7.0 REFERENCES

1. Bruce, J.C. and Roggensack, W.D., "Second Generation Arctic Platforms: Lessons From First Generation Design Experience," Proceedings 1984 Offshore Technology Conference, OTC 4798, Houston, Texas.

2. Matsuishi, M.; Nishimaki, K.; Takeshita, H.; Iwata, S. and Suhara, T.; "On the Strength of New Composite Steel-Concrete Material For Offshore Structure," Proceedings 1977 Offshore Technology Conference, OTC 2804, Houston, Texas.

3. Carino, N.J., "Offshore Concrete Structures in the Arctic: Research Needs," National Bureau of Standards Technical Note 1192, April, 1984.

4. Carino, N.J., Proceedings of the International Workshop on the Performance of Offshore Concrete Structures in the Arctic Environment, National Bureau of Standards, March, 1983.

5. Faulds, E.C., "Structural Inspection and Maintenance in a North Sea Environment," Proceedings 1982 Offshore Technology Conference, OTC 4360, Houston, Texas.

6. ACI Committee 357, "State-of-the-Art Report on Offshore Concrete Structures for the Arctic, Fifth Draft," American Concrete Institute, Detroit, Mich., 1984. Karl H. Runge, Editor.

7. Kivisild, H.R., "Offshore Structures in Arctic Ice," Proceedings of the International Conference on the Behavior of Offshore Structures (BOSS '76), Trondheim, 1976.

8. Tunik, A., Miller, D.N. and Chen, Y.K., "Literature Review on Ice Loadings", American Bureau of Shipping Technical Report OED-83006/TD-8301, 1983.

9. Peyton, H., "Ice and Marine Structures, Part 3," Ocean Industry, Dec., 1968, Vol. 3, No. 12, pp. 51-58.

10. Croasdale, K.R. and Marcellus, R.W., "Ice and Wave Action on Artificial Islands in the Beaufort Sea," Canadian Journal of Civil Engineering, Vol. 5, No. 1, 1978, pp. 98-113.

11. Engelbrektson, A., "Ice Force Design of Offshore Structures in Light of Experiences From the Baltic," Proceedings, Offshore Goteburg-83, VRM 057-003, 1983.

12. Energy Interface Associates, Inc., "Technology Review of Arctic Offshore Oil/Gas Operations," September, 1979.

13. Croasdale, K.R., "Ice Forces on Fixed Rigid Structures," IAHR Special Report 80-26, Ed. T. Carsten, Publ. USA CRREL, June, 1980.

14. Korzhavin, K.N., "Action of Ice on Engineering Structures," (1962) USA CRREL Draft Translation 260, AD723169, 1971.

15. Ralston, T.D., "Sea Ice Loads," Technical Seminar on Alaskan Beaufort Sea Gravel Island Design, Exxon USA, Anchorage, October 15, 1979.

16. API Bulletin 2N, "Planning, Designing, and Constructing Fixed Offshore Structures in Ice Environments," First Edition, January, 1982, American Petroleum Institute, Dallas, Texas.

17. Neill, C.R., "Dynamic Ice Forces on Piers and Piles. An Assessment of Design Guidelines in the Light of Recent Research," Canadian Journal of Civil Engineering, Vol. 3, 1976.

18. Haynes, F.D., Sodhi, D.S., Kato, K. and Hirayama, K., "Ice Forces on Model Bridge Piers," CRREL Report 83-19, 1983.

19. Edwards, R.Y. and Croasdale, K.R., "Model Experiments to Determine Ice Forces on Conical Structures," Symposium on Applied Glaciology, Cambridge, England, 1976.

20. Kry, P.R., "A Statistical Prediction of Effective Ice Crushing Stresses on Wide Structures," IAHR Ice Symposium, Lulea, Sweden, 1978.

21. Vivatrat, V. and Slomski, S., "A Probabilistic Basis for Selecting Design Ice Pressures and Ice Loads for Arctic Offshore Structures," Proceedings 1983 Offshore Technology Conference, OTC 4457, Houston, Texas.

22. ACI Committee 357, "Guide For the Design and Construction of Fixed Offshore Concrete Structures, (ACI 357 R-78)," American Concrete Institute, Detroit, Mich., 1978.

23. Buslov, V.M. and Krahl, N.W. (Brown and Root Inc.), "Fifty-one New Concepts for Arctic Drilling and Production," Part 1, Ocean Engineering, 1983.

24. Bea, R.G., "Design of Offshore Arctic Structures: Advanced Concepts and Recent Developments," ASCE Continuing Education Services, 1983.

25. Schlecten, J.R.; Fernandes, R.L.; Dolan, D.K. and Bivens, H.R.; "Analysis and Design of an Ice Wall Framing System For an Arctic Drilling Structure," Proceedings 1984 Offshore Technology Conference, OTC 4691, Houston, Texas.

26. Byrd, R.C.; Coleman, R.K.; Weiss, R.T.; Boaz, I.B.; Sauve, E.R. and White, R.M.; "The Arctic Cone Exploration Structure: A Mobile Offshore Drilling Unit For Heavy Ice Cover," Proceedings 1984 Offshore Technology Conference, OTC 4800, Houston, Texas.

27. Wetmore, S.B., "The Concrete Island Drilling System: Super Series (Super CIDS)," Proceedings 1984 Offshore Technology Conference, OTC 4801, Houston, Texas.

28. Bruen, F.J.; Byrd, R.C.; Vivatrat, V. and Watt, B.J.; "Selection of Local Design Ice Pressures For Arctic Systems," Proceedings 1982 Offshore Technology Conference, OTC 4334, Houston, Texas.

29. Gerwick, B.C., Potter, R.E. and Rojansky, M., "Development of a Structural Concept to Resist Impacts From Multiyear Ice Floes, Ridges, and Icebergs," Proceedings 1984 Offshore Technology Conference, OTC 4799, Houston, Texas.

30. ACI Committee 318, "Building Code Requirements for Reinforced Concrete (ACI 318-77)," American Concrete Institute, Detroit, Mich., 1977.

31. Bhula, D.N., Birdy, J.N. and Bruen, F.J., "Design of Concrete Gravity Structures to Withstand Concentrated Ridge and Flow Impact Loads," Proceedings 1984 Offshore Technology Conference, OTC 4708, Houston, Texas.

32. ACI Committee 318, "Building Code Requirements for Reinforced Concrete, (ACI 318-83)," American Concrete Institute, Detroit, Mich., 1983.

33. ACI Committee 318, "Commentary on Building Code Requirements for Reinforced Concrete, (ACI 318-83)," American Concrete Institute, Detroit, Mich., 1983.

34. Brian Watt Associates, Inc., "Experimental Work on Punching Shear Resistance of Concrete Structures For the Arctic," AOGA Project No. 152, Nov., 1982.

35. Fitzpatrick, J. and Stenning, D.G., "Design and Construction of Tarsiut Island in the Canadian Beaufort Sea," Proceedings 1983 Offshore Technology Conference, OTC 4517, Houston, Texas.

36. Park, R. and Gamble, W., "Reinforced Concrete Slabs," John Wiley and Sons, 1980.

37. Criswell, M.E. and Hawkins, N.W., "Shear Strength of Slabs: Basic Principle and Their Relation to Current Methods of Analysis," ACI Special Publication 42-29, pp. 641-676, Detroit, Mich., 1974.

38. Winter, G. and Nilson, A.H., "Design of Concrete Structures," Ninth Edition, McGraw Hill Book Company, 1979.

39. Wang, C. and Salmon, C.G., "Reinforced Concrete Design," Third Edition, Harper and Row, 1979.

40. ASCE-ACI Committee 426, "The Shear Strength of Reinforced Concrete Members," Journal of the Structural Division, ASCE, No. ST6, June, 1973, pp. 1091-1187.

also

ASCE-ACI Committee 426, "The Shear Strength of Reinforced Concrete Members - Slabs," Journal of the Structural Division, ASCE, No. ST8, Aug., 1974, pp. 1543-1591.

41. Hawkins, N.M., Criswell, M.E. and Roll, F., "Shear Strength of Slabs Without Reinforcement," ACI Special Publication 42-30, pp. 667-720, Detroit, Mich., 1974.

42. Carino, N.J. and Lew, H.S., "Re-examination of the Relation Between Splitting Tensile and Compressive Strength of Normal Weight Concrete," ACI Journal, May-June, 1982, pp. 214-219.

43. Elstner, R.C. and Hognestad, E., "Shearing Strength of Reinforced Concrete Slabs," ACI Journal, Proceedings, Vol. 53, No. 1, July, 1956, pp. 29-58.

44. Ivy, C.B., Ivey, D.L. and Buth, E., "Shear Capacity of Lightweight Concrete Flat Slabs," ACI Journal, Vol. 66, No. 6, June, 1969, pp. 490-494.

45. Kinnunen, S., "Punching of Concrete Slabs With Two-Way Reinforcement With Special Reference to Dowel Effect and Deviation of Reinforcement From Polar Symmetry," Transactions, No. 198, 1963, Royal Institute of Technology, Stockholm, Sweden.

46. Anis, N.N., "Shear Strength of Reinforced Concrete Flat Slabs Without Shear Reinforcement," Ph.D. Thesis, Imperial College, University of London, 1970.

47. Moe, J., "Shearing Strength of Reinforced Concrete Slabs and Footings Under Concentrated Loads," Development Department Bulletin D47, Portland Cement Association, April, 1961, 130 pp.

48. Roll, F., Zaidi, S.T.H., Sabnis, G.M. and Chuang, K., "Shear Resistance of Perforated Reinforced Concrete Slabs," SP-30, Cracking, Deflection and Ultimate Load of Concrete Slab Systems, American Concrete Institute, Detroit, Mich., 1971, pp. 77-102.

49. Batchelor, B. de V. and Tissington, I.R., "A Study of Partially Restrained Two-Way Bridge Slabs Subjected to Concentrated Loads," Report on Project Q-47 of the Ontario Joint Highway Research Programme, Queen's University, March, 1972.

50. Malhotra, V.M., "Effect of Specimen Size on Tensile Strength of Concrete," Report of Dept. of Energy, Mines, and Resources, Ottawa, Canada, June, 1969, 9 pp.

51. Walraven, J.C., "The Influence of Depth on the Shear Strength of Lightweight Concrete Beams Without Shear Reinforcement," Stevin Laboratory Report No. 5-78-4, Delft University of Technology, The Netherlands.

52. Bazant, Z.P. and Kim, J., "Size Effect in Shear Failure of Reinforced Concrete Beams," Northwestern University, Report 83-5/428s, May, 1983.

53. Kinnunen, S., Nylander, H. and Tolf, P., "Plattjocklekens inverkin pa betongolattors hallfashthet vid genomstansning. Forsok med rektangulara plattor (Effect of Slab Thickness on Punching Shear Strength of Concrete Slabs. Tests on Rectangular Slabs)," Bulletin 137, TRITA-BST-0137, Dept. of Structural Mechanics and Engineering, Royal Institute of Technology, Stockholm, Sweden, 1980.

54. Criswell, M.E., "Static and Dynamic Response of Reinforced Concrete Slab-Column Connections," ACI Special Publication SP 42-31, pp. 721-746, Detroit, Mich., 1974.

55. Vanderbilt, M.D., "Shear Strength of Continuous Plates," Journal of the Structural Division, ASCE, Vol. 98, No. ST5, May, 1972, pp. 961-973.

56. Nightingale, R.I., "Collapse Loads of Concrete Flat Plates," Report No. Ce4, Dept. of Civil Engineering, University of Maine, Orono, Maine, January, 1970.

57. Plisga, S.J., "Punching of Flat Plates," Report No. Ce9, Dept. of Civil Engineering, University of Maine, Orono, Maine, January, 1972.

58. Hawkins, N.M., Fallsen, H.B. and Hinojosa, R.C., "Influence of Column Rectangularity on the Behavior of Flat Plate Structures," SP-30, Cracking, Deflection and Ultimate Load of Concrete Slab Systems, American Concrete Institute, Detroit, Mich., 1971, pp. 127-146.

59. Hawkins, N.M., "Shear Strength of Slabs With Shear Reinforcement," ACI Special Publication SP 42-34, pp. 785-815, Detroit, Mich., 1974.

60. Criswell, M.E., "Strength and Behavior of Reinforced Concrete Slab-Column Connections Subjected to Static and Dynamic Loadings," Technical Report M-70-1, U.S. Army Waterways Experiment Station, Vicksburg, December, 1970.

61. Moll, E.L., "Investigation of Transverse Stressing in Bridge Decks," Masters Thesis, McMaster University, Hamilton, Ontario, April, 1985.

62. Brotchie, J.F. and Holley, M.J., "Membrane Action in Slabs," SP-30, Cracking, Deflection and Ultimate Load of Concrete Slab Systems, American Concrete Institute, Detroit, Mich., 1971, pp. 345-377.

63. Taylor, R. and Hayes, B., "Some Tests on the Effect of Edge Restraint on Punching Shear in Reinforced Concrete Slabs," Magazine of Concrete Research, Vol. 17, No. 50, March, 1965, pp. 39-44.

64. Aoki, Y. and Seki, H., "Shearing Strength and Cracking in Two-Way Slabs Subjected to Concentrated Load," SP-30, Cracking, Deflection and Ultimate Load of Concrete Slab Systems, American Concrete Institute, Detroit, Mich., 1971, pp. 103-126.

65. Hewitt, B.E. and Batchelor, B. de V., "Punching Shear Strength of Restrained Slabs," Journal of the Structural Division, ASCE, No. ST9, September, 1975, pp. 1837-1853.

66. Tong, P.Y. amd Batchelor, B. de V., "Compressive Membrane Enhancement in Two-Way Bridge Slabs," SP-30, Cracking, Deflection and Ultimate Load of Concrete Slab Systems, American Concrete Institute, Detroit, Mich., 1971, pp. 271-286.

67. Masterson, D.M. and Long, A.E., "The Punching Strength of Slabs, A Flexural Approach Using Finite Elements," ACI Special Publication 42-32, pp. 747-768, Detroit, Mich., 1974.

68. Kinnunen, S., and Nylander, H., "Punching of Concrete Slabs Without Shear Reinforcement," Transactions of the Royal Institute of Technology, Stockholm, Sweden, No. 158, 1960.

69. Scordelis, A.C., Lin, T.Y. and May, H.R., "Shearing Strength of Prestressed Lift Slabs," ACI Journal, Proceedings, Vol. 55, No. 4, October, 1958, pp. 485-506.

70. Grow, J.C. and Vanderbilt, M.D., "A Study of the Shear Strength of Lightweight Prestressed Concrete Flat Plates," Structural Research Report No. 2, December, 1966, Civil Eng. Dept., Colorado State University, Fort Collins, Colorado; also Journal of the Prestressed Concrete Institute, Vol. 12, No. 4, August, 1967, pp. 18-28.

71. Gerber, L.L. and Burns, N.H., "Ultimate Strength of Post-Tensioned Flat Plates," PCI Journal, Vol. 16, No. 6, Nov.-Dec., 1971, pp. 40-58.

72. ACI-ASCE Committee 423, "Recommendations for Concrete Members Prestressed with Unbonded Tendons," Concrete International, ACI, Vol. 5, No. 7, July, 1983, pp. 61-76.

73. Abrams, J.H., "The Punching Shear Strength of Precracked Reinforced Concrete in Biaxial Tension," M.S. Thesis, Cornell University, May, 1979.

74. Jau, W.C., White, R.N. and Gergely, P., "Behavior of Reinforced Concrete Slabs Subjected to Combined Punching Shear and Biaxial Tension," Cornell University, NUREG/CR-2920, September, 1982.

75. Johnson, R.P. and Arnouti, C., "Punching Shear Strength of Concrete Slabs Subjected to In-Plane Biaxial Tension," Magazine of Concrete Research, Vol. 32, No. 110, March, 1980.

76. Hognestad, E., "Shearing Strength of Reinforced Concrete Column Footings," ACI Journal, Proceedings, Vol. 50, No. 3, November, 1953, pp. 189-208.

77. Tasker, H.E. and Wyatt, R.J., "Shear in Flat-Plate Construction Under Uniform Loading," Special Report No. 23, October, 1963, Australian Commonwealth Experimental Building Station, Sydney, Australia.

78. Herzog, M., "A New Evaluation of Earlier Punching Tests," Conrete, Vol. 4, No. 12, December, 1970, pp. 448-450.

79. Mowrer, R.D. and Vanderbilt, M.D., "Shear Strength of Lightweight Aggregate Reinforced Concrete Flat Plates," Proceedings, American Concrete Institute, Vol. 64, November, 1967, pp. 722-729.

80. Whitney, C.S., "Ultimate Shear Strength of Reinforced Concrete Flat Slabs, Footings, Beams, and Frame Members Without Shear Reinforcement," ACI Journal, Proceedings, Vol. 54, No. 4, October, 1957, pp. 265-298.

81. Yitzhaki, D., "Punching Strength of Reinforced Concrete Slabs," Proceedings, American Concrete Institute, Vol. 63, May, 1966, pp. 527-542.

82. Blakey, F.A., "A Review of Some Experimental Studies of Slab-Column Connections," Constructional Review, Vol. 39, No. 8, July, 1966, pp. 17-24.

83. Gesund, H. and Kaushik, Y.P., "Yield Line Analysis of Punching Failures in Slabs," Publications, International Association for Bridge and Structural Engineering, Vol. 30-1, 1970.

84. Long, A.E., "A Two-Phase Approach to the Prediction of Punching Strength of Slabs," ACI Journal, Proceedings, February, 1975.

85. Anderson, J.L., "Punching of Concrete Slab With Shear Reinforcement," Stockholm Royal Institute of Technology, Transaction No. 212, 1963.

86. Nielsen, M.P., Braestrup, M.W., Jensen, B.C. and Bach, F., "Concrete Plasticity. Beam Shear - Punching Shear - Shear in Joints," Copenhagen, Danish Society for Structural Science and Engineering, Special Publication, 1978.

87. Braestrup, M.W., "Punching Shear in Concrete Slabs," IABSE Colloquium, Copenhagen, 1979. Plasticity in Reinforced Concrete, Introductory Reports.

88. Braestrup, M.W., Nielsen, M.P., Jensen, B.C. and Bach, F., "Axisymmetric Punching of Plain and Reinforced Concrete," Copenhagen Technical University of Denmark, Structural Research Laboratory, Report R 75.

89. CEB-FIP, "Model Code for Concrete Structures," Comite Euro-International du Beton et Federation International de la Preconstrainte, London, 1978.

90. CP110: Part 1, "British Unified Code of Practice for the Structural Use of Concrete," British Standards Institute, London, 1972.

91. Comite Europeen du Beton: Dalles, Structure Planes. Theme II, Poinconnement, Bulletin d'Information, No. 57, Sept., 1966, pp. 175.

92. Regan, P.E., "A Comparison of British and ACI 318-71 Treatments of Punching Shear," ACI Special Publication 42-37, pp. 881-903, Detroit, Mich., 1974.

93. Nylander, H. and Sundquist, H., "Genomstansning av pelar-understodd plattbro av betong med ospand armering (Punching-Through of Column-Supported Slab Bridges Made of Concrete With Untensioned Reinforcement)," Report 104, Inst. foer Byggnadsstatik, KTH, Stockholm, Sweden, 1972.

94. Nylander, H., Kinnunen, S. and Ingvarsson, H., "Genomstansning av pelarunderstodd plattbro av betong med spand och ospand armering (Punching-Through of Column-Supported Slab Bridges Made of Concrete With Prestressed and Untensioned Reinforcement), Report 123, Inst. foer Byggnadsstatik, KTH, Stockholm, Sweden, 1975.

95. Cheung, K.C., Gotschall, H.L. and Liu, T.C., "Ultimate Strength of Prestressed Concrete Reactor Vessel End Slabs," General Atomic Projects 1900 and 1901 (GA-A13057), May, 1975.

96. Langan, D. and Garas, F.K., "Behavior of End Slabs in Cylindrical Prestressed Concrete Pressure Vessels," Structural Mechanics in Reactor Technology, Vol. H, No. 3/4, 1971, pp. 187-230.

97. Paul, S.L., Sozen, M.A., Schnobrich, W.C., Karlsson, B.I. and Zimmer, A., "Strength and Behavior of Prestressed Concrete Vessels For Nuclear Reactors - Volumes I and II," University of Illinois, Structural Research Series No. 346, July, 1969.

98. Karlsson, B.I. and Sozen, M.A., "Shear Strength of End Slabs With and Without Penetrations in Prestressed Concrete Reactor Vessels," University of Illinois, Structural Research Series No. 380, July, 1971.

99. Elstner, R.C. and Hognestad, E., "Shearing Strength of Reinforced Concrete Slabs," ACI Journal, Proceedings, Vol. 52, May, 1956, pp. 913-986.

100. Brown, I. and Perry, S., "An Experimental Method to Investigate Impact on Concrete Slabs," BAM Proceedings, 1982, pp. 202-212.

101. Wittman, F. and Boulahdour, T., "Variability of Resistance of Concrete Slabs Under Impact Load," Structural Mechanics in Reactor Technology, Vol. J, No. 7/2, 1981, 7 pp.

102. Berriaud, C., Verpeaux, P., Hoffmann, A., Jamet, P. and Avet-Flancard, R., "Test and Calculation of Concrete Structures Under Missile Impact," Structural Mechanics in Reactor Technology, Vol. J, No. 7/1, 1979, 7 pp.

103. McMahon, P., Sen, S. and Meyers, B., "Behavior of Reinforced Concrete Barriers Subject to the Impact of Turbine Missiles," Structural Mechanics in Reactor Technology, Vol. J, No. 7/6, 1979, 8 pp.

104. Jonas, W., Meschkat, R., Riech, H. and Rudiger, E., "Experimental Investigations to Determine the Kinetic Ultimate Bearing Capacity of Reinforced Concrete Slabs Subject to Deformable Missiles," Structural Mechanics in Reactor Technology, Vol. J, No. 8/5, 1979, 7 pp.

105. Davies, I., Carlton, D. and O'Brien, T., "Scaling Laws Applied to Impact Testing and Computer Assessments Made to Compare Tests at Two Scales," Structural Mechanics in Reactor Technology, Vol. J, No. 8/1, 1979, 8 pp.

106. Barr, P., Brown, M., Carter, P., Howe, W., Jowett, J., Neilson, A. and Young, R., "Studies of Missile Impact With Reinforced Concrete Structures," Nuclear Energy, Vol. 19, No. 3, June, 1980, pp. 179-189.

107. Berrieaud, C., Sokolovsky, A., Gueraud, R., Dulac, J. and Labrot, R., "Local Behavior of Reinforced Concrete Walls Under Missile Impact," Nuclear Engineering and Design, Vol. 45, 1978, pp. 457-469.

108. Sage, F. and Pfeiffer, A., "Response of Reinforced Concrete Targets to Impacting Soft Missiles, An FRGMRT-UKAEA Co-Operation in Tests to Validate Computer Codes and Scaling Laws," Structural Mechanics in Reactor Technology, Vol. J, No. 8/4, 1979, 8 pp.

109. Woodfin, R.L., "Full-Scale Turbine Missile Concrete Impact Tests," EPRI NP-2745, Sandia National Laboratories, January, 1983.

110. Woodfin, R.L. and Sliter, G.L., "Results of Full Scale Turbine Missile Concrete Impact Experiments," Structural Mechanics in Reactor Technology, Vol. J, No. 8/2, 1981, 8 pp.

111. Sliter, G.E., Chu, B.B. and Ravindra, M.K., "EPRI Research on Turbine Missile Effects in Nuclear Power Plants," Structural Mechanics in Reactor Technology, Vol. J, No. 8/5, 1983, pp. 403-409.

112. Nachtsheim, W. and Stangenberg, F., "Selected Results of Meppen Slab Tests - State of Interpretation, Comparison With Computational Investigations," Structural Mechanics in Reactor Technology, Vol. J, No. 8/1, 1983, pp. 379-386.

113. Rudiger, E. and Riech, H., "Experimental and Theoretical Investigations on the Impact of Deformable Missiles onto Reinforced Concrete Slabs," Structural Mechanics in Reactor Technology, Vol. J, No. 8/3, 1983, pp. 387-394.

114. Barr, P., Carter, P.G., Howe, W.D. and Nielson, A.J., "Replica Scaling Studies of Hard Missile Impacts on Reinforced Concrete," BAM Proceedings, 1982, pp. 329-344.

115. Brandes, K., Limberger, E. and Herter, J., "Strain Rate Dependent Energy Absorption Capacity of Reinforced Concrete Members Under Aircraft Impact," Structural Mechanics in Reactor Technology, Vol. J, No. 9/5, 1983, pp. 431-438.

116. Brandes, K., Limberger, E. and Herter, J., "Experimental Verification of Punching Shear Failure of RC Slabs Subjected to Aircraft Impact Loads," Structural Mechanics in Reactor Technology, Vol. J, No. 5/6, 1985, pp. 197-201.

117. Dulac, J. and Giraud, J., "Impact Testing of Reinforced Concrete Slabs," Structural Mechanics in Reactor Technology, Vol. J, No. 7/1, 1981, 7 pp.

118. Romander, C. and Florence, A., "Scale Model Tests of Turbine Missile Containment by Reinforced Concrete," EPRI Report NP-2747, March, 1983.

119. McHugh, S., Seaman, L. and Gupta, Y., "Scale Modeling of Turbine Missile Impact into Concrete," EPRI Report NP-2746, Feb., 1983.

120. Bauer, J., Scharpf, F. and Schwarz, R., "Analysis of Reinforced Concrete Structures Subjected to Aircraft Impact Loading," Structural Mechanics in Reactor Technology, Vol. J, No. 9/4, 1983, pp. 423-430.

121. Buchhardt, F., Magiera, G., Matthees, W. and Weber, M., "A Non-linear 3D Containment Analysis for Airplane Impact," Structural Mechanics in Reactor Technology, Vol. J, No. 9/6, 1983, pp. 439-446.

122. Crutzen, Y. and Teynen, J., "Disintegration of Concrete Shell Structures Under Violent Dynamic Loading Conditions," Structural Mechanics in Reactor Technology, Vol. J, No. 7/1, 1983, pp. 347-354.

123. Filho, F., Coumbs, R. and Burieto, L., "Design of the RC Containment Shell of a Nuclear Reactor for Aircraft Impact," Structural Mechanics in Reactor Technology, Vol. J, No. 9/11, 1981, 7 pp.

124. Puttonen, J., "The Local Deformations Caused by an Aircraft Impact on a Containment Building," Structural Mechanics in Reactor Technology, Vol. J, No. 9/12, 1981.

125. Zimmerman, T., Rebora, B. and Rodriguez, C., "Aircraft Impact on Reinforced Concrete Shells," Computers and Structures, Vol. 13, 1981, pp. 263-274.

126. Jamet, P., Berriaud, C., Millard, A., Nahas, G. and Yuritzin, T., "Perforation of a Concrete Slab by a Missile: Finite Element Approach," Structural Mechanics in Reactor Technology, Vol. J, No. 7/6, 1983, pp. 373-378.

127. Jonas, W., Meschkat, R., Reich, H. and Rudiger, E., "Approximate Calculation of the Impact of Missiles onto Reinforced Concrete Structures and Comparison of Test Results," Structural Mechanics in Reactor Technology, Vol. J, No. 8/6, 1979, 7 pp.

128. Ree, H. and Hock, M., "Analysis of the Behavior of a Concrete Structure Due to an Airplane Impact and the Effects of the Reinforcements," Structural Mechanics in Reactor Technology, Vol. J, No. 9/5, 1979, 10 pp.

129. Adamik, V., "A Theoretical Study of Reinforced Concrete Structures Under Missile Impact Loading," Nuclear Technology, Vol. 46, Dec., 1979, pp. 369-377.

130. Brown, M., Curtress, N. and Jowett, J., "Local Failure of Reinforced Concrete Under Missile Impact Loading," Structural Mechanics in Reactor Technology, Vol. J, No. 8/7, 1979, 9 pp.

131. Eibl, J. "The Design of Impact Endangered Concrete Structures," Structural Mechanics in Reactor Technology, Vol. J, No. 6/3, 1985, pp. 265-270.

132. Maurel, P., Lacoste, J.M., Hoffmann, A. and Jamet, P., "Three Dimensional Dynamic Analysis of a Thick Reinforced Concrete Slab Subjected to the Impact of a Projectile," Structural Mechanics in Reactor Technology, Vol. J, No. 6/1, 1985, pp. 203-207.

133. Marti, J., Kalsi, G.S. and Attalla, I., "Three-Dimensional Non-Linear Aircraft Impact Analysis," Structural Mechanics in Reactor Technology, Vol. J, No. 9/7, 1983, pp. 447-454.

134. Henager, C., "The Use of Steel Fiber Reinforced Concrete in Containment and Exlosive-Resistant Structures," Proceedings, The Interaction of Non-Nuclear Munitions With Structures, U.S. Air Force Academy, Colorado, May, 1983, pp. 199-203.

135. Ramakrishnan, V., Coyle, W.V., Kulandaisamy, V. and Schrader, E.V., "Performance Characteristics of Fiber Reinforced Concrete With Low Fiber Contents," ACI Journal, Sept.-Oct., 1981, pp. 388-394.

136. Kormeling, H.A., "Energy Absorbtion of Steel Fibre Reinforced Concrete Subjected to Tensile Impact Loading at +20°C and -170°C," New York - Delft Exchange Papers, Delft University of Technology, The Netherlands, Nov., 1984.

137. Arockiasamy, M., Swamidas, A.S.J., Munaswamy, K., and Cheema, P.S., "Impact Strength of Fibre Reinforced Concrete Cylindrical Panels," Structural Mechanics in Reactor Technology, Vol. H, No. 3/9, 1985, pp. 125-130.

138. Schupack, M., "Design of Permanent Seawater Structures to Prevent Deterioration," Concrete International, March, 1982, pp. 19-27.

139. ACI Committee 544, "Guide for Specifying, Mixing, Placing, and Finishing Steel Fiber Reinforced Concrete," ACI Journal, March-April, 1984, pp. 140-148.

140. Swamy, R. and Ali, S., "Punching Shear Behavior of Reinforced Slab-Column Connection Made With Steel Fiber Concrete," ACI Journal, Sept.-Oct., 1982, pp. 392-406.

141. Walraven, J.C., "Steel Fibre as Punching Shear Reinforcement," New York - Delft Exchange Papers, Delft University of Technology, The Netherlands, Nov., 1984.

142. Fujii, M. and Miyamoto, A., "Improvement of the Impact Resistance for Prestressed Concrete Slabs," Proceedings, Concrete Structures Under Impact and Impulsive Loading, West Berlin, June, 1982, pp. 266-278.

143. Hulsewig, M., Schneider, E. and Stilp, A., "Behavior of Fiber Reinforced Concrete Slabs Under Impact Loading," Proceedings, The Interaction of Non-Nuclear Munitions With Structures, U.S. Air Force Academy, Colorado, May, 1983, pp. 91-94.

144. Stangenberg, F. and Buttmann, P., "Impact Testing of Steel Fibre Reinforced Concrete Slabs With Liner," Structural Mechanics in Reactor Technology, Vol. J, No. 7/5, 1979, 8 pp.

145. Anderson, W.F., Watson, A.J. and Armstrong, P.J., "Fibre Reinforced Concretes for the Protection of Structures Against High Velocity Impact," Proceedings of the International Conference on Structural Impact and Crashworthiness, Vol. 2, Conference Papers, London, 1984, pp. 687-695.

146. Jamrozy, Z., "Lightweight Aggregate Concrete With Steel Fiber Admixture," 1978 RILEM Symposium on Testing and Test Methods of Fiber Cement Composites, The Construction Press, pp. 121-127.

147. Arockiasamy, M., Swamidas, A.S.J., Hamlyn, D. and Mumaswamy, K., "Response Studies of Concrete Shell Panel Models to Simulated Bergy-Bit Impact," 1984 IAHR Symposium on Ice, Hamburg, 12 pp.

148. Gerwick, B.C., Litton, R.W. and Reimer, R.B., "Resistance of Concrete Walls to High Concentrated Ice Loads," Proceedings 1981 Offshore Technology Conference, OTC 4111, Houston, Texas.

149. Colbjornsen, A. and Lenschow, R., "Forspente Sylinderskall Lastflatens Innvirkning Ved Local Belastning (Prestressed Cylindrical Shells Subjected to Local Loadings)," SINTEF Report No. STF65 A78036, Research Institute for Cement and Concrete, June 27, 1978, Trondheim, Norway.

150. Det norske Veritas, "Rules for the Design, Construction and Inspection of Offshore Structures, 1977.

151. Sorensen, K.A., "Behavior of Reinforced and Prestressed Concrete Tubes Under Static and Impact Loading," Proceedings of the International Conference on the Behavior of Offshore Structures (BOSS '76), Trondheim, 1976, pp. 798-813.

152. Regan, P.E. and Hamadi, V.D., "Behavior of Concrete Caisson and Tower Members," Concrete in the Oceans Technical Report No. 4, London, 1981.

153. Kavyrchine, M., "Punching Strength of Cylindrical Concrete Shells," BAM Proceedings, 1982, pp. 304-314.

154. ASCE, "Finite Element Analysis of Reinforced Concrete," Task Committee on Finite Element Analysis of Reinforced Concrete Structures of the Structural Division Committee on Concrete and Masonry Structures, American Society of Civil Engineers, New York, 1982.

155. Noguchi, H. and Inoue, N., "Analytical Techniques of Shear in Reinforced Concrete Structures by Finite Element Method," Proceedings of the ACI Colloquiem on Shear Analysis of RC Structures, June, 1982, pp. 57-92.

156. Ottosen, N.S., "A Failure Criterion for Concrete," Journal of the Engineering Mechanics Division, ASCE, Vol. 103, No. EM4, Aug., 1977, pp. 527-535.

157. Ottosen, N.S., "Constitutive Model for Short-Time Loading of Concrete," Journal of the Engineering Mechanics Division, Vol. 105, No. EM1, Feb., 1979, pp. 127-141.

158. Willam, K.J. and Warnke, E.P., "Constitutive Model For the Triaxial Behavior of Concrete," International Association of Bridge and Structural Engineers, Seminar on Concrete Structures Subjected to Triaxial Stresses, Paper III-1, Bergamo, Italy, May 17-19, 1974.

159. Bazant, Z.P. and Bhat, P., "Endochronic Theory of Inelasticity and Failure of Concrete," Journal of the Engineering Mechanics Division, ASCE, Vol. 102, 1976, pp. 701-722.

160. Scordelis, A.C., "Finite Element Analysis of Reinforced Concrete Structures," Proceedings of the Specialty Conference on Finite Element Method in Civil Engineering, Montreal, Canada, June, 1972.

161. Ingraffea, A.R., Gerstle, W.H., Gergely, P. and Saouma, V., "Fracture Mechanics of Bond in Reinforced Concrete," Journal of Structural Engineering, Vol. 110, No. 4, April, 1984, pp. 871-890.

162. Ngo, D. and Scordelis, A.C., "Finite Element Analysis of Reinforced Concrete Beams," Journal of the American Concrete Institute, Vol. 64, No. 3, March, 1967, pp. 152-163.

163. Nilson, A.H., "Nonlinear Analysis of Reinforced Concrete by the Finite Element Method," Journal of the American Concrete Institute, Vol. 65, No. 9, Sept., 1968, pp. 757-766.

164. Kesler, C.E., Naus, D.J. and Lott, J.L., "Fracture Mechanics - Its Applicability to Concrete," Proceedings of the 1971 International Conference on Mechanical Behavior of Materials, Vol. IV, Japan, 1972, pp. 113-124.

165. Ingraffea, A.R. and Gerstle, W.H., "Non-Linear Fracture Models for Discrete Crack Propagation," Application of Fracture Mechanics to Cemetitious Composites, NATO-ARW - September 4-7, 1984, Northwestern University, S.P. Shah, editor, pp. 171-209.

166. Ingraffea, A.R. and Saouma, V., "Numerical Modeling of Discrete Crack Propagation in Reinforced and Plain Concrete," Application of Fracture Mechanics to Concrete Structures, G.C. Sih and A. DiTommaso, eds, The Hague, Martinus Nijhoff Publishers, 1984.

167. Walraven, J.C., "Aggregate Interlock: A Theoretical and Experimental Analysis," Dissertation, Delft University of Technology, The Netherlands, 1980.

168. Pruijssers, A.F., "Description of the Stiffness Relation for Mixed-Mode Fracture Problems in Concrete Using the Rough Crack Model of Walraven," Report No. 5-85-2, Delft University of Technology, The Netherlands, 1985.

169. Bazant, Z.P. and Gambarova, P., "Rough Cracks in Reinforced Concrete," Journal of the Structural Division, ASCE, Vol. 106, No. ST4, April, 1980, pp. 819-842.

170. Hand, F.R., Pecknold, D.A. and Schnobrich, W.C., "Nonlinear Layered Analysis of RC Plates and Shells," Journal of the Structural Division, ASCE, Vol. 99, No. ST7, July, 1973, pp. 1491-1505.

171. Lin, C.S. and Scordelis, A., "Nonlinear Analysis of RC Shells of General Form," Journal of the Structural Division, ASCE, No. ST3, March, 1975.

172. Loseth, S., Slatto, A. and Syvertsen, T.G., "Finite Element Analysis of Punching Shear Failure of Reinforced Concrete Slabs," Nordic Concrete Research, No. 1, Dec., 1982, 17 pp., Trondheim, Norway.

173. Tao, Xuekang and White, R.N., "Finite Element Prediction of Punching Shear Failure of Axisymmetric Reinforced Concrete Slabs," Report No. 84-9, Cornell University, Ithaca, New York, July, 1984.

174. Scanlon, A., "Time Dependent Deflections of Reinforced Concrete Slabs," Dissertation, Department of Civil Engineering, University of Alberta, Edmonton, Canada, Dec., 1971.

175. Borst, R. de and Nauta, P., "Smeared Crack Analysis of Reinforced Concrete Beams and Slabs Failing in Shear," Proceedings of the International Conference on Computer-Aided Analysis and Design of Concrete Structures, Part I, Sept., 1984, Split, Yugoslavia, pp. 261-273.

176. Litton, R.W., "A Contribution to the Analysis of Concrete Structures Under Cyclic Loadings," Dissertation, University of California, Berkeley, 1976.

Table 1 Comparison of effective ice pressures for vertical piles and piers (from Reference 13)

Source		Range of Pressures Specified or Implied (psi), kPa
Korzhavin 1962: USSR rivers, spring break-up		(70 - 270 psi) 490 - 1860
AASHO and CSA (old), Highway bridge codes		(400 psi) 2760
New CSA Code S-6 (1974), Highway Bridges		(100 - 400 psi) 690 - 2760
USSR Code SN 76-66: River Structures		(45 - 190 psi) 295 - 1320
Canada Ministry of Transport - Navigation Lightpiers, St. Lawrence		(140 - 175 psi) 965 - 1210
Canada Dept. of Public Works - Wharf Piles		(200 - 250 psi) 1380 - 1720
Wedge Formula (warm ice -1.5°C)	3 m dia structure	(250 psi) 1755
	30 m dia structure	(200 psi) 1390
Michel and Toussaint (warm ice -1.5°C)	Ductile	(690 psi) 4810
	Brittle	(230 psi) 1620
Tryde (-1.5°C)	3 m dia structure	(555 psi) 3860
	30 m dia structure	(370 psi) 2580
Wedge Formula (cold ice -10°C	3 m dia structure	(585 psi) 4095
	30 m dia structure	(460 psi) 3255
Michel and Toussaint (cold ice -10°C)	Ductile	(1600 psi) 11230
	Brittle	(580 psi) 4050
Tryda (-10°C)	3 m dia structure	(1300 psi) 9070
	30 m dia structure	(860 psi) 5990

Table 2 Expressions for ultimate shear strength (adapted from Reference 37)

Investigator	Nominal Shear Stress	Limiting Shear Stress	Eq. No.	Remarks
EXPRESSIONS DEPENDENT PRIMARILY ON CONCRETE STRENGTH				
Hognestad [76]	$\frac{V_u}{7/8\ bd}$	$= (0.035 + \frac{0.07}{\phi_o})\ f'_c + 130$ psi	(1)	$f'_c > 1800$ psi (126 kgf/cm^2) Stages I and II, Fig. 2
Elstner and Hognestad [43]	$\frac{V_u}{7/8\ bd}$	$= 333$ psi $+ \frac{0.046\ f'_c}{\phi_o}$	(2)	
Moe [47]	$\frac{V_u}{bd}$	$= \frac{15(1 - 0.075c/d)\sqrt{f'_c}}{1 + \frac{5.25\ bd\sqrt{f'_c}}{V_{flex}}}$	(3)	Not intended for c/d ratios much larger than 3.0
Moe [47]	$\frac{V_u}{bd}$	$= (9.23 - 1.12\ c/d)\sqrt{f'_c}$ for $c/d \leq 3$	(4a)	Modifications of Eq. 3 for design
	$\frac{V_u}{bd}$	$= (2.5 + 10d/c)\sqrt{f'_c}$ for $c/d > 3$	(4b)	
Tasker and Wyatt [77]	$\frac{V_u}{b'd}$	$= [8.27\ (1 + 1.21\ d/c) - 5.25\ \phi_o]\sqrt{f'_c}$	(5)	Modification of Eq. 3
Tasker and Wyatt [77]	$\frac{V_u}{b'd}$	$= (2.5 + \frac{10}{1 + c/d})\sqrt{f'_c}$	(6)	Lower bound of Eq. 5 for design
Herzog [78]	$\frac{V_u}{4\ (c + d)d}$	$= (2.64 + 0.00477\ \rho f_y)\sqrt{f'_c} \leq 6.3\ f'_c$	(7)	For design
Mowrer and Vanderbilt [79]	$\frac{V_u}{bd}$	$= \frac{9.7\ (1.0 + d/c)\sqrt{f'_c}}{1 + \frac{5.25\ bd\sqrt{f'_c}}{V_{flex}}}$	(8)	
Long [84]	$\frac{V_u}{bd}$	$= \frac{\rho f_y d\ (1 - 0.59)\rho f_y/f'_c}{b\ (0.2 - 0.9\ c/L)}$	(9a)	Whichever is smaller
or	$\frac{V_u}{bd}$	$= \frac{20\ (c + d)(100\rho)^{.25}\sqrt{f'_c}}{b\ (0.75 + 4\ c/L)}$	(9b)	
EXPRESSIONS DEPENDENT PRIMARILY ON FLEXURAL EFFECTS				
Whitney [80]	$\frac{V_u}{4d\ (r + d)}$	$= 100$ psi $+ 0.75\ \frac{M_u\sqrt{d/l_s}}{d^2}$	(10)	
Yitzhaki [81]	$\frac{V_u}{bd}$	$= 8\ (1 - \frac{\rho f_y}{2f'_c})\ \frac{d}{b}\ (149.3 + 0.164\ \rho f_y)\ (1 + \frac{c}{2d})$	(11)	
Blakey [82]	V_u	$= \frac{-2\pi\ (m_x + m_y)}{\ln \frac{c}{L} + 1.31}$	(12)	Expression for V_u, not a nominal shear stress
Gesund and Kaushik [83]	V_u = Yield line capacity if $Q = \frac{\rho^2 f_y d^2 10^4}{\sqrt{f'_c}\ bB} \leq 2$		(13)	Based on $f_y = 40$ ksi (2812 kgf/cm^2)
	If $Q \geq 4$ Shear failure.			ρ = negative moment steel ratio unless positive steel stops short of column
				then $\rho = \rho + \rho'$

Table 2 (continued) Notation used in expressions
(adapted from Reference 37)

b = perimeter of loaded area

b' = perimeter of column collar (Eqs. 5 and 6)

b_o = perimeter of critical section located d/2 from column perimeter

c = side length of square column or diameter of circular column

d = effective depth

f'_c = concrete cylinder compressive strength

f_y = yield strength of reinforcement

h = overall depth of slab

l_s = shear span of slab=distance from face of column or cap to line of contraflexure

L = span between center of columns

m_x, m_y = moments in x, y direction per unit width

v_u = ultimate nominal shear stress

V_u = ultimate shear force

V_{flex} = ultimate flexural capacity determined from yield line analysis

ϕ_o = V_u/V_{flex}

ρ = negative moment reinforcement ratio

ρ' = positive moment reinforcement ratio

PARAMETERS	ACI 318-83	CEB-FIP	CP110
critical section	d/2	d/2	1.5h
lightweight agg. factor	0.75 all lightweight/ 0.85 sand-lightweight	K = 1.0 always	0.80
flex. reinf. factor	——	$50\rho_\ell$, $\rho_\ell \leq 0.008$	in v_o term
thickness factor	——	K = 1.6 - d ≥ 1.0 m	in ε_o term
shape factor	β_c = long side / short side	for aspect ratios > 2, special provisions	——
axial restraint factor	none, except for special provisions for two-way prestress	$\beta_1 = 1+(M_o/M_{sdu}) \leq 2$ where the concrete shear strength is multplied by β_1	none, except for special provisions for prestress
shear strength of concrete w/o shear reinforcement	$V_c=(2+4/\beta_c)\sqrt{f'_c}b_od \leq 4\sqrt{f'_c}b_od$ or for two-way prestress $V_c=(3.5\sqrt{f'_c}+.3f_{pc})b_od+V_p$ where $f'_c \leq 5000$ psi and 125 psi $\leq f_{pc} \leq$ 500 psi	$V_{Rd1}=1.6\,\tau_{Rd}K(1+50\rho_\ell)ud$ τ_{Rd} given in tables	$V = v\,u_{crit}\,d$ where $v = v_o\,\varepsilon_o$ and v_o, ε_o are given in tables, special provisions for prestressed slabs
shear strength of concrete w/ shear reinforcement	$V_c = 2\sqrt{f'_c}b_od$	as above	as above
limitations on total shear	$V_{max} \leq 6\sqrt{f'_c}b_od$ for bar reinforcement, or $V_{max} \leq 7\sqrt{f'_c}b_od$ for shearhead reinforcement	$V_{max} \leq 1.6\,V_{Rd1}$	V_{max} specified in tables

Table 3 Summary of code provisions on punching shear

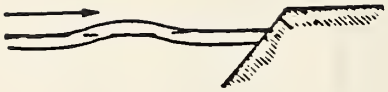

Buckling

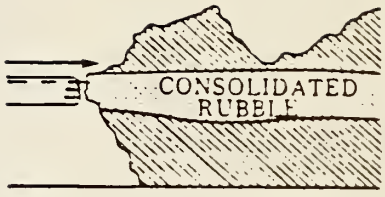

Crushing

Flexure

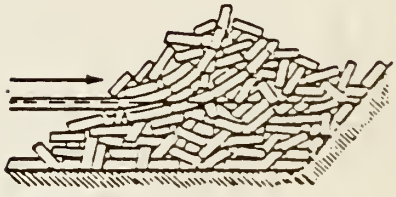

Rubble formation

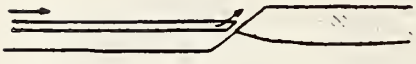

Adfreeze bond fails then ice fails in flexure

Ductile flow of ice around structure

Figure 1 Possible ice failure modes (adapted from References 7, 9 and 10)

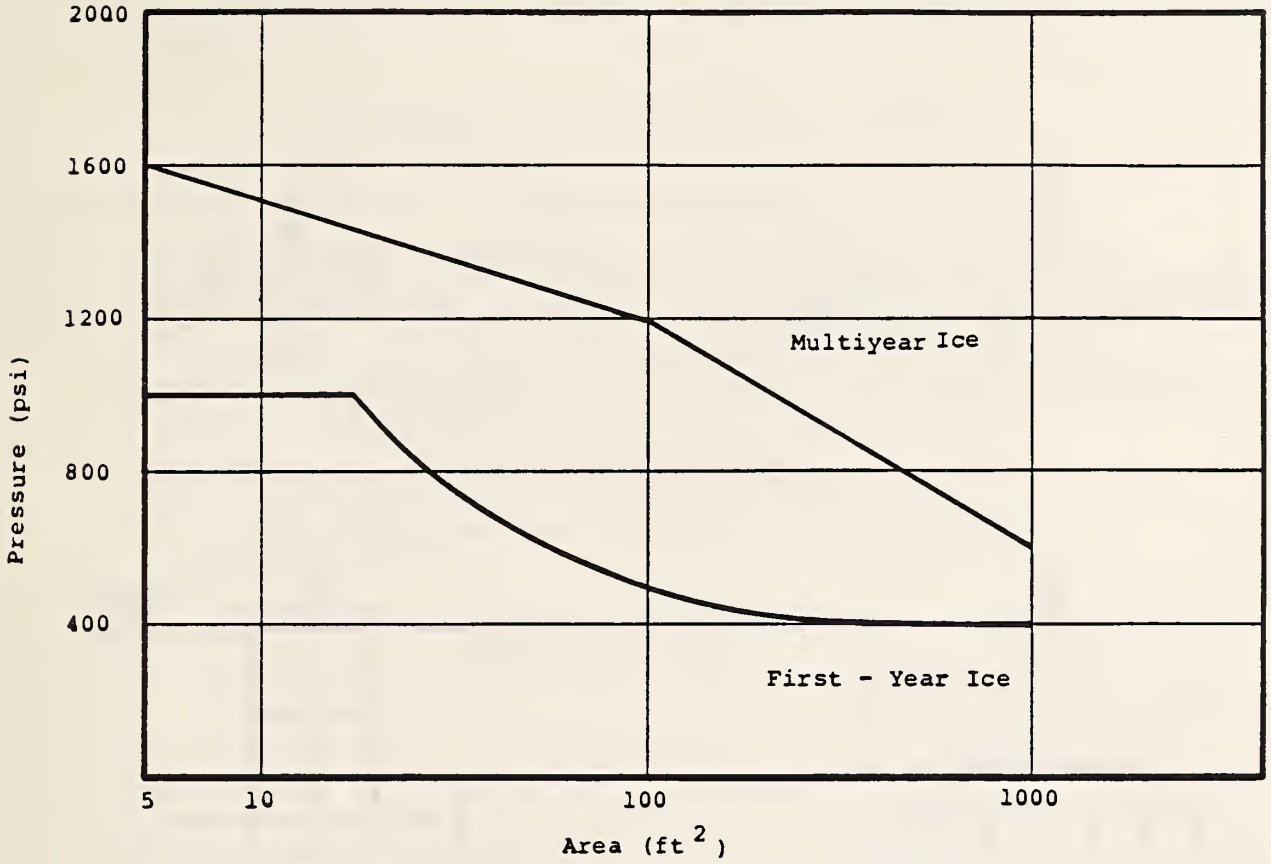

(a) — Comparison of pressure from first and multiyear floes
(from Reference 28)

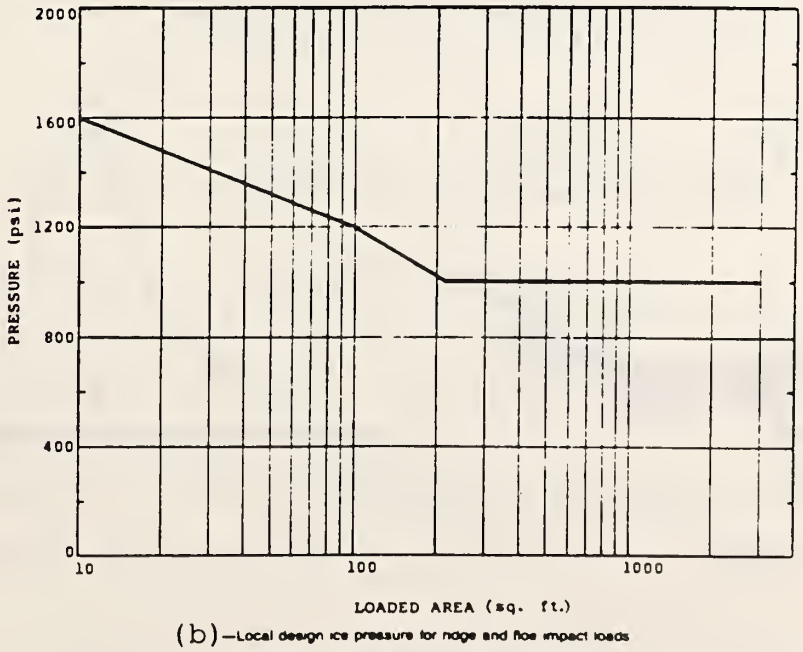

(b)—Local design ice pressure for ridge and floe impact loads
(from Reference 26)

Figure 2 Local ice pressure design curves

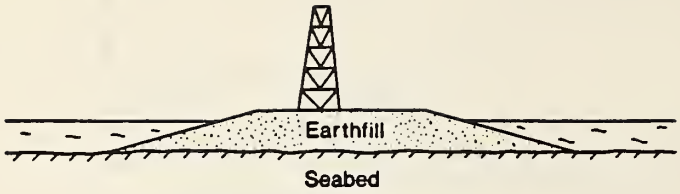

a) artificial island

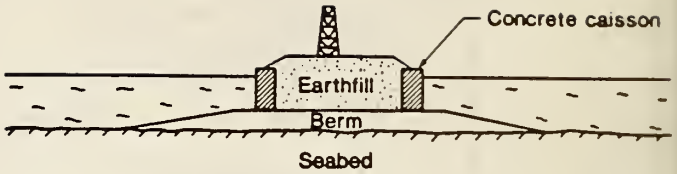

b) caisson-retained island

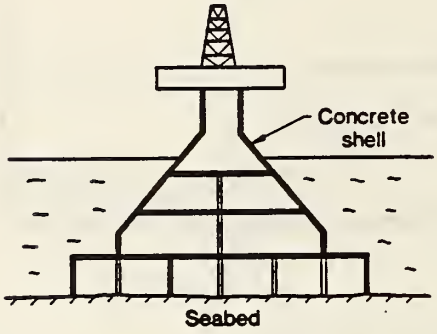

c) conical gravity structure

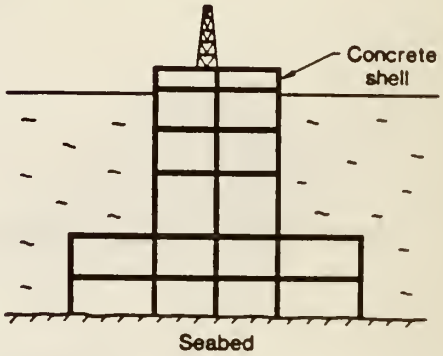

d) caisson gravity structure

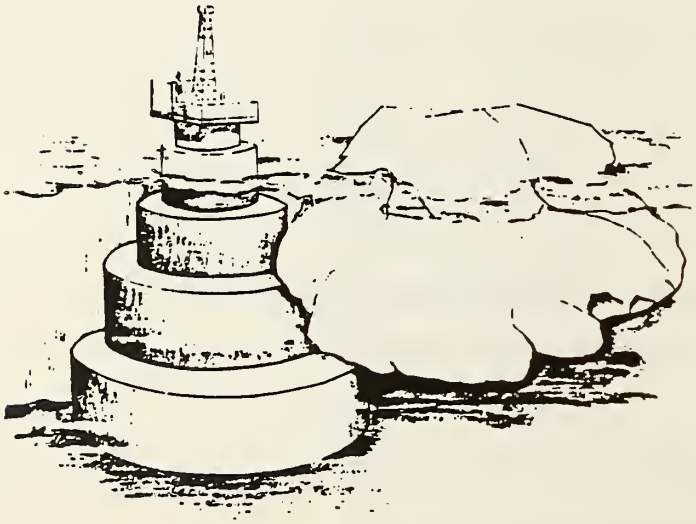

e) stepped structure

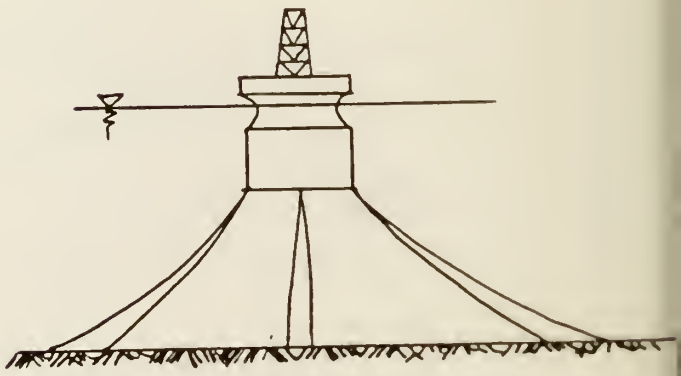

f) floating structure

Figure 3 Example configurations of Arctic offshore structures (adapted from References 3 and 29)

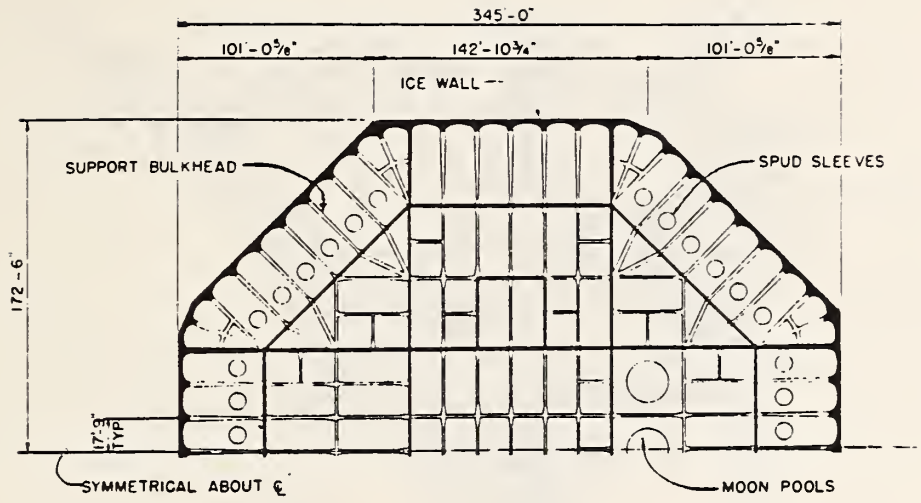

(a) plan view

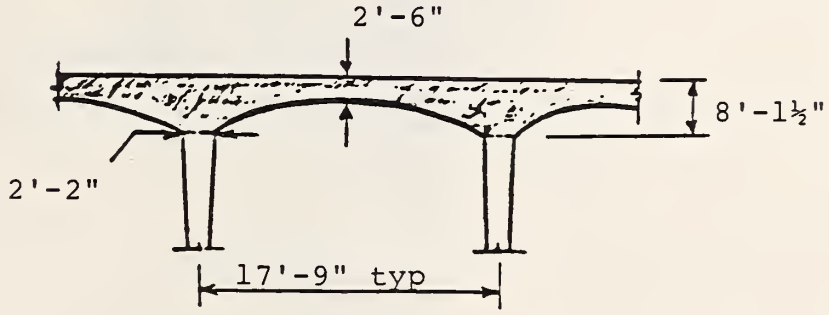

(b) detail of wall

Figure 4 SOHIO Arctic Mobile Structure (SAMS)
(from Reference 25)

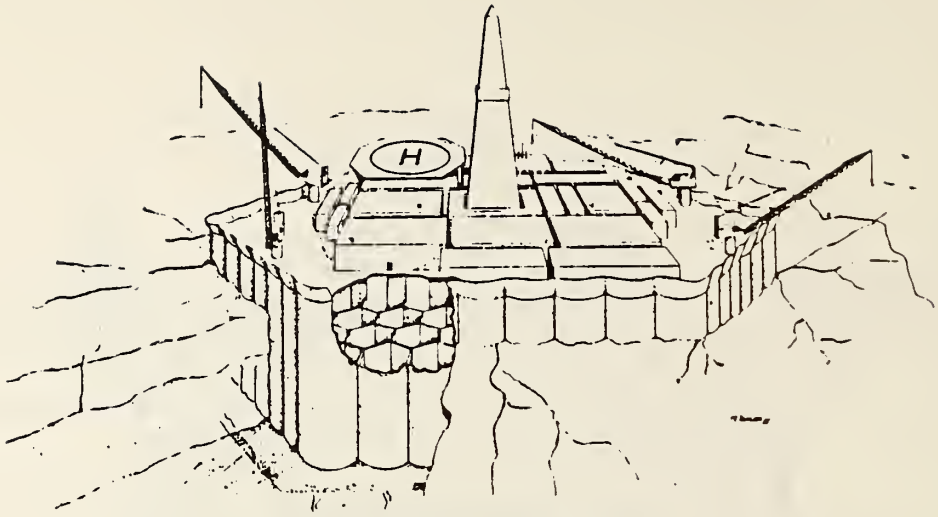

(a) perspective view

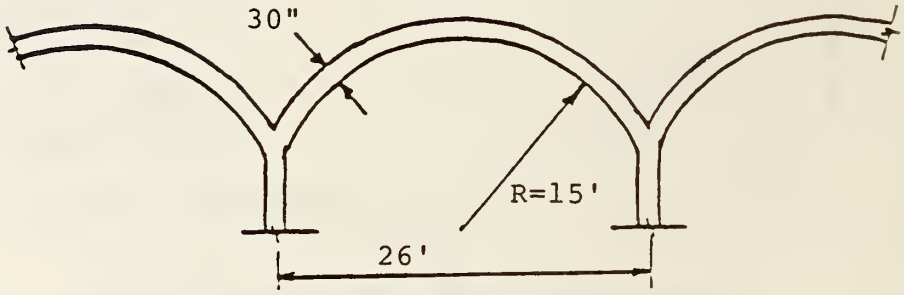

(b) wall detail

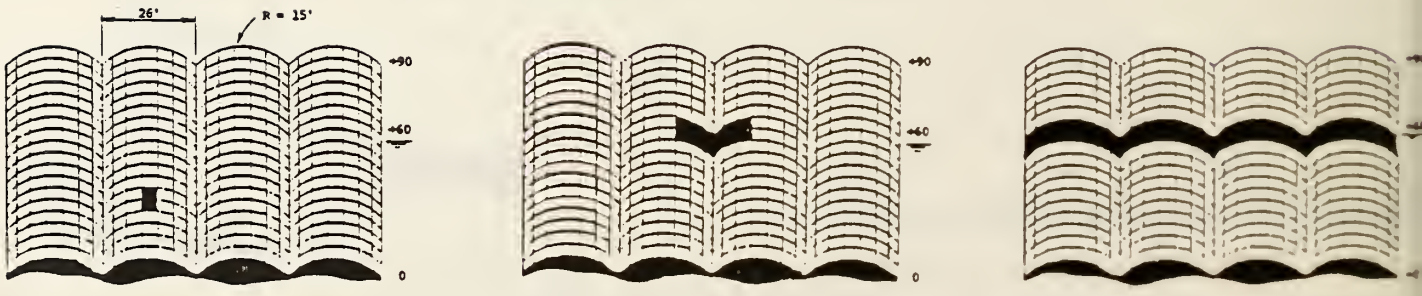

(c) typical extreme ice load patterns for BWACS design

Figure 5 Brian Watt Associates Caisson System (BWACS) (from Reference 31)

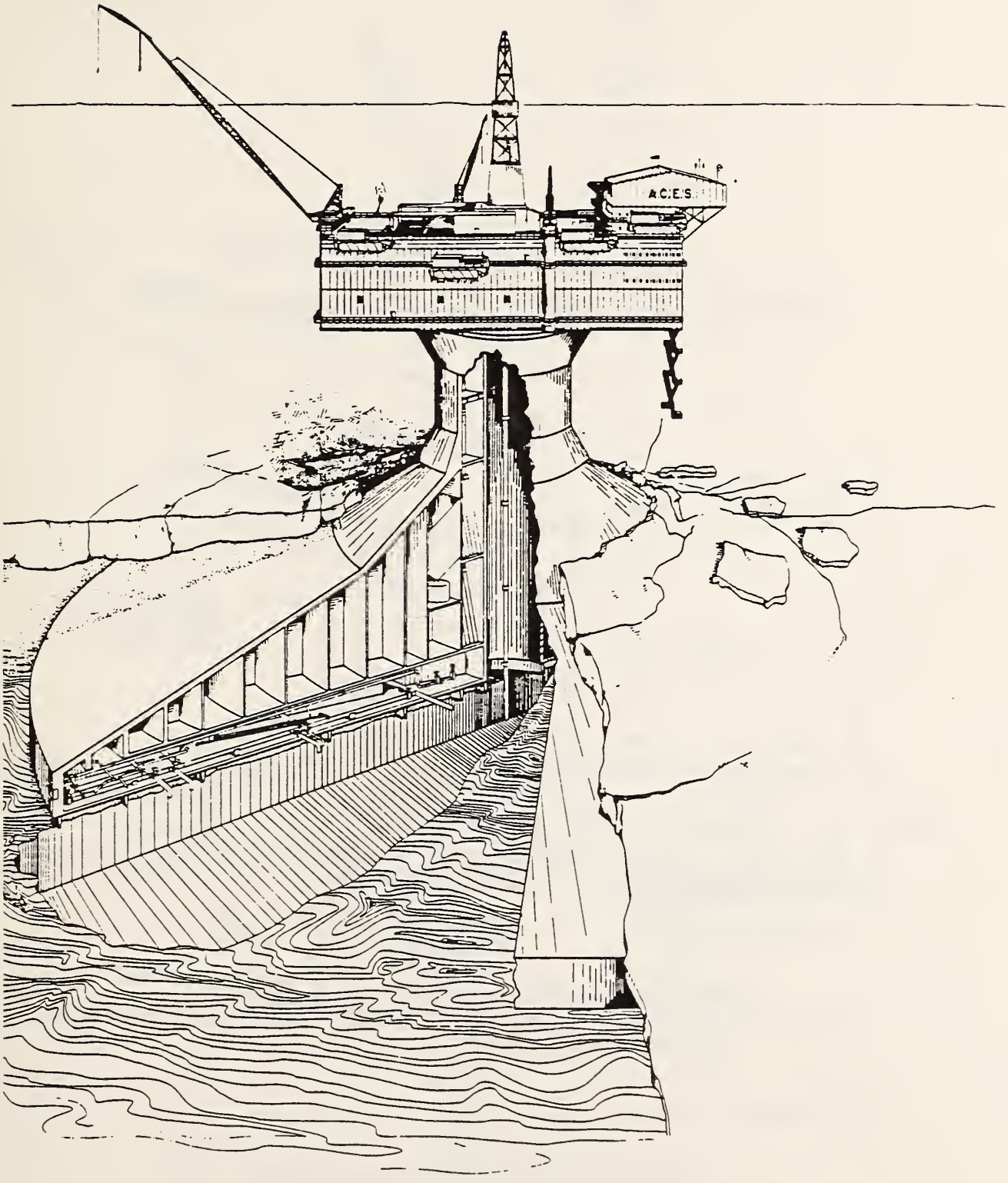

Figure 6 Artist's sketch of the Arctic Cone Exploration Stucture (ACES) (from Reference 26)

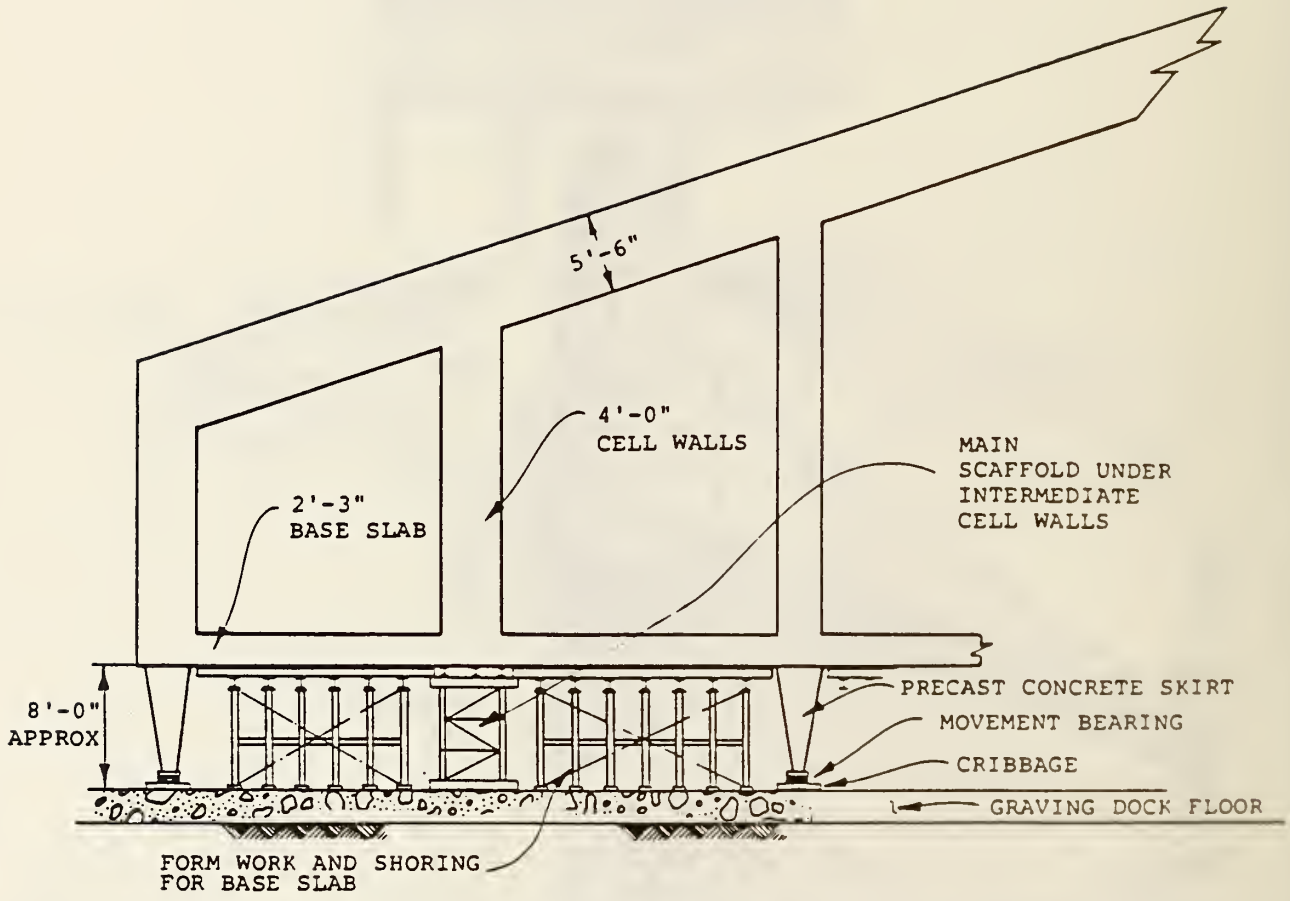

Figure 7 Typical details of initial construction (ACES) (from Reference 26)

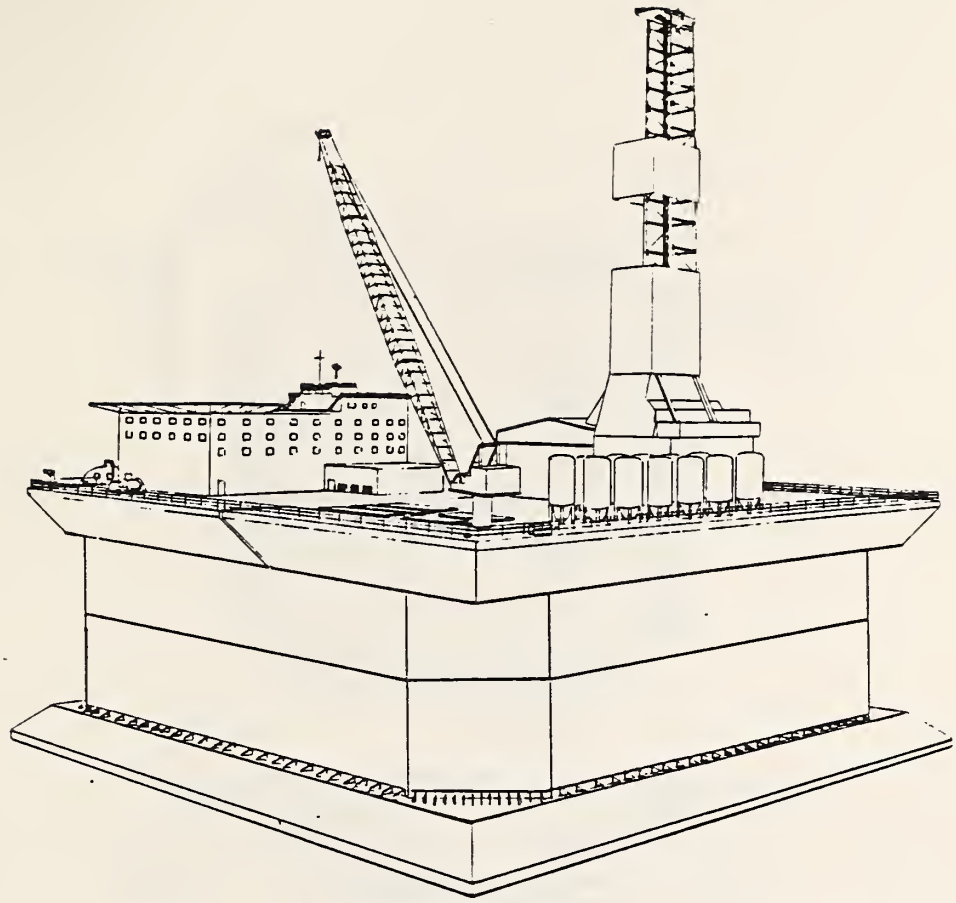

(a)—Super CIDS—isometric.

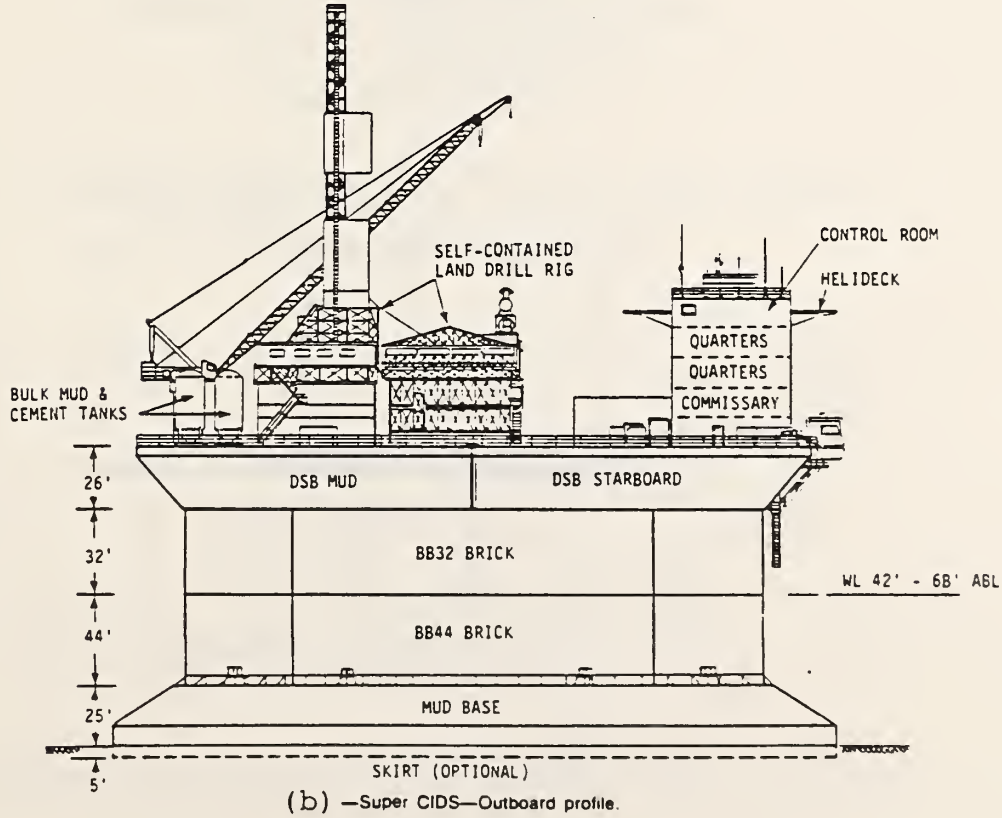

(b) —Super CIDS—Outboard profile.

Figure 8 Concrete Island Drilling System: Super Series (Super CIDS) (from Reference 27)

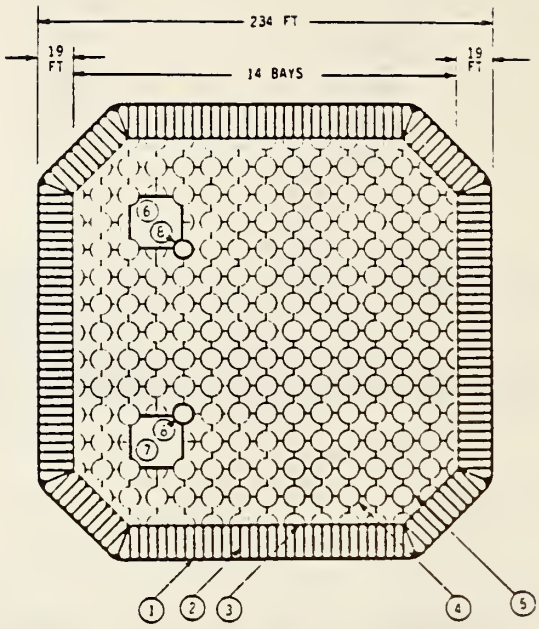

(a) brick structural arrangement

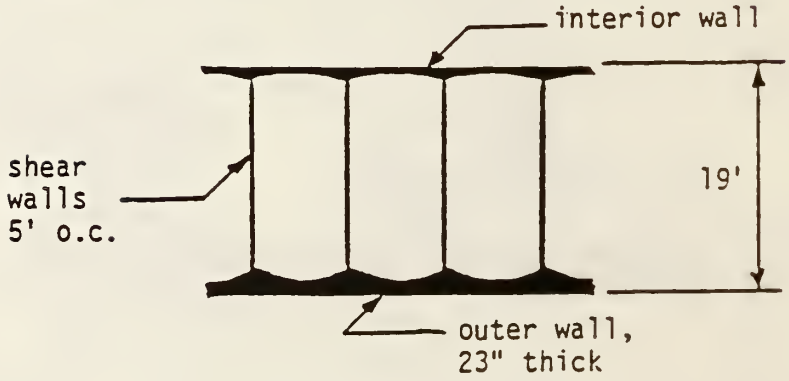

(b) outer wall dimensions

Figure 9 Super CIDS brick dimensions and details (from Reference 27)

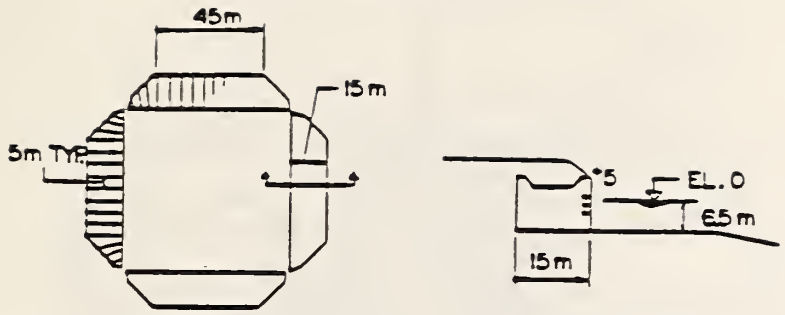

Figure 10 Tarsiut Island, general arrangement (from Reference 35)

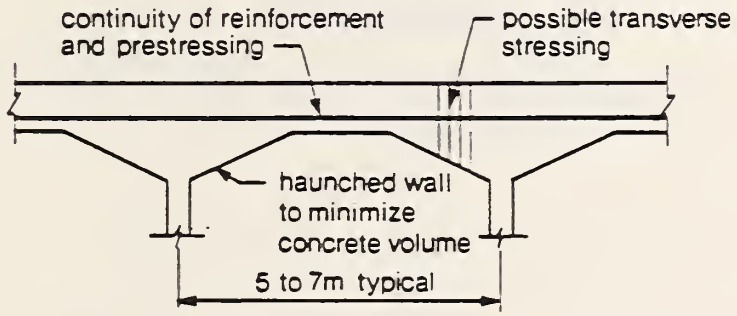

Figure 11 Structural arrangement for concrete ice wall (from Reference 1)

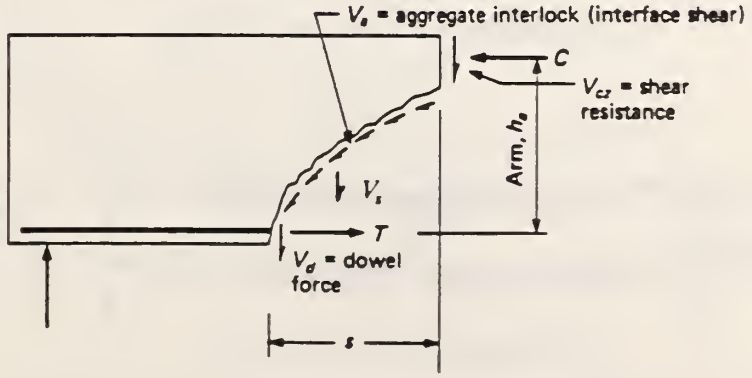

Figure 12 Shear transfer mechanisms in a cracked beam (adapted from Reference 39)

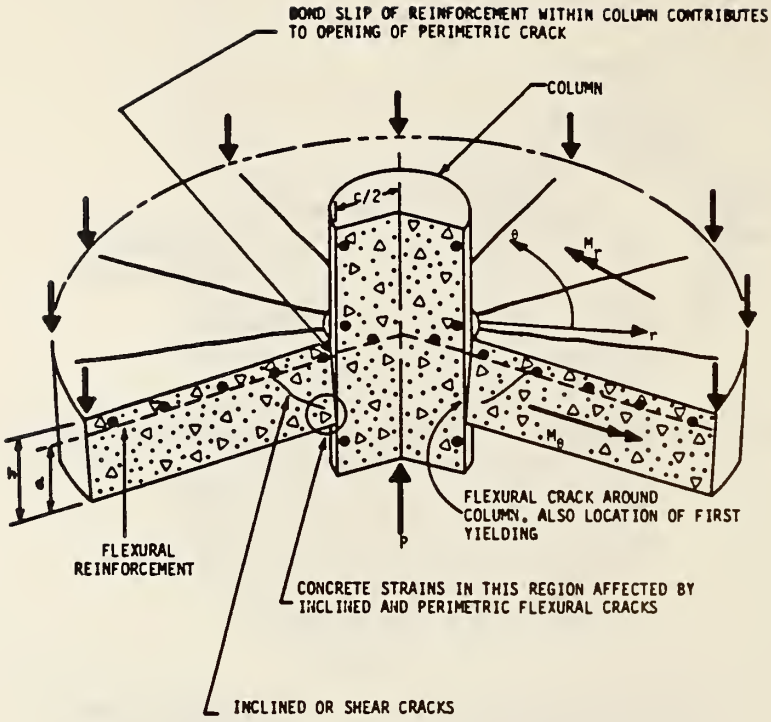

Figure 13 Crack formation in the column area of a slab (from Reference 40)

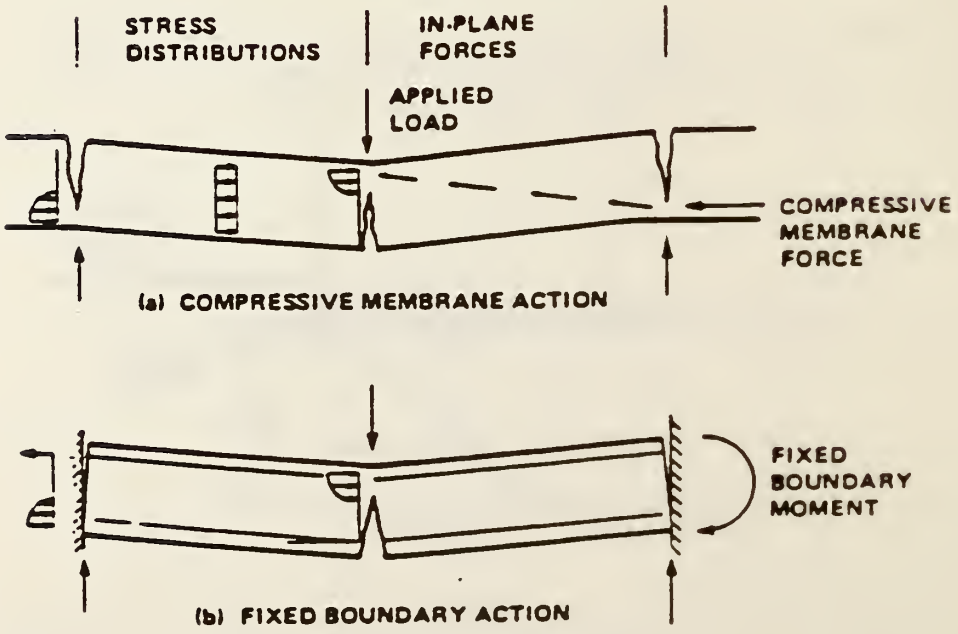

Figure 14 Arching action in slabs (from Reference 61)

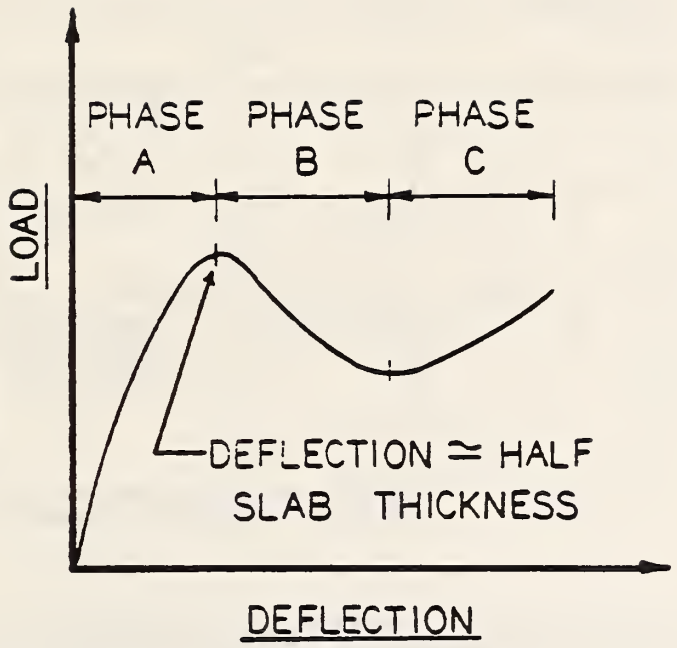

(a) load-deflection curve

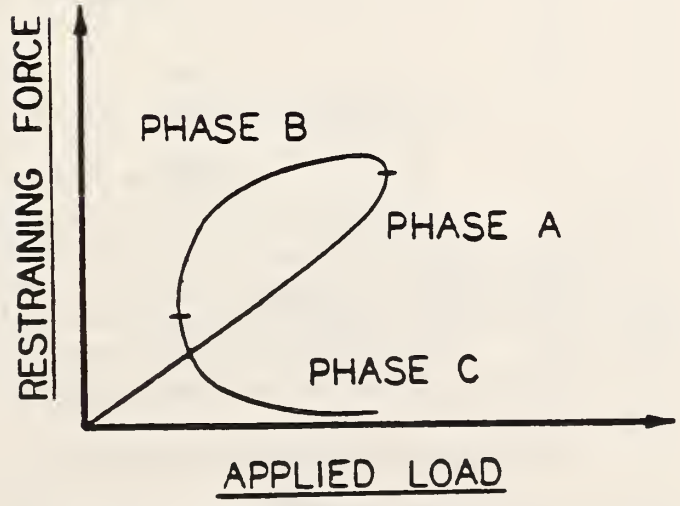

(b) load-restraining force curve

Figure 15 Typical curves for an underreinforced slab (from Reference 61)

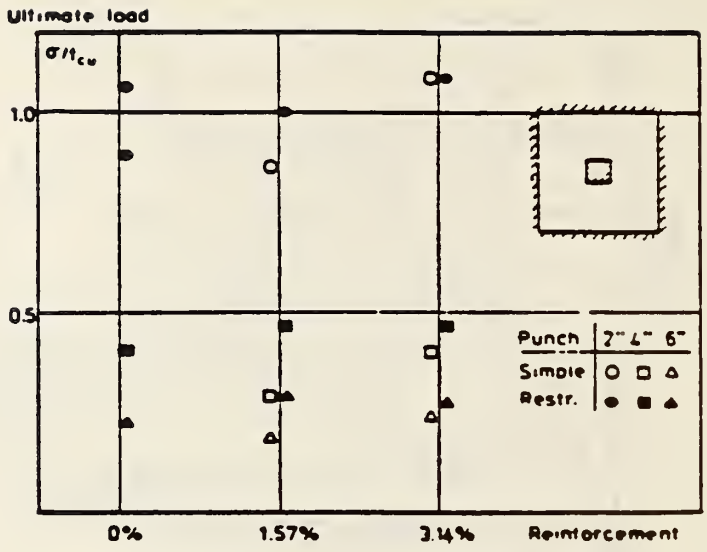

Figure 16 Punch load vs. flexural reinforcement for the simple and restrained slabs tested by Taylor and Hayes [63] (from Reference 87)

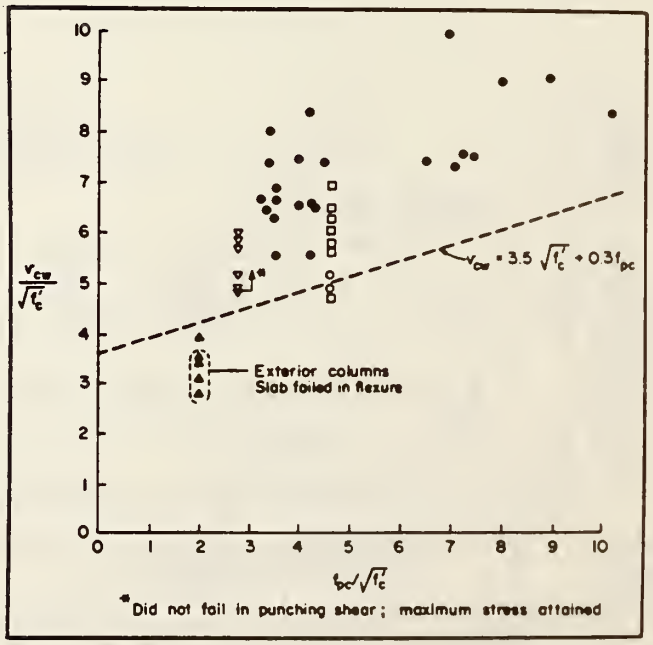

Figure 17 Shear test data vs. Eq. 11-37 of ACI 318-83 for two-way prestressed slabs (from Ref. 72)

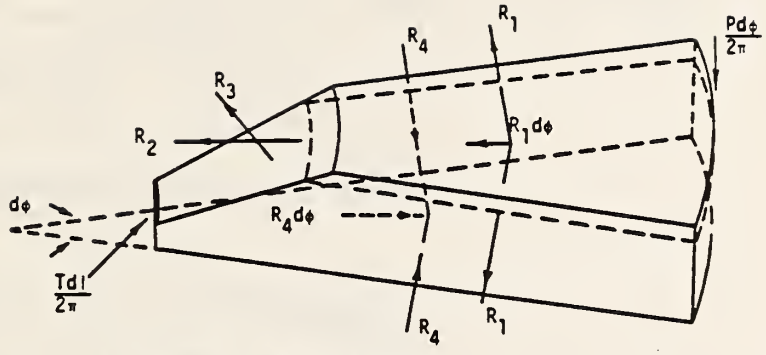

(A) FORCES ACTING ON A SLAB

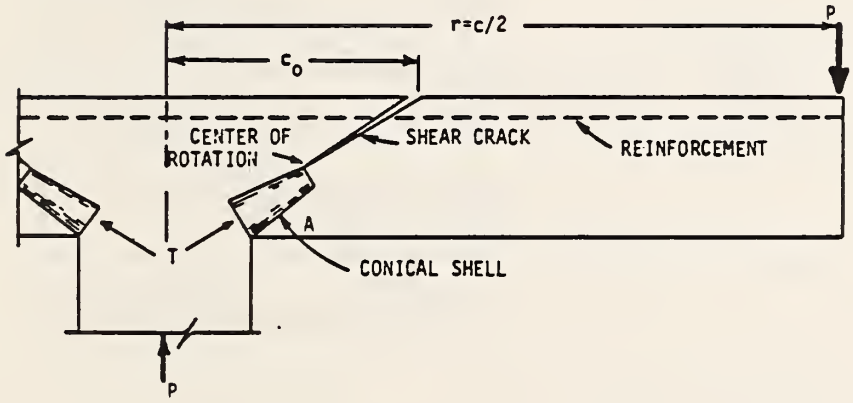

(B) ASSUMED GEOMETRY OF CONNECTION

LEGEND

P = Applied Load at the Slab Periphery
T = Inclined Compressive Force Acting on the Conical Shell
R_1 = Resultant Perpendicular to Radial Crack of the Reinforcement
R_2 = Resultant Perpendicular to Shear Crack of the Reinforcement
R_3 = Resultant of Shear Reinforcement, If Any
R_4 = Tangential Resultant of the Concrete Compressive Stresses

Figure 18 Idealized connection model of Kinnunen and Nylander [68] (from Reference 37)

(a) American building code

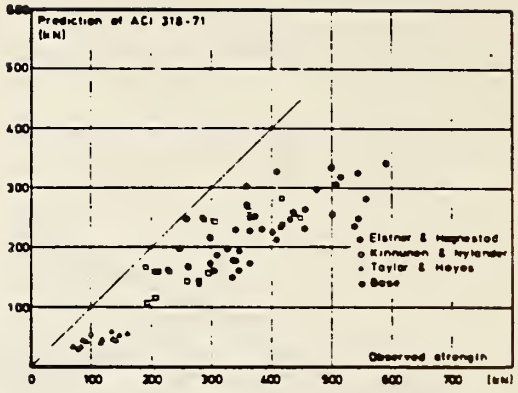

(b) European Model Code

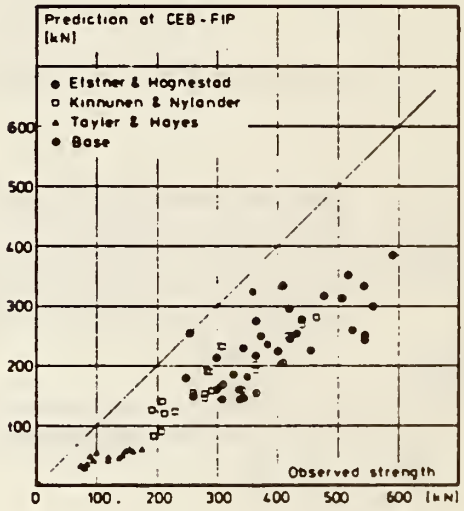

(c) British code of practice

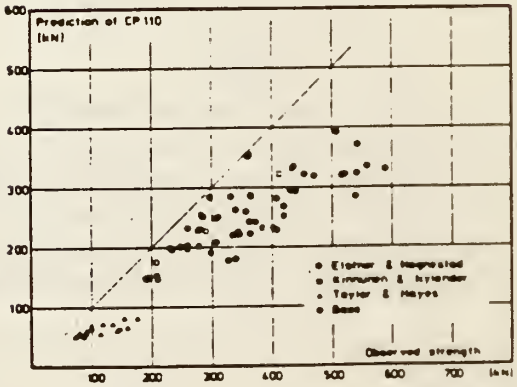

Figure 19 Punching test results compared with code predictions (from Reference 87)

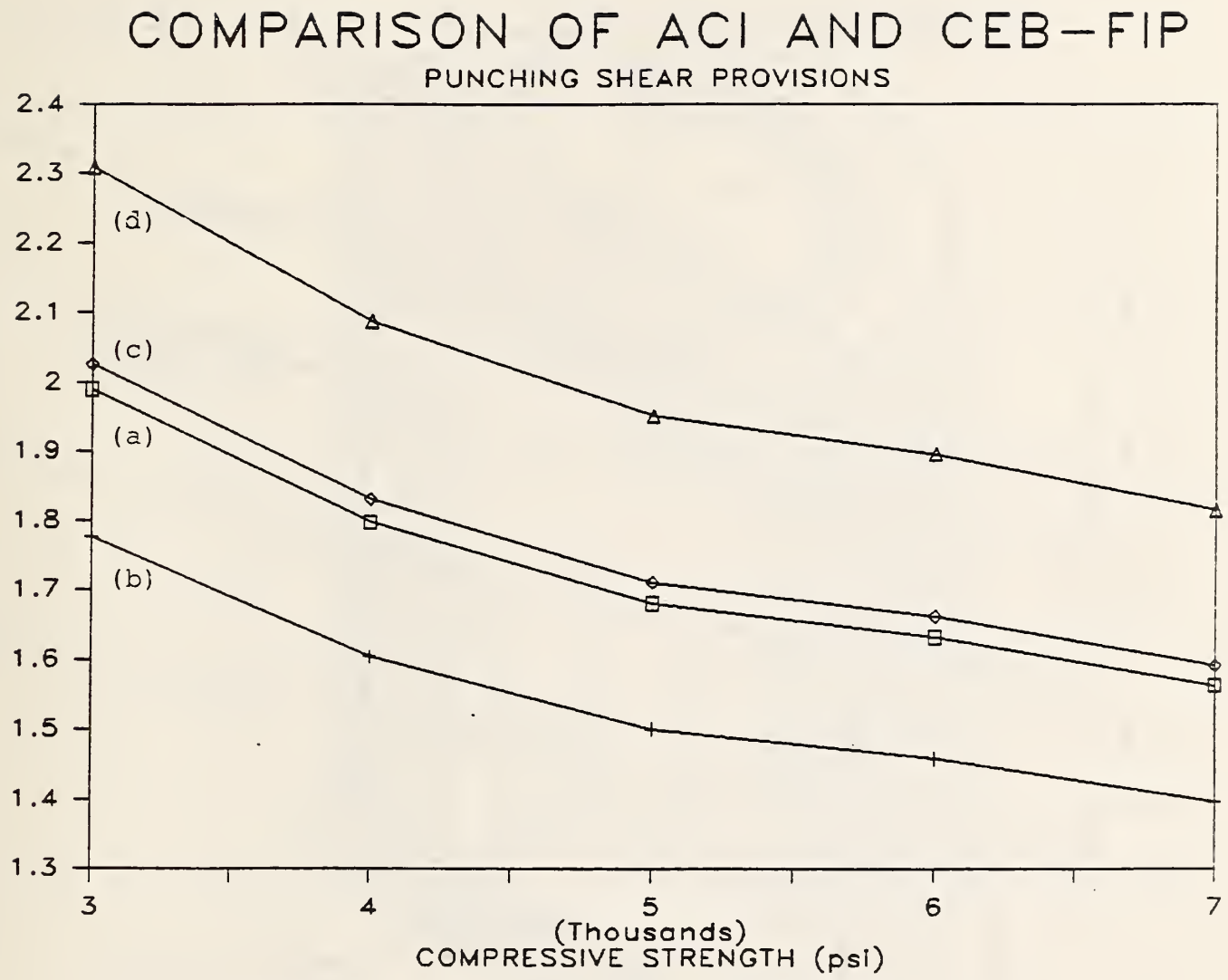

(a) diameter of load = 12 in., d = 12 in., ρ_f = 0.005
(b) diameter of load = 12 in., d = 12 in., ρ_f = 0.01
(c) diameter of load = 36 in., d = 18 in., ρ_f = 0.01
(d) diameter of load = 36 in., d = 36 in., ρ_f = 0.02

Figure 20 Comparison of punching shear provisions for selected parameters: ACI vs. CEB-FIP

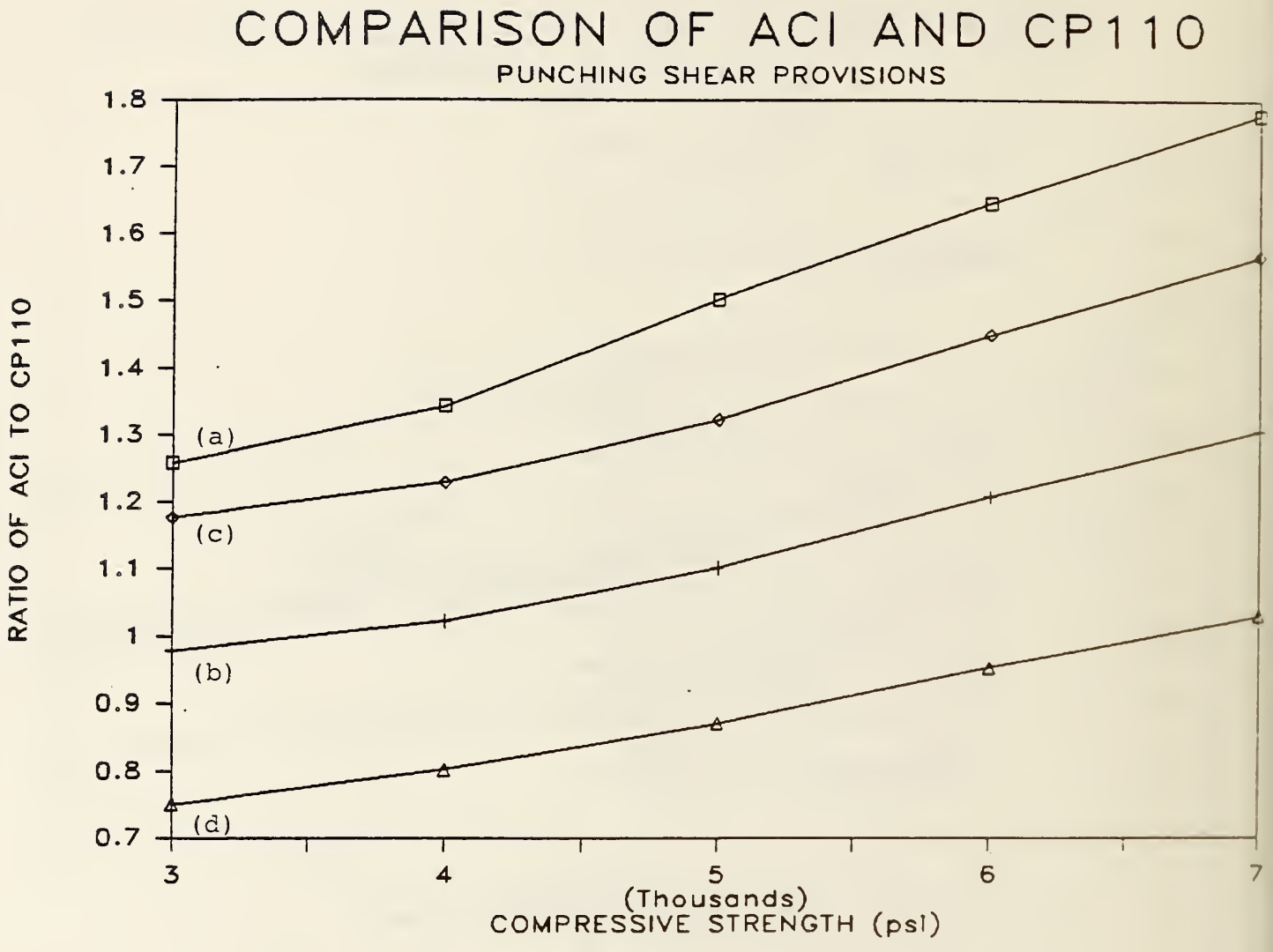

(a) diameter of load = 12 in., d = 12 in., ρ_f = 0.005
(b) diameter of load = 12 in., d = 12 in., ρ_f = 0.01
(c) diameter of load = 36 in., d = 18 in., ρ_f = 0.01
(d) diameter of load = 36 in., d = 36 in., ρ_f = 0.02

Figure 21 Comparison of punching shear provisions for selected parameters: ACI vs. CP110

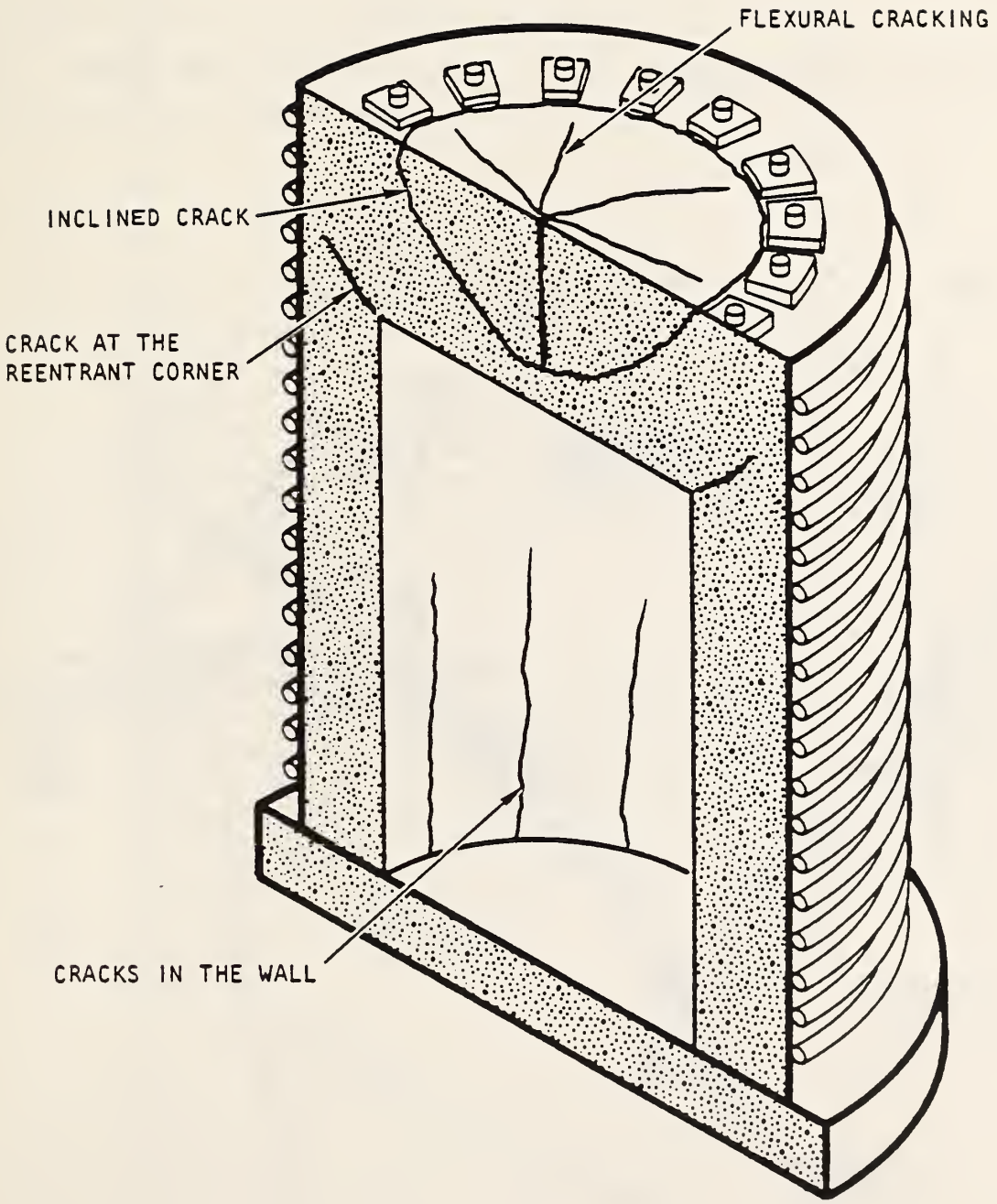

Figure 22 Different types of cracks observed in pressure vessels (from Reference 98)

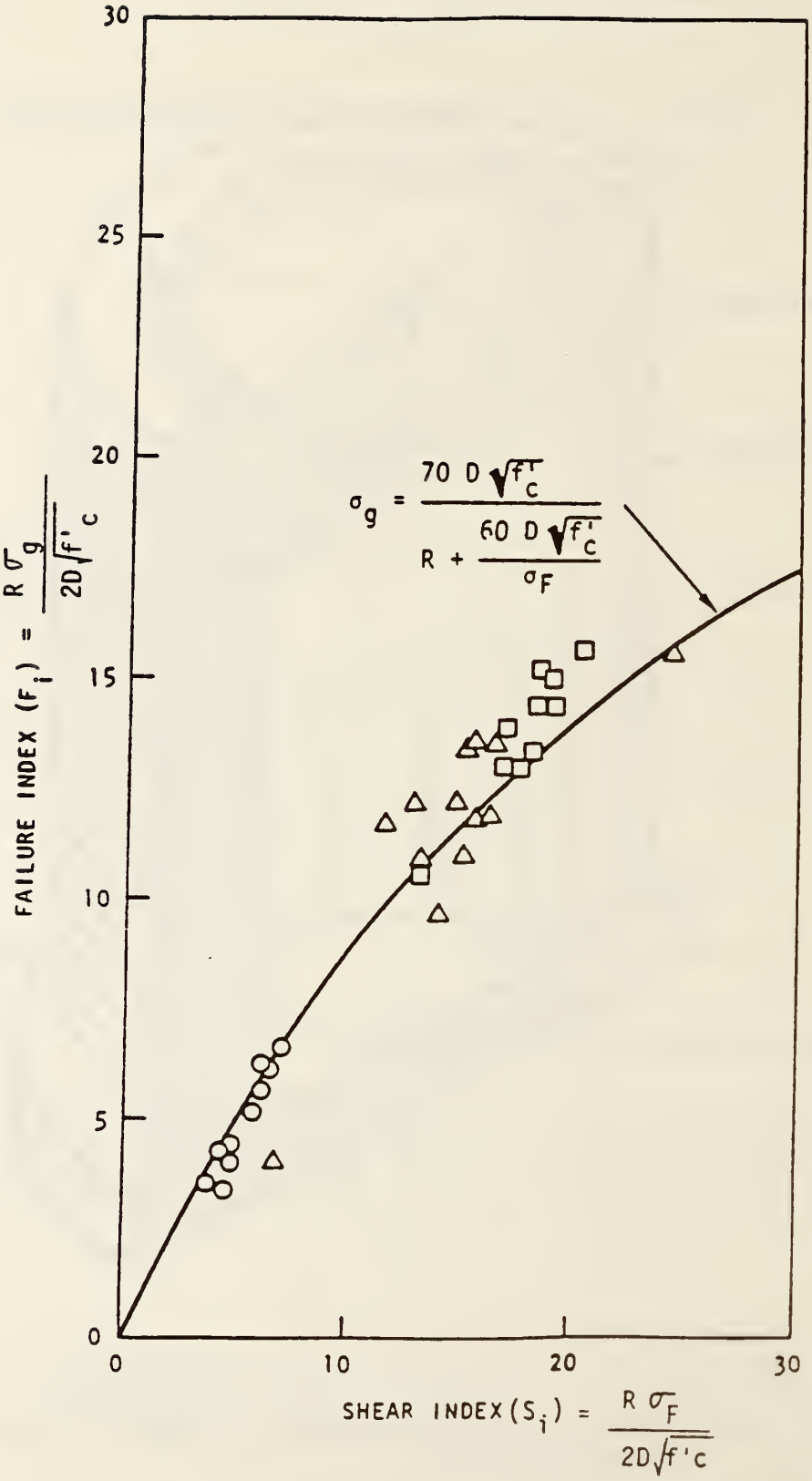

Figure 23 Shear-flexure interaction curve (adapted from Reference 95)

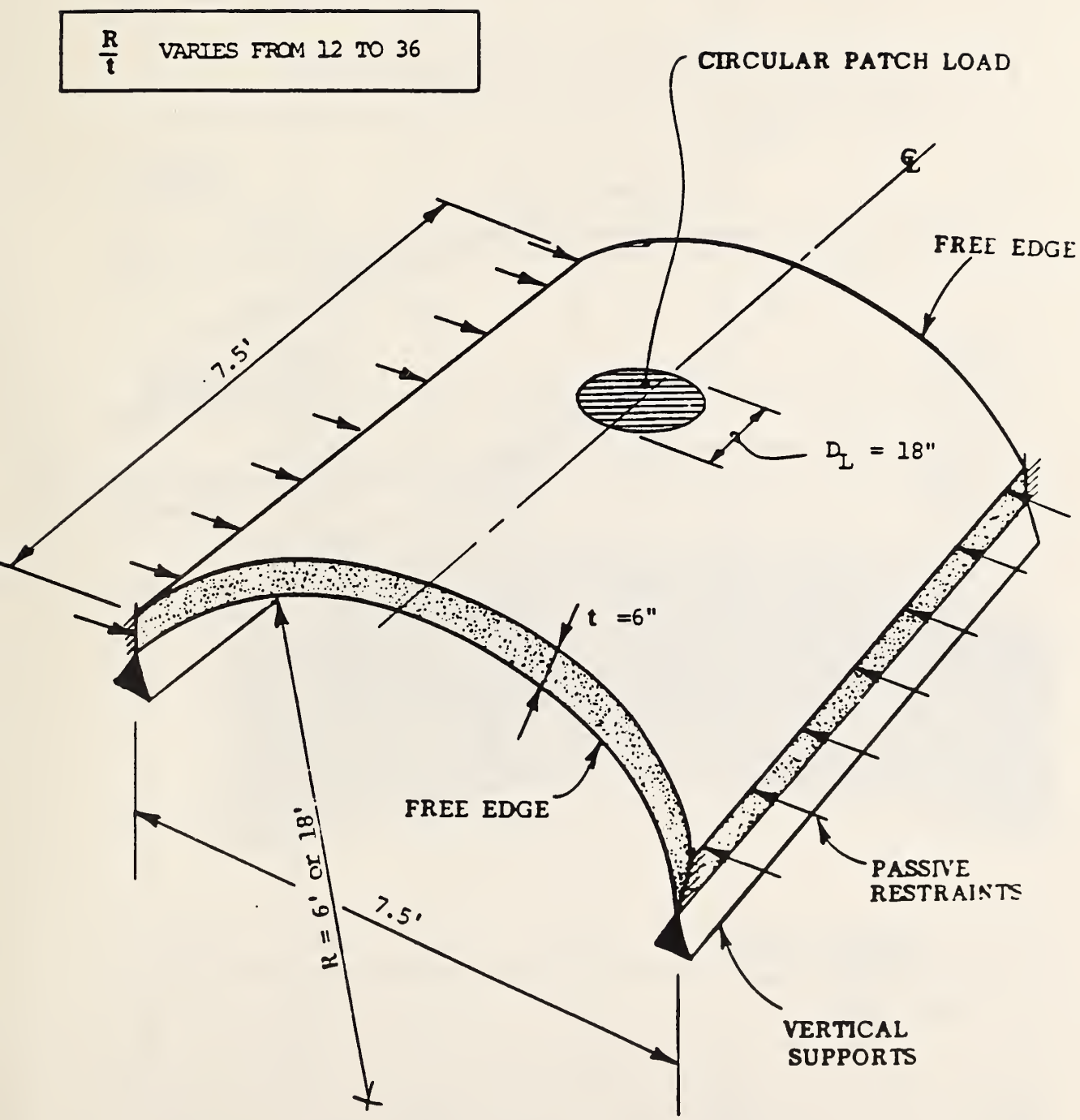

Figure 24 General characteristics of a typical test panel used in the BWA study [34]

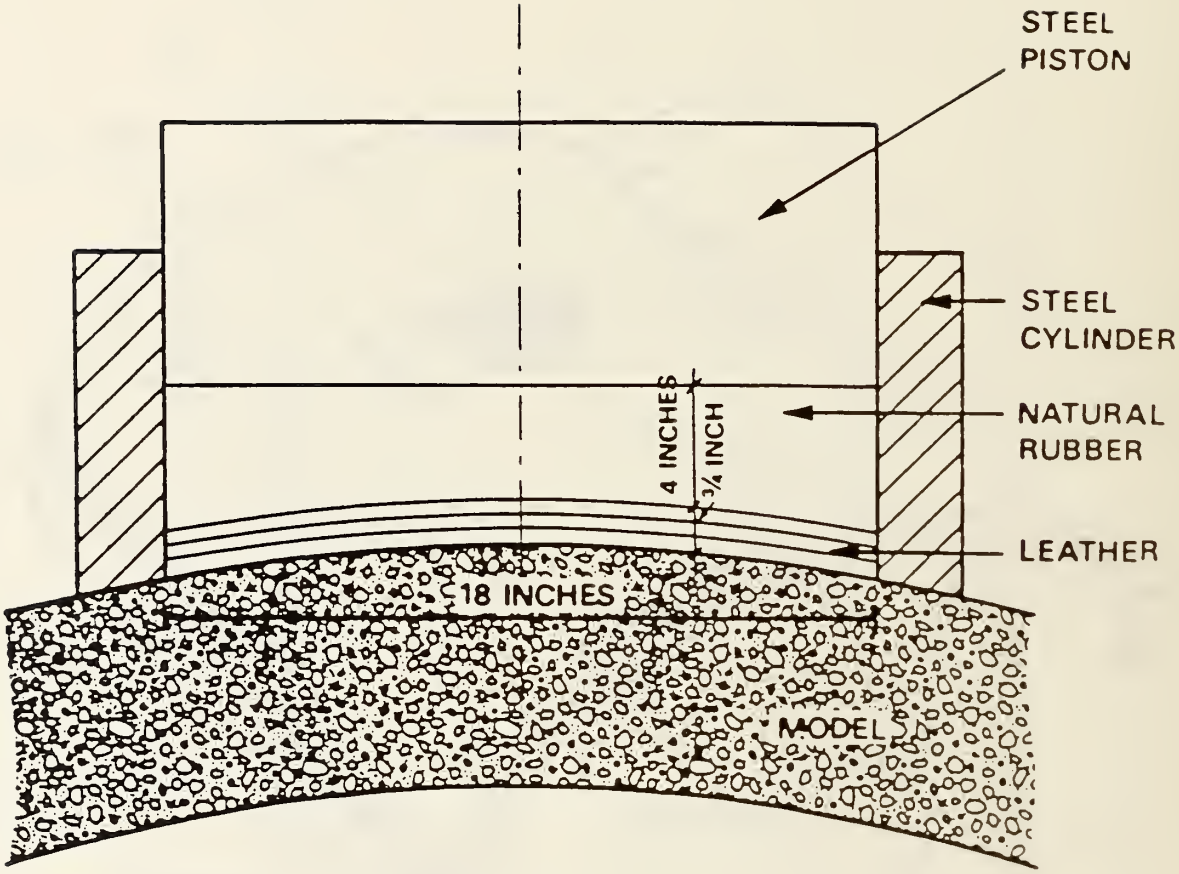

Figure 25 BWA punching shear study loading system (from Reference 34)

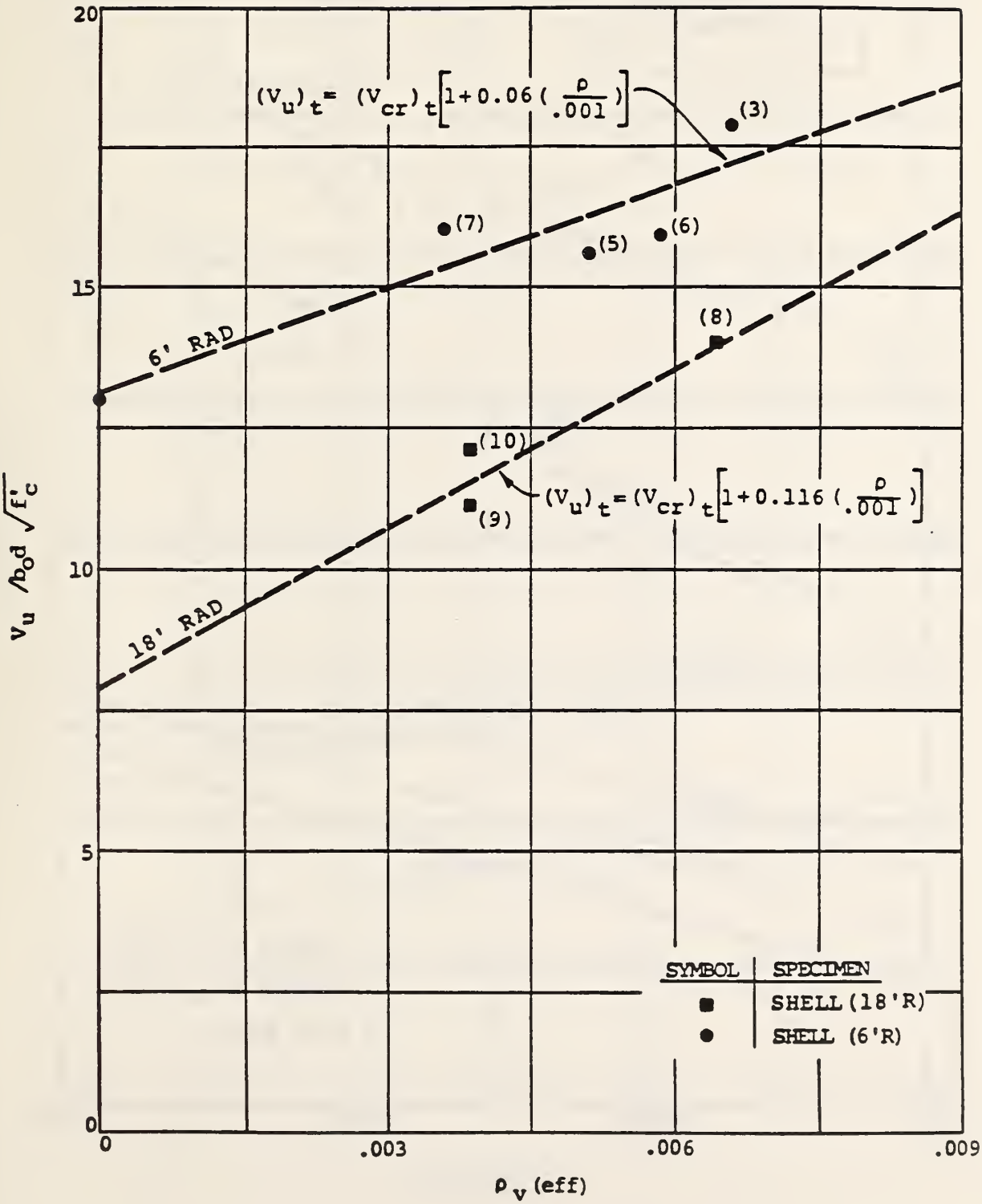

Figure 26 Effect of shear reinforcement quantity on ultimate shear resistance in BWA study [34]

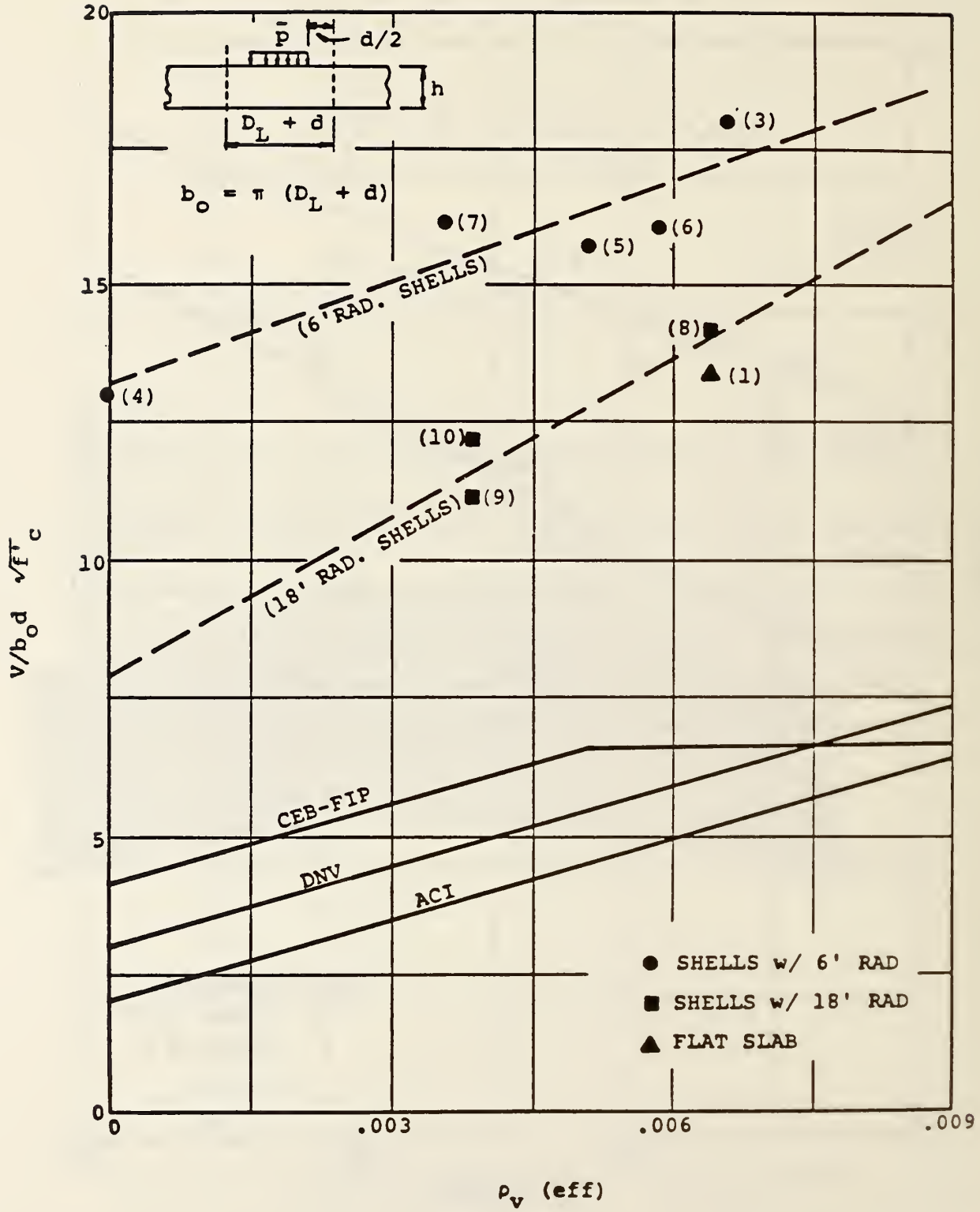

Figure 27 Test results of BWA study compared with "conventional slab methods" [34]

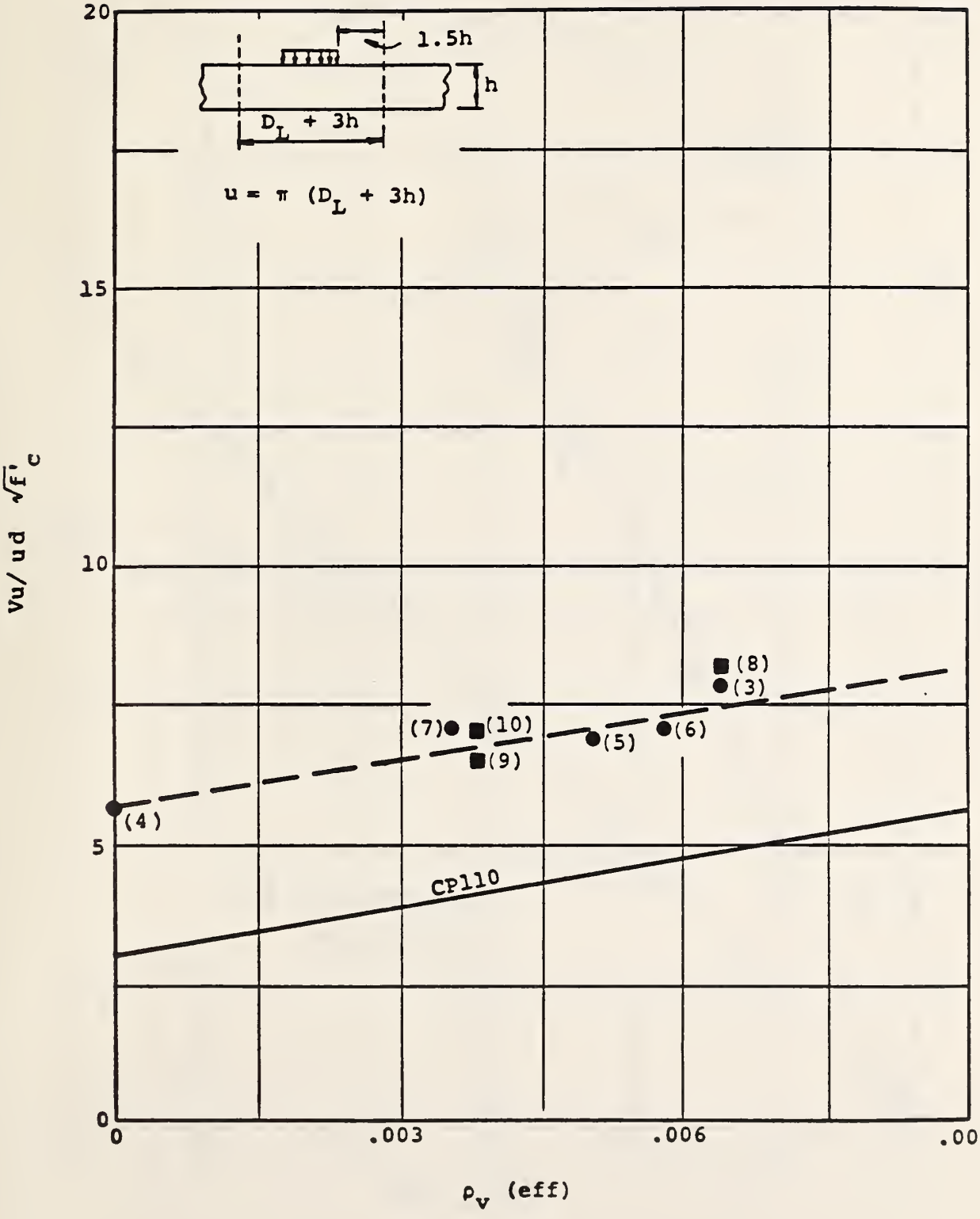

Figure 28 Test results of BWA study compared with "conventional slab method" (CP110) [34]

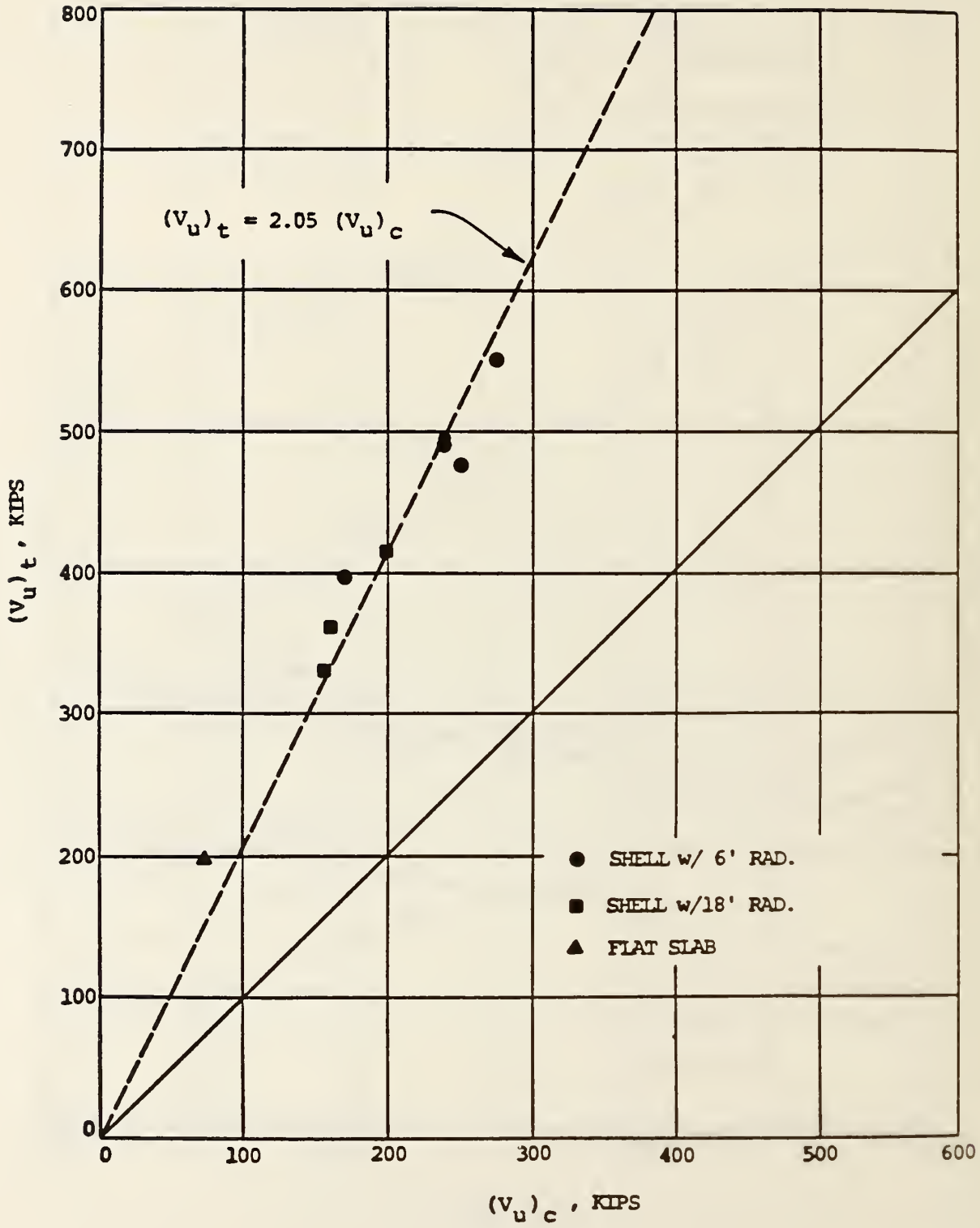

Figure 29 Comparison of tested vs. calculated ultimate shear resistance, Vu ("ACI modified punching shear method"), from BWA study [34]

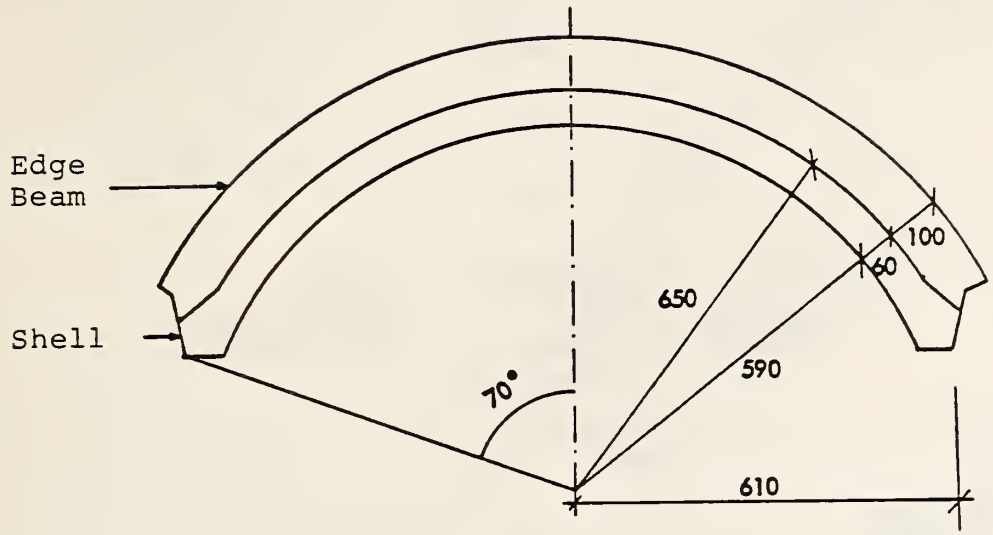

END VIEW

(all dimensions in mm)

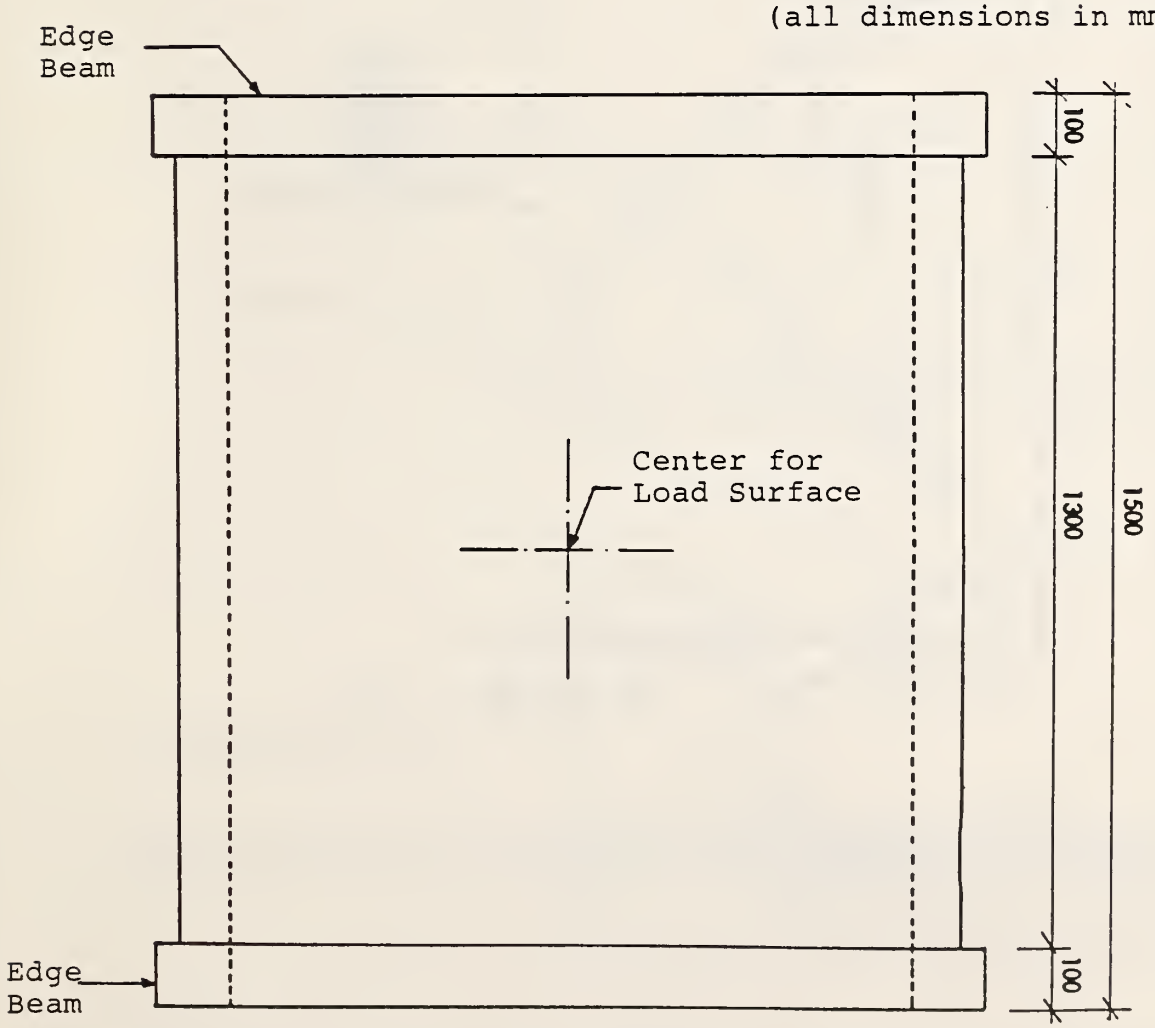

TOP VIEW

Figure 30 Geometry and dimensions for shell specimens of Reference 149

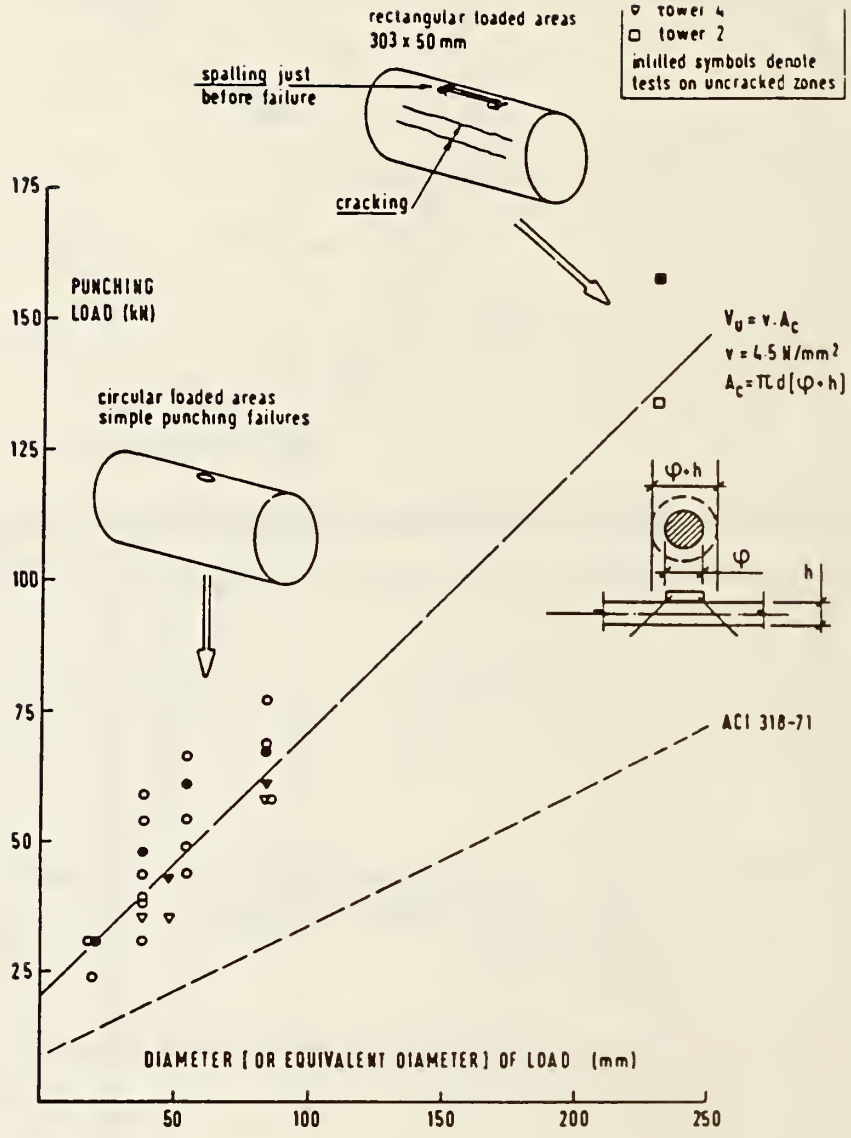

Figure 31 Results of punching tests of Reference 152

(a)

from Reference 172

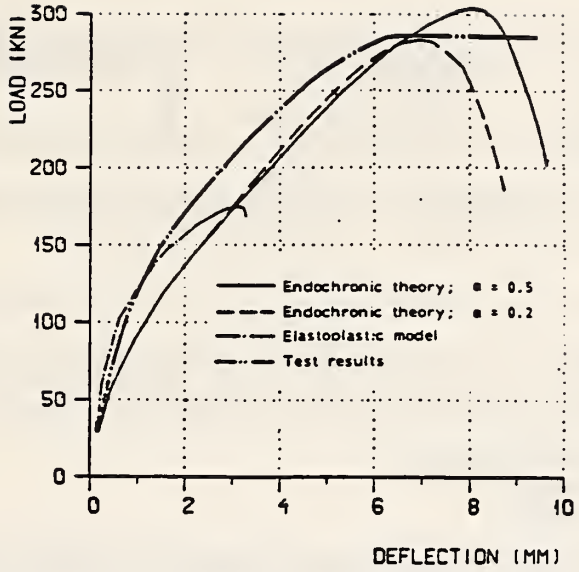

(b)

from Reference 173

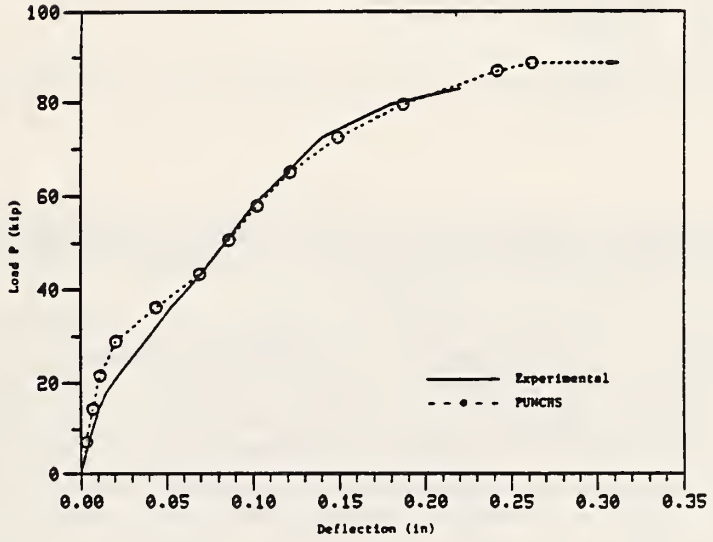

(c)

from Reference 175

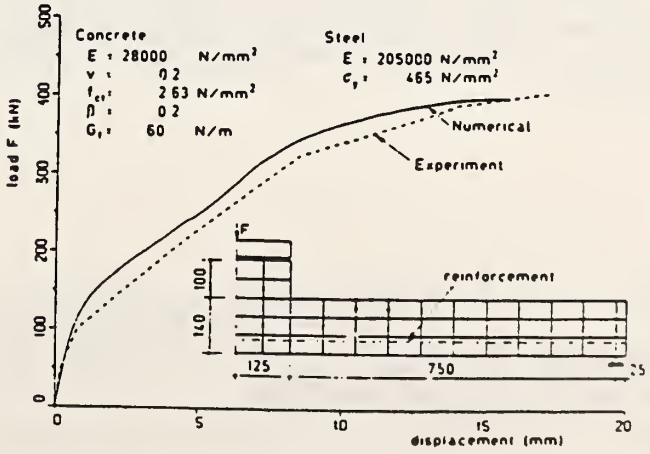

Figure 32 Finite element predictions of punching shear strength: load vs. deflection curves

NBS-114A (REV. 2-8C)

U.S. DEPT. OF COMM. BIBLIOGRAPHIC DATA SHEET (See instructions)	1. PUBLICATION OR REPORT NO. NBSIR 86-3388	2. Performing Organ. Report No.	3. Publication Date MAY 1986

4. TITLE AND SUBTITLE

Punching Shear Resistance of Lightweight Concrete Offshore Structures for the Arctic: Literature Review

5. AUTHOR(S)

David I. McLean, H. S. Lew, Long T. Phan, Mary J. Sansalone

6. PERFORMING ORGANIZATION (If joint or other than NBS, see instructions)

NATIONAL BUREAU OF STANDARDS
DEPARTMENT OF COMMERCE
WASHINGTON, D.C. 20234

7. Contract/Grant No.

8. Type of Report & Period Covered

9. SPONSORING ORGANIZATION NAME AND COMPLETE ADDRESS (Street, City, State, ZIP)

Technology Assessment and Research Branch; Mineral Management Service
U.S. Department of the Interior
Reston, VA. 22091

10. SUPPLEMENTARY NOTES

☐ Document describes a computer program; SF-185, FIPS Software Summary, is attached.

11. ABSTRACT (A 200-word or less factual summary of most significant information. If document includes a significant bibliography or literature survey, mention it here)

The punching shear resistance of lightweight concrete offshore structures for the Arctic is being investigated at the National Bureau of Standards on the behalf of the Minerals Management Service of the U.S. Department of the Interior in cooperation with five American oil companies. This report serves as an introduction to the project and reviews current knowledge on material relevant to the punching shear behavior of concrete offshore structures subjected to Arctic ice loads. A brief review of available information on Arctic ice loads and a discussion of some of the proposed offshore structural concepts are presented. The general mechanics of punching shear failures and the factors affecting punching resistance are discussed along with a comparison of current U.S. and European code provisions on punching shear. Available literature on experimental and analytical investigations on punching shear relevant to this project is also reviewed.

12. KEY WORDS (Six to twelve entries; alphabetical order; capitalize only proper names; and separate key words by semicolons)

Artic environment; lightweight concrete; literature review; offshore structure; punching shear; reinforced concrete.

13. AVAILABILITY

☐ Unlimited

☒ For Official Distribution. Do Not Release to NTIS

☐ Order From Superintendent of Documents, U.S. Government Printing Office, Washington, D.C. 20402.

☐ Order From National Technical Information Service (NTIS), Springfield, VA. 22161

14. NO. OF PRINTED PAGES

15. Price

USCOMM-DC 6043-P80